3. Cromatografía de Líquidos-Espectrometría de Masas

3.1. INTRODUCCIÓN GENERAL

Como se ha expuesto anteriormente en la presente memoria, la cromatografía de líquidos es la técnica de separación más comunmente utilizada para llevar a cabo la separación de las HAs y su determinación en matrices alimentarias, ya que a diferencia de la cromatografía de gases no se requiere una etapa de derivatización previa a su inyección en el sistema cromatográfico. Tal y como se comentó en el Apartado 1.2.2.2, si se combina la cromatografía de líquidos con la espectrometría de masas el resultado es una metodología analítica de elevada selectividad y sensibilidad. Por este motivo, cada vez son más numerosas las publicaciones relacionadas con las aminas heterocíclicas que aplican técnicas basadas en el acoplamiento LC-MS.

Los primeros trabajos que utilizaron métodos LC-MS para analizar HAs emplearon fuentes de ionización por termopulverización (TSP) (Edmons *et al.*, 1986). Posteriormente y siguiendo la evolución de las técnicas de ionización en espectrometría de masas acoplada a la cromatografía de líquidos, el TSP fue desplazado por las técnicas de ionización a presión atmosférica (API), que incluyen la electropulverización o *electrospray* (ESI) (Johansson *et al.*, 1995) y la ionización química a presión atmosférica (APCI) (Holder *et al.*, 1997).

En la fuente ESI, desarrollada a mediados de los años 80 (Yamashita *et al.*, 1984; Aleksandrov *et al.*, 1985), la muestra líquida se introduce a través de un capilar al que se aplica un elevado potencial (± 3-5 kV), lo que permite producir un spray de microgotas cargadas, las cuales debido a repulsiones electrostáticas se dividen hasta provocar la desolvatación y evaporación de los iones. La fuente ESI trabaja a flujos entre 0,5 y 10 μL min^{-1}, aunque se pueden aumentar hasta 300-400 μL min^{-1} utilizando el denominado *ionspray* (ISP), una variante del *electrospray* en la cual la formación del aerosol y la desolvatación están facilitadas por una corriente coaxial de gas. La electropulverización es una técnica de ionización suave, de manera que los iones producidos son principalmente los derivados de la incorporación o cesión de uno o varios protones a las moléculas, aunque también se pueden originar iones correspondientes a aductos con otras especies presentes en la fase móvil.

En las fuentes de APCI, desarrolladas a mediados de los años 70 (Horning *et al.*, 1973), la fase móvil se introduce a través de una cámara de vaporización cilíndrica que se encuentra a elevada temperatura, lo que provoca la evaporación del efluente

cromatográfico. La ionización se induce aplicando un elevado voltaje (± 3-5 kV) a un electrodo en forma de aguja, lo que produce una corriente de hasta 10 μA. Esta corriente eléctrica origina un plasma de iones de la fase móvil que provoca un proceso de ionización química. La ionización química a presión atmosférica es una técnica de ionización suave, aunque en algunos casos además de los iones correspondientes a la molécula protonada o desprotonada pueden aparecer fragmentos en el espectro.

En la Tabla 3.1 se resumen las principales características de las fuentes API. La principal diferencia entre las dos fuentes de ionización radica en el mecanismo de ionización. En ESI, los iones preformados en fase líquida son a continuación desolvatados y evaporados. En cambio, en APCI la ionización se produce en fase gas debido a reacciones ion-molécula entre el plasma generado a partir de la fase móvil y los analitos. Otra diferencia importante está relacionada con el caudal de fase móvil óptimo. Mientras que ESI funciona óptimamente a caudales bajos, el APCI permite trabajar sin pérdida de sensibilidad a caudales de 1 mL min^{-1}. Además, esta última técnica de ionización se ve menos afectada por componentes iónicos presentes en la matriz, aunque la elevada temperatura de trabajo del APCI limita su aplicación a sustancias no termolábiles.

Tabla 3.1.- Principales características de las fuentes de ionización a presión atmosférica.

Fuentes de ionización	ESI	APCI
Ionización	En fase líquida (evaporación iónica)	En fase gas
pH	Influencia importante	Poca influencia
Caudal fase móvil	0,5-400 μL min^{-1}	0,5-2 mL min^{-1}
Polaridad analito	Iónicos/polares	Ionizables/intermedia
Peso molecular	Sin límite	< 1200 Da
Inconvenientes	Mayor efecto matriz	Degradación térmica

La mayoría de los trabajos publicados en la literatura que hacen referencia a la utilización de fuentes API para analizar HAs mediante LC-MS emplean la ionización por electropulverización (Johansson *et al.*, 1995; Richling *et al.*, 1996; Fay *et al.*, 1997; Pais *et al.*, 1997b). Sin embargo, la fuente de ionización APCI también ha sido utilizada, y tanto los parámetros de calidad establecidos como los resultados obtenidos han sido equivalentes a los proporcionados por la fuente de ionización de ESI (Holder *et al.*, 1997; Pais *et al.*, 1997a; Stavric *et al.*, 1997a; Guy *et al.*, 2000). Por este motivo, en este trabajo se ha estudiado la potencialidad del APCI para el análisis de HAs en muestras de alimentos. En concreto, el objetivo principal de esta parte del trabajo ha sido el desarrollo de metodología

analítica basada en LC-MS utilizando para ello dos instrumentos diferentes, uno con un analizador de trampa de iones y otro con uno de triple cuadrupolo.

3.2. ESPECTROMETRÍA DE MASAS CON UN ANALIZADOR DE TRAMPA DE IONES

3.2.1. Introducción y objetivos

Aunque el funcionamiento del analizador de trampa de iones fue descrito por primera vez a mediado de los años 50, los espectrómetros de masas con este tipo de analizador no empezaron a comercializarse hasta 1983. Actualmente, las aplicaciones descritas en la bibliografía que utilizan este tipo de instrumentación son innumerables, y abarcan campos tan variados como por ejemplo estudios de reactividad en fase gaseosa, análisis de péptidos o aplicaciones medioambientales (March, 2000; Hao *et al.*, 2001).

Como se expuso en el Capítulo 1 de la presente memoria, las mejoras introducidas en el acoplamiento LC-MS en la última década ha posibilitado que esta técnica sea ampliamente utilizada para el análisis de HAs en diversos tipos de muestra. Sin embargo, las aplicaciones en las que se describe el uso de un analizador de trampa de iones eran prácticamente nulas en el momento de iniciar nuestro trabajo experimental, por lo que en esta parte de la tesis doctoral nos propusimos evaluar el uso de este tipo de instrumentación y poner a punto metodología analítica para el análisis de HAs.

Con este objetivo, se utilizó un espectrómetro de masas Finnigan LCQ, cuyo esquema se muestra en la Figura 3.1. Como puede observarse en esta figura, el efluente cromatográfico se introduce en una fuente de ionización a presión atmosférica, en este caso APCI. El spray formado con la ayuda de los gases auxiliar y envolvente se vaporiza a continuación mediante la aplicación de energía térmica, provocándose seguidamente la ionización mediante la aplicación de un elevado potencial en la aguja de descarga. Los iones producidos se dirigen entonces hacia el *heated capillary*, un tubo de acero inoxidable que, al estar calentado a una temperatura de entre 150-250 ºC, ayuda a la desolvatación de los iones. Una vez atravesado este capilar, los iones se introducen en el tubo de lentes. Al aplicar a este componente el potencial adecuado, los iones se focalizan y atraviesan el *skimmer*. La aplicación de un potencial extra, denominado *tube lens offset voltage*, contribuye a la desolvatación de los iones mediante colisiones con el gas presente en la zona. Sin embargo, si el voltage aplicado es muy elevado, las colisiones son tan energéticas que provocan la fragmentación de las moléculas, lo que disminuye la sensibilidad del método. A continuación, los iones atraviesan el *skimmer*,

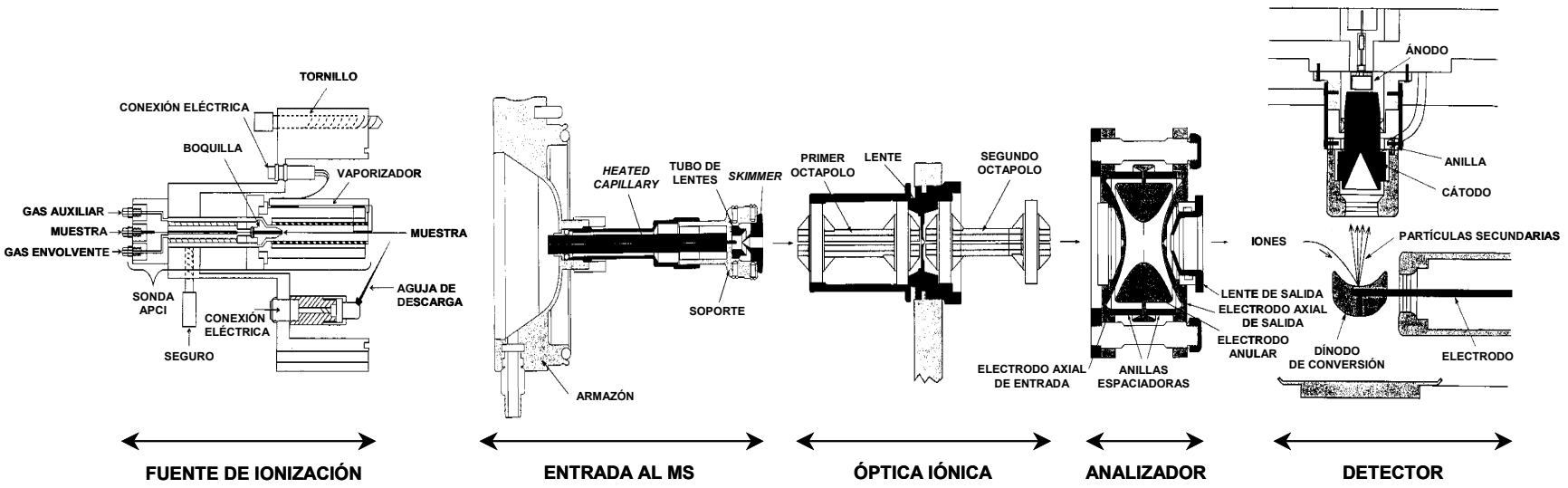

Figura 3.1.- Esquema del espectrómetro de masas con analizador de trampa de iones utilizado.

el cual tiene como función mantener la diferencia de vacío entre la zona del *heated capillary* (1 Torr) y el primer octapolo (10^{-3} Torr), y se dirigen a la zona de óptica iónica. La óptica iónica, consistente en dos octapolos y una lente intermedia, se encarga de transmitir los iones hasta el analizador de masas mediante la creación de campos eléctricos.

La trampa de iones está compuesta por dos electrodos axiales y uno anular, dispuestos de manera que forman una cavidad en la que se produce el análisis de masas. Dependiendo del tipo de corriente alterna aplicado en los diferentes electrodos, los iones son atrapados, fragmentados o eyectados dependiendo de su relación masa/carga. Así, la aplicación de un voltaje de frecuencia constante y amplitud variable en el electrodo anular provoca el atrapamiento de los iones con trayectoria estable. Para obtener el espectro de masas, los iones atrapados se desestabilizan en función de su relación masa/carga mediante el aumento de la radiofrecuencia del potencial aplicado. La eyección de un tipo concreto de iones puede ser también originada por la aplicación de una corriente alterna en los electrodos axiales, con un desfase de 180º entre ellos. Además, cuando la radiofrecuencia del voltaje aplicado iguala la frecuencia de resonancia de un ion, la cual depende de su *m/z*, dicho ion incrementa su energía cinética y colisiona con el He presente en la trampa de iones, lo que provoca su disociación en iones producto. El último componente del espectrómetro de masas, el detector, incluye un dínodo de conversión y un canal multiplicador de electrones.

El trabajo experimental realizado en el presente capítulo se inició con la optimización de la composición de la fase móvil para hacerla compatible con el espectrómetro de masas, para lo cual se partió de la separación cromatográfica establecida en el capítulo precedente (Apartado 2.2.2.1). Se compararon también diferentes propiedades del tampón basado en fosfato utilizado para la detección UV y del tampón basado en formiato propuesto para ser usado con el sistema MS. Este estudio se expone detalladamente en el Apartado 3.2.2.1 de la memoria.

A continuación, utilizando el sistema de espectrometría de masas anteriormente descrito, se estudiaron los espectros de los analitos en modo *full scan* y se establecieron las condiciones experimentales óptimas para realizar la determinación de las HAs mediante LC-APCI-MS(IT). Después de evaluar diferentes parámetros de calidad del método, éste se aplicó al análisis de un extracto de carne liofilizado cuya preparación se describió en la Tesis Doctoral de P. Pais (Pais, 1996). Este trabajo experimental se encuentra descrito en el Artículo IV, titulado "*Determination of heterocyclic aromatic amines in meat extracts by*

liquid chromatography-ion trap atmospheric pressure chemical ionization mass spectrometry", el cual se incluye en el Apartado 3.2.2.2.

Posteriormente nos propusimos utilizar la espectrometría de masas en tándem (MS/MS) acoplada a la cromatografía de líquidos (LC-MS/MS) para la cuantificación de HAs. Con este fin, se estudió en primer lugar la fragmentación de los analitos en una trampa de iones utilizando espectrometría de masas en tándem múltiple (MS^n), lo que nos permitió establecer rutas de fragmentación para cada analito. El trabajo de elucidación de rutas de fragmentación ha dado lugar al Artículo V de esta memoria, que se incluye en el Apartado 3.2.2.3 y lleva por título "*Multistep mass spectrometry of heterocyclic amines in a quadrupole ion trap mass analyser*". Después de identificar los iones producto más característicos en MS^2, se optimizaron los diferentes parámetros que influyen en la fragmentación del ion precursor y la estabilidad tanto del ion precursor como de los iones producto. Tras estudiar las prestaciones de la metodología LC-MS/MS establecida, se analizó el extracto de carne liofilizado citado con anterioridad. Esta última parte del trabajo experimental realizada con el instrumento de trampa de iones se incluye en el Artículo VI, titulado "*Ion-trap tandem mass spectrometry for the determination of heterocyclic amines in food*" (Apartado 3.2.2.4).

3.2.2. Trabajo experimental

3.2.2.1. Comparación de los sistemas reguladores fosfórico/fosfato y fórmico/formiato

El ácido fosfórico es el ácido utilizado tradicionalmente en las fases móviles utilizadas en el análisis por cromatografía de líquidos con detección UV de las HAs. Ello es principalmente debido a la baja absorbancia de este ácido, lo que contribuye a la obtención de una línea de base estable. A fin de obtener picos cromatográficos simétricos y estrechos para compuestos básicos como las HAs se añade trietilamina a la fase móvil, ya que esta base neutraliza los grupos silanol libres de la columna. Sin embargo, la pareja ácido/base obtenida no tampona en la zona de pH 3-4 utilizada normalmente para la separación de las HAs, ya que la primera constante de acidez del ácido fosfórico es 1,96. Además, a la hora de acoplar la cromatografía de líquidos a la espectrometría de masas este tampón debe ser sustituido por uno volátil. Así, con el objetivo de emplear la espectrometría de masas como sistema de detección, nos propusimos la utilización de un sistema regulador basado en el uso de amoníaco y ácido fórmico. Este nuevo sistema

regulador no sólo es volátil, sino que tampona en la zona de pH de trabajo por tener el ácido fórmico una constante de acidez de 3,75.

Con el fin de evaluar la aplicabilidad de la nueva fase móvil, nos propusimos comparar las características proporcionadas por el sistema cromatográfico fórmico/formiato con las correspondientes al tampón fosfórico/fosfato normalmente utilizado en los métodos LC-UV. Así, se utilizaron ambas fases móviles y se evaluó la precisión del método cromatográfico en diferentes condiciones: en determinaciones secuenciales (repetitividad o precisión *run-to-run*), en diferentes días (precisión a medio plazo o *day-to-day*), y tras ocasionar pequeños cambios en los valores nominales de algunas variables (robustez).

La separación cromatográfica de las HAs se llevó a cabo utilizando un sistema de elución por gradiente compuesto de dos bombas con un mezclador de alta presión y un módulo controlador (Pharmacia LKB 2150-2152, Uppsala, Suecia) y una columna cromatográfica TSK-Gel ODS 80TM (TosoHaas, Sttutgart, Alemania) (5 μm, 25 cm x 4,6 mm) equipada con una precolumna Supelguard LC-8-DB (Supelco, Gland, Suiza). Para la inyección se utilizó un inyector manual de seis válvulas (Rheodyne 7125, Cotati, CA), y la detección se realizó empleando un detector UV con diodos en serie (Beckman System Gold 168, Fullerton, CA). Se utilizaron cinco disoluciones patrón, con concentraciones de los analitos comprendidas entre 0,36 y 6,85 μg mL^{-1} y con TriMeIQx como patrón interno a 1,68 μg mL^{-1}.

Los dos sistemas de elución utilizados fueron los que se describen a continuación. El primero consistió en un gradiente ternario cuyos disolventes eran A: trietilamina 10 mM en agua ajustando pH a 3,25 con ácido fosfórico, B: trietilamina 10 mM en agua ajustando pH a 3,7 con ácido fosfórico y C: acetonitrilo. El segundo sistema de elución consistió también en un gradiente ternario, pero constituido esta vez por A: ácido fórmico 30 mM y trietilamina 7 mM en agua ajustando pH a 3,25 con amoníaco, B: ácido fórmico 30 mM y trietilamina 7 mM en agua ajustando pH a 3,7 con amoníaco y C: acetonitrilo. En ambos casos el flujo se mantuvo a 1 mL min^{-1} y se programó el siguiente gradiente: 5-23 % C en A, 0-18 min; 23 % C en A, 18-20 min; 23 % C en B, 20-25 min; 23-55 % C en B, 25-35 min, 55 % C en B, 35-40 min. En la Figura 3.2 se muestran a modo de ejemplo los cromatogramas obtenidos al inyectar 15 μL de una disolución patrón que contenía los analitos a un nivel aproximado de 4 μg mL^{-1} (~ 60 ng inyectados) con los dos sistemas cromatográficos utilizados.

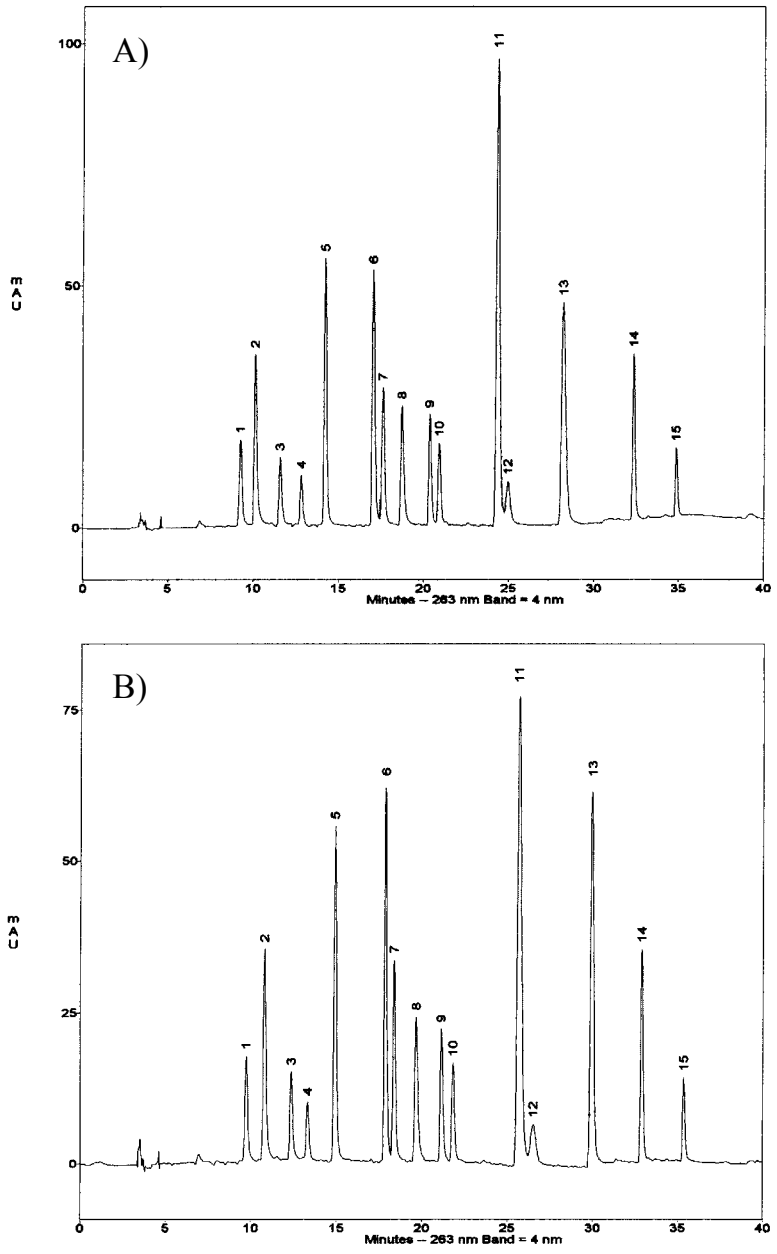

Figura 3.2.- Cromatograma obtenido con la fase móvil A) fosfórico/fosfato y B) fórmico/formiato tras inyectar 15 µL de una disolución patrón de ~4 µg mL^{-1}. Identificación de los picos: 1. Glu-P-2, 2. IQ, 3. MeIQ, 4. Glu-P-1, 5. MeIQx, 6. 7,8-DiMeIQx, 7. 4,8-DiMeIQx, 8. Norharman, 9. TriMeIQx (P.I.), 10. Harman, 11. Trp-P-2, 12. PhIP, 13. Trp-P-1, 14. AαC, 15. MeAαC.

La primera característica del sistema cromatográfico estudiada fue la precisión *run-to-run* o repetitividad, la cual se define como la precisión del método cuando se analiza la muestra repetidamente, en un corto plazo de tiempo y siendo utilizado el mismo procedimiento e instrumento por un mismo analista. Para la determinación de la repetitividad de la cuantificación y de los tiempos de retención, se inyectaron el mismo día los cinco patrones de la recta de calibrado y se realizaron cinco análisis de una disolución

que contenía los analitos a un nivel de ~1,7 μg mL^{-1}. Los valores medios obtenidos para la concentración así como los respectivos valores de desviación estándar se indican en la Tabla 3.2. También se han incluido en esta tabla las diferencias relativas porcentuales del valor de concentración calculado con respecto al teórico.

Tabla 3.2.- Repetitividad del método (desviación estándar relativa de la concentración) y diferencias porcentuales relativas del valor calculado con respecto a la concentración nominal.

Analito	**Conc. Nominal**	**Fosfórico/Fosfato**			**Fórmico/Formiato**		
	μg mL^{-1}	*Media (μg mL^{-1})*	*RSD %*	*Dif. rel %*	*Media (μg mL^{-1})*	*RSD %*	*Dif. rel %*
Glu-P-2	1,556	1,64	3	5	1,58	3	2
IQ	2,311	2,26	2	2	2,14	4	7
MeIQ	1,215	1,20	7	1	1,24	3	2
Glu-P-1	1,390	1,37	7	1	1,40	4	1
MeIQx	1,556	1,59	4	2	1,52	3	2
7,8-DiMeIQx	1,704	1,75	3	3	1,65	2	3
4,8-DiMeIQx	1,244	1,25	4	0	1,29	1	4
Norharman	1,670	1,67	4	0	1,80	3	8
Harman	1,556	1,64	5	5	1,51	2	3
Trp-P-2	1,972	2,03	4	3	1,89	2	4
PhIP	1,644	1,69	3	3	1,57	4	5
Trp-P-1	1,639	1,71	4	4	1,65	2	1
AαC	2,533	2,61	2	3	2,61	1	3
MeAαC	1,644	1,68	2	2	1,56	2	5

En la tabla anterior puede observarse que los valores medios de concentración calculados con los dos sistemas de elución son muy similares. Las diferencias relativas porcentuales del valor de concentración calculado con respecto al nominal, muy inferiores al 10 % en la mayoría de los casos, indican una buena correspondencia entre estos dos valores de concentración. En el caso de las RSD %, éstas oscilan entre 1,6 y 7,1 en el caso del ácido fosfórico y entre 1,0 y 4,1 % para el ácido fórmico.

Los valores de repetitividad para los tiempos de retención se indican en la Tabla 3.3, donde además se muestran los valores medios obtenidos con cada sistema tamponador. Según el test F realizado al 95 % de confianza, la mayoría de valores de desviación estándar son significativamente superiores en el caso del tampón fosfórico/fosfato, siendo además las diferencias superiores en la primera mitad del cromatograma.

Tabla 3.3.- Valores medios y de repetitividad (expresado como RSD %) de los tiempos de retención con las fases móviles de ácido fosfórico y ácido fórmico.

Analito	**Fosfórico/Fosfato**		**Fórmico/Formiato**	
	Media (min)	*RSD %*	*Media (min)*	*RSD %*
Glu-P-2	9,2	1,3	9,9	0,5
IQ	10,0	1,2	11,1	0,3
MeIQ	11,5	1,3	12,8	0,3
Glu-P-1	12,6	1,3	13,5	0,3
MeIQx	14,0	1,1	14,9	0,2
7,8-DiMeIQx	16,9	0,8	17,7	0,3
4,8-DiMeIQx	17,4	0,9	18,3	0,2
Norharman	18,6	0,6	19,6	0,1
Harman	20,8	0,4	21,8	0,2
Trp-P-2	24,2	0,4	25,7	0,4
PhIP	24,8	0,4	26,7	0,3
Trp-P-1	28,1	0,2	29,9	0,3
AαC	32,3	0,2	33,1	0,1
MeAαC	34,9	0,2	35,5	0,1

A continuación, se estudió la precisión a medio plazo o *day-to-day* proporcionada por los dos sistemas de elución. La precisión *day-to-day* de un resultado cuantitativo se obtiene cuando el mismo analista determina el contenido de analito en la misma muestra, utilizando el mismo método e instrumento, en días diferentes. Para su determinación, se inyectaron durante cinco días una recta de calibrado y una disolución que contenía las HAs a un nivel de ~1,7 μg mL^{-1}. Los resultados obtenidos para la cuantificación se indican en la Tabla 3.4, donde además se muestran las diferencias porcentuales relativas entre los valores de concentración calculada y teórica. La aplicación de un test estadístico t con un 95 % de confianza indica que la media calculada con los dos sistemas de elución son equivalentes en todos los casos. De manera similar, la realización de un test F al 95% de grado de confianza revela que la desviación estándar relativa sólo es significativamente diferente para 4,8-DiMeIQx y norharman. En cuanto a la exactitud del método, para ambos sistemas de elución las diferencias porcentuales relativas entre el valor de concentración calculado y el nominal fueron inferiores al 4 % en la mayoría de los casos.

El estudio de precisión a medio plazo para los tiempos de retención originó los resultados mostrados en la Tabla 3.5. Al igual que en el caso de la repetitividad, la variabilidad mostrada por el sistema regulador fosfórico/fosfato es en general superior a la obtenida con el tampón fórmico/formiato, debido a su peor capacidad tamponadora en el pH de trabajo.

Tabla 3.4.- Precisión a medio plazo de la concentración (desviación estándar relativa) y diferencias porcentuales relativas del valor calculado con respecto a la concentración nominal. La concentración nominal de cada analito es la misma que en la Tabla 3.2.

Analito	**Fosfórico/Fosfato**			**Fórmico/Formiato**		
	Media (μg mL^{-1})	*RSD %*	*Dif .rel %*	*Media (μg mL^{-1})*	*RSD %*	*Dif. rel %*
Glu-P-2	1,57	6	1	1,55	3	0
IQ	2,26	3	2	2,22	4	4
MeIQ	1,13	5	7	1,19	3	2
Glu-P-1	1,37	6	1	1,39	5	0
MeIQx	1,55	3	0	1,58	3	2
7,8-DiMeIQx	1,71	1	0	1,72	2	1
4,8-DiMeIQx	1,26	3	1	1,27	2	2
Norharman	1,71	2	2	1,67	3	0
Harman	1,58	5	2	1,56	3	0
Trp-P-2	1,98	2	0	2,01	2	2
PhIP	1,62	4	1	1,67	4	2
Trp-P-1	1,63	2	1	1,67	2	2
AαC	2,55	2	1	2,60	2	3
MeAαC	1,65	2	0	1,63	3	1

Tabla 3.5.- Valores medios y de precisión a medio plazo (expresado como RSD %) de los tiempos de retención con las fases móviles de ácido fosfórico y ácido fórmico.

Analito	**Fosfórico/Fosfato**		**Fórmico/Formiato**	
	Media (min)	*RSD %*	*Media (min)*	*RSD %*
Glu-P-2	9,3	3,30	10,0	0,53
IQ	10,1	3,41	11,1	1,60
MeIQ	11,6	2,83	12,7	1,81
Glu-P-1	12,8	2,35	13,5	0,73
MeIQx	14,2	2,02	14,9	0,48
7,8-DiMeIQx	17,0	1,74	17,7	0,37
4,8-DiMeIQx	17,6	1,73	18,3	0,36
Norharman	18,8	1,81	19,6	0,47
Harman	20,9	1,60	21,8	0,51
Trp-P-2	24,4	1,69	25,7	0,65
PhIP	25,0	1,88	26,6	0,86
Trp-P-1	28,3	1,73	29,9	0,36
AαC	32,3	0,66	33,0	0,48
MeAαC	34,9	0,34	35,4	0,27

La robustez fue el último aspecto estudiado del método analítico. Este parámetro es una medida de la capacidad del método de reproducir resultados cuando el procedimiento es repetido bajo circunstancias diferentes. Tradicionalmente, la robustez se ha definido desde dos puntos de vista, bien en diferentes laboratorios o dentro de un mismo

laboratorio. En el primer caso, se debe evaluar el grado de reproducibilidad al alterar condiciones externas tales como el analista o el instrumento, mientras que en el segundo se estudia el efecto producido por pequeños cambios en el valor nominal de variables experimentales como el pH, la concentración del tampón o la composición de la fase móvil. Estos valores nominales deben ser los recomendados en el caso de utilizar un método estándar, o los optimizados si se aplica un método desarrollado en el propio laboratorio.

A pesar de ser una importante característica del sistema, en la bibliografía se presentan pocos trabajos que propongan una metodología para realizar el test de robustez. Además, al ser diferente el diseño aplicado en cada caso, los resultados no son directamente comparables. En general, todos los trabajos coinciden en aconsejar que la variación del valor nominal sea lo suficientemente grande como para producir una variación en la respuesta analítica mayor que el error aleatorio inherente al método estudiado (Molnár, 1996). Asimismo, se sugiere que la alteración provocada debe simular variaciones incontroladas del sistema.

Nosotros centramos esta parte del estudio en la comparación de la robustez obtenida con las dos fases móviles estudiadas, consistentes en ácido fórmico o fosfórico y sus respectivas formas básicas. Con este fin, se seleccionaron únicamente las variables más importantes (pH, concentración del tampón, porcentaje de acetonitrilo en la fase móvil) y se diseñó un diseño factorial de estrella, con tres variables y tres niveles cada una de ellas, tal y como se muestra en la Figura 3.3. En la Tabla 3.6 se indican las variaciones realizadas en las tres variables fijadas en el sistema. La alteración producida, mantenida a lo largo de todo el cromatograma, fue de 0,1 unidades en el valor nominal del pH, mientras que la concentración del tampón se modificó en un 5 % y el porcentaje de acetonitrilo un 1 %.

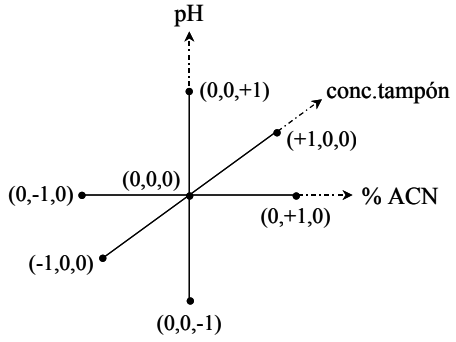

Figura 3.3.- Diseño de estrella utilizado para el estudio de la robustez.

Tabla 3.6.- Alteración producida en las variables estudiadas.

Variable	Variación aplicada		Valor inferior (-1)	Valor central (0)	Valor superior (+1)
pH	± 0,1	t < 20 min	3,15	3,25	3,35
		t > 20 min	3,6	3,7	3,8
Conc.tampón	± 5 %	fosfórico/fosfato	9,5 mM TEA	10 mM TEA	10,5 mM TEA
		fórmico/formiato	28,5 mM HCOOH	30 mM HCOOH	31,5 mM HCOOH
% ACN	± 1	t = 0 min	4	5	6

En cada una de las condiciones propuestas, se inyectó una recta de calibrado y se efectuaron cinco análisis de una disolución que contenía los analitos a un nivel de concentración de ~1,7 μg mL^{-1}. Se calcularon a continuación los valores medios de concentración y tiempo de retención en las condiciones iniciales óptimas y en las modificadas. El valor obtenido se normalizó dividiendo por el valor calculado en las condiciones sin alterar y se multiplicó por 100, obteniéndose los datos que se indican en la Tabla 3.7. Como puede observarse, los valores de la tabla son generalmente inferiores al 6 %, por lo que podría decirse que la variabilidad producida al alterar los parámetros estudiados es equivalente a la propia variabilidad del método. La única excepción es MeAαC con el sistema fosfórico/fosfato, en cuyo caso ya se habían observado anteriormente ciertos problemas de estabilidad (Toribio, 1998).

Tabla 3.7.- Variaciones porcentuales normalizadas obtenidas en el estudio de la robustez del cálculo de concentración.

Analitos	Fosfórico/Fosfato						Fórmico/Formiato					
	pH		Conc.		% ACN		pH		Conc.		% ACN	
	-1	*+1*	*-1*	*+1*	*-1*	*+1*	*-1*	*+1*	*-1*	*+1*	*-1*	*+1*
Glu-P-2	-1,7	-3,2	2,2	-2,0	0,5	-3,2	-3,7	-1,3	4,4	-2,4	-3,5	-0,3
IQ	1,6	-2,4	0,5	0,1	-0,5	0,8	3,3	3,8	4,4	4,3	5,0	-0,1
MeIQ	0,9	0,7	4,8	0,6	-0,1	2,8	4,6	0,2	-2,5	-1,6	-0,4	0,3
Glu-P-1	2,0	5,3	6,0	4,5	-3,3	2,6	3,3	-0,4	0,2	-1,1	-2,8	-1,0
MeIQx	-2,2	-3,1	-2,1	-4,5	-3,0	-2,0	2,6	2,0	4,2	0,2	2,9	2,0
7,8-DiMeIQx	-3,2	2,4	-2,1	-2,7	-2,4	-1,7	-2,1	-1,8	1,4	-1,2	0,9	-1,8
4,8-DiMeIQx	-2,1	-2,3	-1,2	-1,3	-1,1	-0,2	-2,8	-0,8	-1,4	-2,5	-2,7	-1,3
Norharman	-1,0	-3,0	-0,8	-1,9	-2,9	-0,4	0,2	2,4	-0,8	-2,1	1,5	2,2
Harman	-4,5	-0,7	-0,1	-4,2	3,9	-3,7	2,5	3,0	5,0	4,5	-4,4	-2,7
Trp-P-2	-5,1	-4,8	-2,4	-3,1	2,6	-0,7	-2,6	-1,8	-0,3	-4,0	-2,7	-3,6
PhIP	-0,8	-6,0	0,7	-5,7	4,1	-4,0	3,7	3,8	1,0	2,9	4,3	-3,6
Trp-P-1	-5,2	-5,7	-4,5	-5,1	-1,6	-0,6	-1,7	-4,1	-0,6	-2,2	-4,0	-3,4
AαC	-3,1	-3,9	0,4	-2,9	-2,5	0,9	-3,0	-1,7	2,7	-5,2	-3,4	-0,9
MeAαC	-11,1	-7,7	-0,4	0,1	-9,4	-0,9	-2,5	0,9	0,6	-3,7	5,1	-1,9

Los resultados derivados del estudio de la robustez de los tiempos de retención de los analitos se muestra en las figuras siguientes. En la primera de ellas (Figura 3.4), puede observarse que el tiempo de retención de algunas HAs muestra cierta dependencia con la variación de pH. Este efecto se aprecia más claramente en la gráfica correspondiente al sistema de ácido fórmico (Figura 3.4 b), y la tendencia general es la de eluir más tarde al incrementar el pH. En la siguiente figura (Figura 3.5) se muestran los resultados obtenidos en el estudio de la robustez de los tiempos de retención al alterar la concentración del tampón. La tendencia observada no es clara, y además la variabilidad es en la mayoría de los casos inferior al 1 %. Por lo tanto, puede concluirse que la magnitud de la alteración de la concentración del tampón no parece afectar el tiempo de retención. Para finalizar, la Figura 3.6 muestra los resultados derivados del estudio de robustez con respecto a los tiempos de retención al modificar el porcentaje de acetonitrilo de la fase móvil. Como era de esperar, el tiempo de disminuye al aumentar el contenido de acetonitrilo en la fase móvil, debido a la mayor fuerza elutrópica de la fase móvil.

En resumen, los estudios de precisión muestran que, mientras que los valores de concentración son equivalentes con las dos fases móviles estudiadas, la variabilidad en los tiempos de retención se ve reducida con el uso del tampón basado en ácido fórmico, debido a la mayor capacidad tamponadora de este sistema en el pH de trabajo. Por otro lado, el estudio de la robustez proporcionada por los dos sistemas cromatográficos indica que no existen diferencias en los resultados cuantitativos obtenidos utilizando ambos tampones. En cuanto a los tiempos de retención, éstos se ven afectados en ambos casos por variaciones producidas en el pH y en el contenido de modificador orgánico de la fase móvil. Por lo tanto, la fase móvil de ácido fosfórico puede ser sustituida por la de ácido fórmico, posibilitando de esta manera el acoplamiento entre la cromatografía de líquidos y la espectrometría de masas.

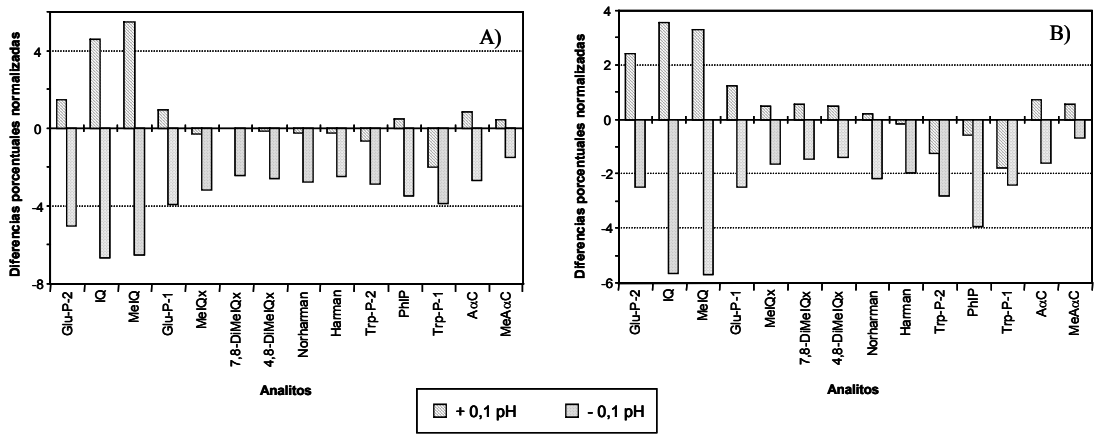

Figura 3.4.- Resultados derivados del estudio de robustez de los tiempos de retención al variar el pH. Sistema A) fosfórico/fosfato y B) fórmico/formiato.

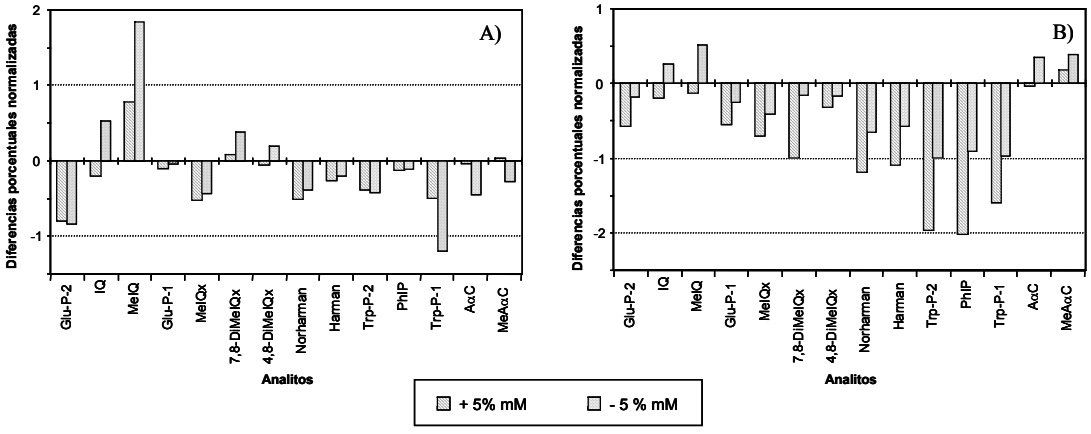

Figura 3.5.- Resultados derivados del estudio de robustez de los tiempos de retención al variar la concentración de tampón. Sistema A) fosfórico/fosfato y B) fórmico/formiato.

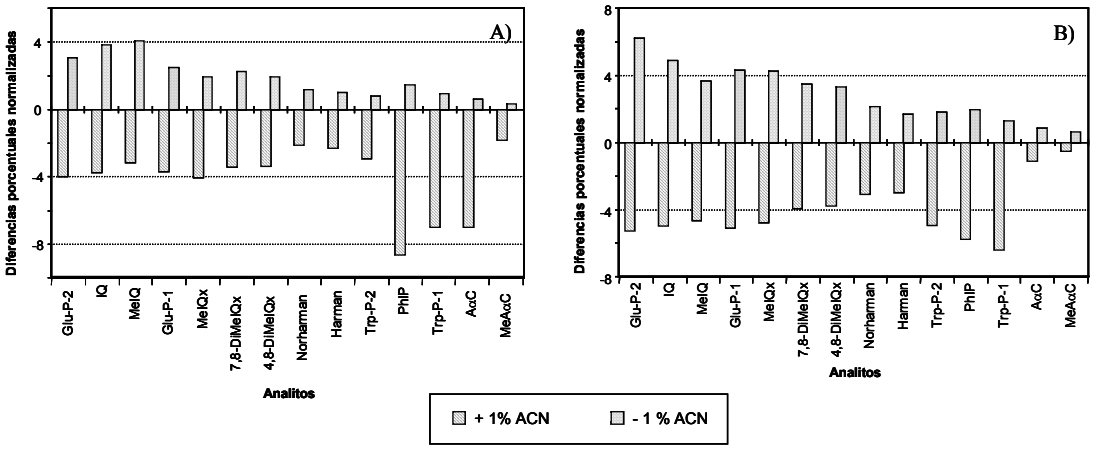

Figura 3.6.- Resultados derivados del estudio de robustez de los tiempos de retención al variar el porcentaje de acetonitrilo de la fase móvil. Sistema A) fosfórico/fosfato y B) fórmico/formiato.

3.2.2.2. **Artículo IV**

Determination of heterocyclic aromatic amines in meat extracts by liquid chromatography-ion trap atmospheric pressure chemical ionization mass spectrometry

F. Toribio, E. Moyano, L. Puignou y M.T. Galceran.

Journal of Chromatography A, 869 (2000) 307-317.

3.2.2.3. **Artículo V**

Multistep mass spectrometry of heterocyclic amines in a quadrupole ion trap mass analyser

F. Toribio, E. Moyano, L. Puignou y M.T. Galceran.

Journal of Mass Spectrometry, 37 (2002) 812-828.

3.2.2.4. **Artículo VI**

Ion-trap tandem mass spectrometry for the determination of heterocyclic amines in food

F. Toribio, E. Moyano, L. Puignou y M.T. Galceran.

Journal of Chromatography A, 948 (2002) 267-281.

3.3. ESPECTROMETRÍA DE MASAS CON UN ANALIZADOR DE TRIPLE CUADRUPOLO

3.3.1. Introducción y objetivos

A diferencia de los espectrómetros de masas de trampa de iones, los analizadores cuadrupolares se han empleado frecuentemente para determinar HAs. Los primeros trabajos publicados utilizaban instrumentos de cuadrupolo sencillo y una fuente de ionización de *termospray* y trabajaban en modo MS (Edmons *et al.*, 1986; Milon *et al.*, 1987; Turesky *et al.*, 1988). Años después, se sustituyó dicha fuente de ionización por la electropulverización (ESI) y la ionización química a presión atmosférica (Johansson *et al.*, 1995; Galceran *et al.*, 1996; Fay *et al.*, 1997; Pais *et al.*, 1997a; Stavric *et al.*, 1997a; Pais *et al.*, 1997b; Stavric *et al.*, 1997b). Más tarde, empezaron a aparecer publicaciones que utilizaban instrumentos de triple cuadrupolo en modo MS/MS (Richling *et al.*, 1996; Holder *et al.*, 1997; Richling *et al.*, 1997; Richling *et al.*, 1998). En la Tabla 1.11 incluida en el Capítulo 1 de esta memoria se incluye una lista exhaustiva de la literatura relacionada con el análisis de HAs utilizando este tipo de metodología analítica.

Aunque la información disponible acerca del análisis de HAs mediante LC-MS es abundante, los resultados no son contrastables debido a diferencias en las condiciones experimentales utilizadas por los distintos autores, como por ejemplo las columnas o fases móviles empleadas en la separación cromatográfica o las muestras analizadas. Por ello, en esta parte del trabajo nos propusimos desarrollar metodología analítica basada en LC-MS y LC-MS/MS en un instrumento de triple cuadrupolo y comparar sus prestaciones con las del espectrómetro de masas de trampa de iones.

El espectrómetro de masas utilizado (Figura 3.7) es un PE Sciex 3000. Al igual que en el caso del instrumento de trampa de iones, la fuente de ionización utilizada fue de ionización química a presión atmosférica. Como puede observarse con mayor detalle en la Figura 3.7 B, la muestra líquida introducida en la sonda se pulveriza con la ayuda de un gas de nebulización y se evapora a continuación con la aplicación de energía térmica. Una vez en fase gas, la muestra es arrastrada hacia la zona de ionización mediante otro gas, el gas auxiliar. En ese punto, se aplica un elevado voltage en un electrodo en forma de aguja que provoca la creación de un plasma reactivo, de manera que la muestra se ioniza por colisión con los iones presentes en dicho plasma.

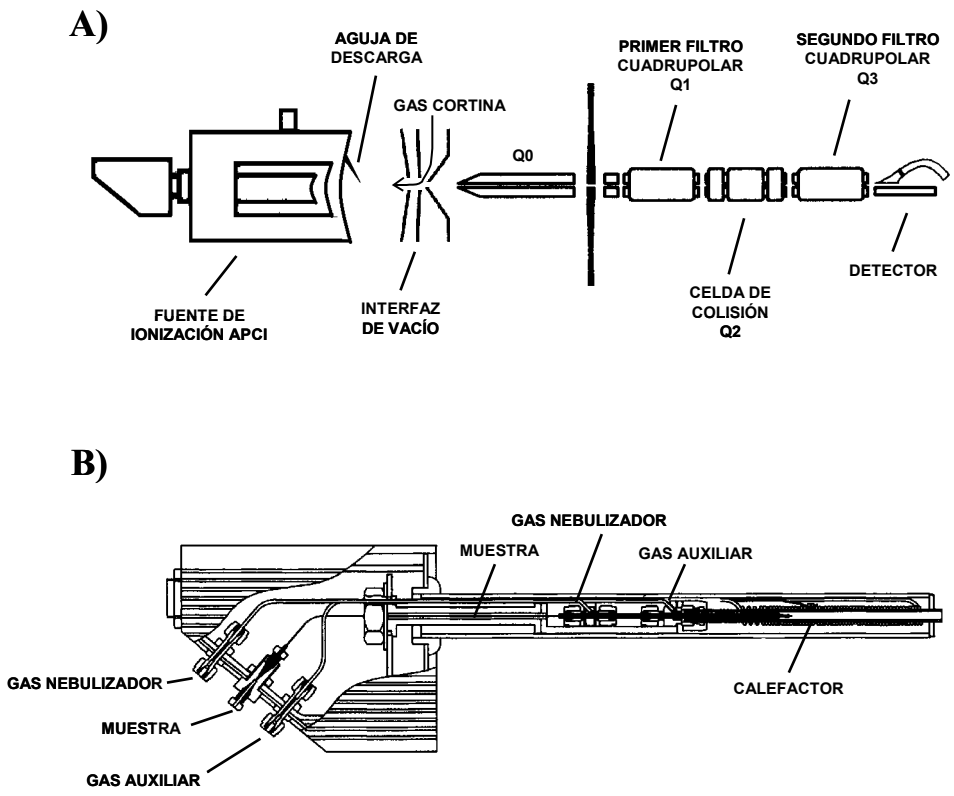

Figura 3.7.- Esquemas correspondientes al instrumento de triple cuadrupolo utilizado. A) Representación general; B) Sonda APCI.

Los iones generados en la fuente de ionización son conducidos a una zona de vacío intermedio ($8x10^{-3}$ torr) a través de un pequeño orificio, el cual está protegido por una cortina de gas inerte que minimiza la entrada de moléculas neutras y contribuye a la ruptura de clústers. La eliminación de aductos está también favorecida por la aplicación de una diferencia de potencial (*declustering potential*). Si dicho voltaje es suficientemente elevado puede provocarse fragmentación, con la consecuente aparición de iones producto. Una vez en la zona de vacío intermedio, los iones deben atravesar un cuadrupolo al que se aplican únicamente radiofrecuencias (Q0) y una lente, tras lo cual entran en la zona de elevado vacío del instrumento. En esta región, además se una serie de lentes se encuentran los dos filtros cuadrupolares (Q1 y Q3) y la cámara de colisión (Q2), consistente en un cuadrupolo al que se aplican únicamente radiofrecuencias. Mientras que Q1 y Q3 son capaces de permitir únicamente el paso de iones con una determinada relación masa/carga, Q2 no tiene propiedades de filtración de iones. Sin embargo, cuando se introduce un gas en su interior éste colisiona con los iones provocando su fragmentación.

Tras atravesar el sistema analizador, los iones finalmente impactan en el detector, produciendo un pulso de electrones que es amplificado por un multiplicador de electrones originando una señal digital.

El trabajo experimental realizado en esta parte del capítulo consistió en primer lugar en el estudio de las principales rutas de fragmentación de los analitos, utilizando para ello los espectros MS, MS/MS así como MS/MS con colisión en la fuente. Los resultados se compararon con los obtenidos en los estudios de espectrometría en tándem múltiple en el instrumento de trampa de iones que se han comentado en el subapartado precedente de este capítulo. A continuación, se estableció metodología analítica LC-MS y LC-MS/MS con el instrumento de triple cuadrupolo y se estudiaron las correspondientes prestaciones. Este trabajo se incluye en el Artículo VII, titulado "*Analysis of heterocyclic amines by liquid chromatography-tandem mass spectrometry: triple quadrupole vs. ion trap*", el cual ha sido enviado para su publicación en la revista *Rapid Communications in Mass Spectrometry*.

3.3.2. Trabajo experimental

Artículo VII

Analysis of heterocyclic amines by liquid chromatography-tandem mass spectrometry: triple quadrupole vs. ion trap

F. Toribio, E. Moyano, L. Puignou y M.T. Galceran.

Enviado para su publicación en: Rapid Communications in Mass Spectrometry (2003)

3.4. DISCUSIÓN DE RESULTADOS

3.4.1. Límites de detección de los métodos LC-MS

En este capítulo, se han establecido las condiciones óptimas de trabajo para analizar las HAs mediante métodos LC-MS y LC-MS/MS, utilizando para ello un instrumento dotado de un analizador de trampa de iones y otro de triple cuadrupolo. Para cada uno de los métodos se han estudiado los límites de detección (LODs), los cuales se recogen en la Tabla 3.8 para cada uno de los analitos en términos absolutos (pg inyectados). A fin de evaluar la mejora que comporta el trabajar con espectrometría de masas, se han incluido además en la citada tabla los LODs obtenidos con el método LC-UV del Apartado 3.2.2.1. Como se puede observar, los valores correspondientes a la detección UV son entre 4 y 650 veces mayores que los obtenidos en espectrometría de masas, dependiendo del modo de trabajo y del instrumento utilizado.

Aunque los LODs obtenidos con el modo de trabajo *fullscan MS* en el instrumento de trampa de iones se encuentran descritos por primera vez en el artículo incluido en el Apartado 3.2.2.2, la incorporación de la DMIP y de analitos trideuterados al análisis así como el reajuste de ciertos parámetros de adquisición nos obligaron a recalcular los LODs en este modo de trabajo. Los valores obtenidos, incluidos en el trabajo del apartado 3.2.2.4, son los mostrados en la Tabla 3.8. Si comparamos los LODs calculados en ambos trabajos, observaremos que en la mayoría de los casos los valores son ligeramente superiores en el último. Este aumento podría ser explicable por el envejecimiento del fotomultiplicador, ya que ambos experimentos se realizaron con una diferencia de dos años.

Al observar los valores mostrados en la Tabla 3.8, puede observarse que en el caso de los métodos LC-MS los valores disminuyen al aumentar el tiempo de retención, debido a que el incremento del porcentaje de acetonitrilo en la fase móvil origina picos más estrechos. Otro hecho destacable es que la mayor selectividad de la espectrometría de masas en tándem permite obtener LODs más bajos. En el caso del instrumento de trampa de iones la mejora en modo MS/MS con respecto al modo MS es de entre 2 y 8 veces, mientras que para el instrumento de triple cuadrupolo los valores disminuyen entre 3 y 24 veces.

Si se comparan los LODs obtenidos con los dos instrumentos, se puede observar que tanto en modo MS como en modo MS/MS los valores obtenidos al utilizar el triple cuadrupolo son entre 2 y 6 veces menores que los correspondientes al instrumento de trampa de iones. Esta diferencia puede ser debida al distinto diseño de la fuente de ionización y especialmente a la existencia del gas cortina en el instrumento de triple cuadrupolo (Figura 3.7 A), que incrementa la eficacia del proceso de desolvatación y minimiza la entrada en el analizador cuadrupolar de especies neutras.

Tabla 3.8.- Límites de detección, expresados como pg inyectados, para los diferentes métodos LC-MS y LC-UV desarrollados.

Analitos	**Límites de detección (pg inyectados)**				
	LC-UV	**Trampa de iones**		**Triple cuadrupolo**	
		Fullscan MS	*Product ion scan*	*SIM*	*MRM*
DMIP	-	358	44	239	10
Glu-P-2	1100	283	45	180	12
IQ	900	235	38	66	10
MeIQ	1500	202	39	57	10
Glu-P-1	1700	259	41	48	10
MeIQx	600	196	24	-[a]	9
7,8-DiMeIQx	500	79	33	65	9
4,8-DiMeIQx	400	66	34	68	8
Norharman	1000	215	64	40	10
Harman	800	158	46	43	8
Trp-P-2	300	62	18	24	8
PhIP	1400	41	16	29	4
Trp-P-1	200	53	12	31	6
AαC	800	40	10	-[a]	4
MeAαC	2000	46	11	15	3

[a] Presencia de un ion interferente.

En la tabla anterior puede observarse la existencia para MeIQx y para AαC de especies interferentes en el modo de trabajo MS con el triple cuadrupolo. La existencia de iones con la misma relación *m/z* que el ion $[M+H]^+$ de los dos analitos mencionados ha producido un aumento de sus LODs (~3500 pg inyectados para MeIQx y ~230 pg inyectados para AαC). El efecto negativo de estos iones interferentes ha podido ser evitado utilizando el modo de trabajo MS/MS, ya que sus principales iones producto son diferentes a los proporcionados por los analitos. A modo de ejemplo, la Figura 3.8 muestra los espectros en *fullscan* MS y en *product ion scan* obtenidos al realizar una infusión de una disolución de MeIQx (~ 7 μg mL^{-1}) con fase móvil, además del espectro en *product ion*

scan obtenido para la interferencia al introducir únicamente fase móvil en el espectrómetro de masas. Se han incluido también en la figura los cromatogramas obtenidos en modo SIM y MRM al inyectar una disolución que contenía MeIQx a un nivel de concentración de ~0,5 μg mL^{-1}.

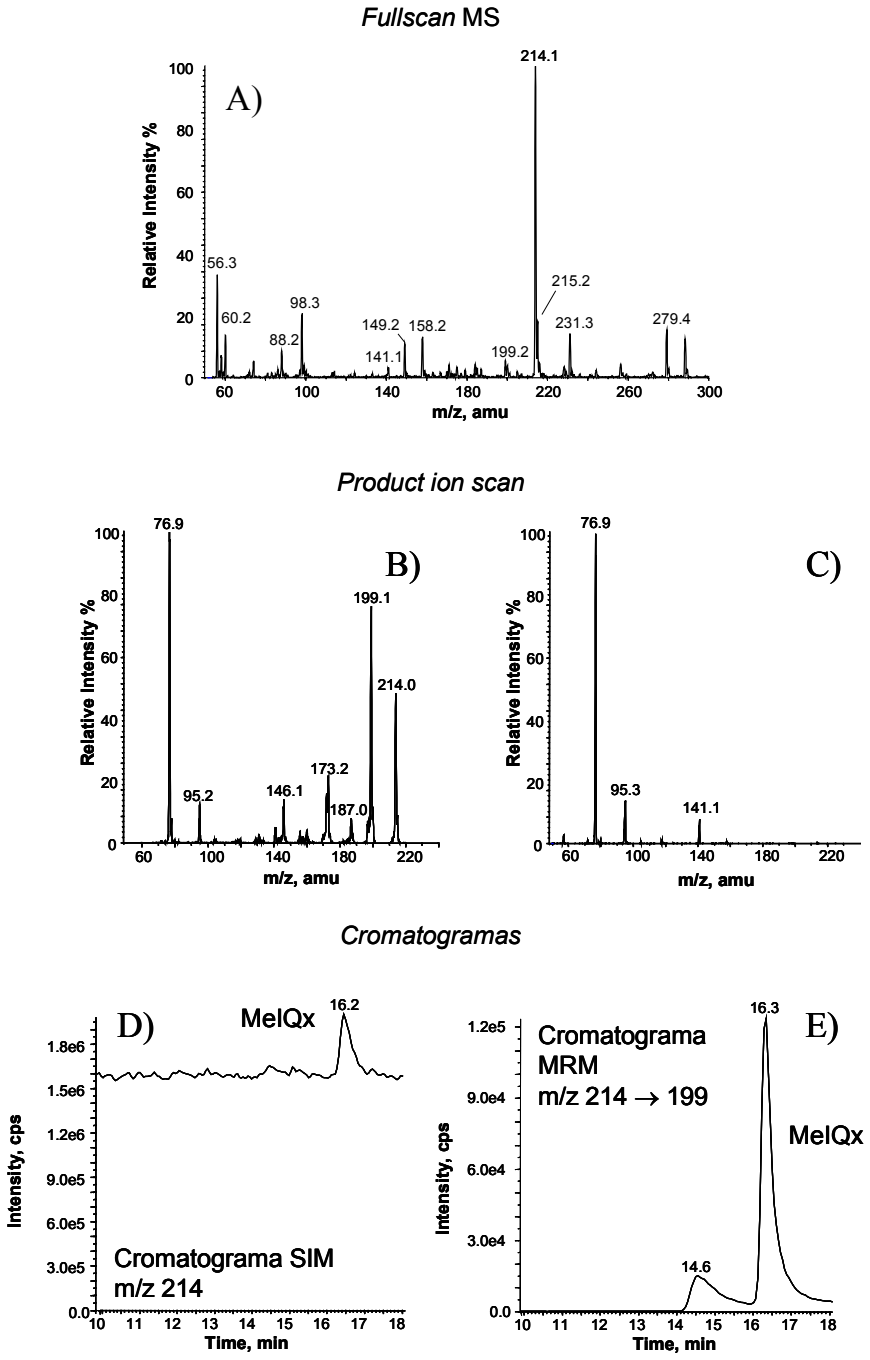

Figura 3.8.- Espectros obtenido en modo A) *fullscan* MS y B) *product ion scan* al infusionar una disolución de MeIQx con fase móvil. El espectro en modo *product ion scan* de la especie interferente se muestra en C). Cromatogramas obtenidos en modo D) SIM y E) MRM al inyectar 15 μL de una disolución de MeIQx a una concentración de ~0,5 μg mL^{-1}. Condiciones experimentales descritas en el Apartado 3.3.2.

Además de con disoluciones estándar, los límites de detección de todos los analitos se han estudiado para muestras de alimentos. Los valores obtenidos en muestras de extracto de carne y de ternera a la plancha, incluidos en los Artículos IV, VI y VII para los diferentes métodos LC-MS, siguen el mismo comportamiento que el observado con patrones. Así, los LODs han sido generalmente más bajos para los analitos con tiempos de retención mayores, el modo tándem ha favorecido la disminución de los LODs y los analitos han podido ser detectados a menores concentraciones con el instrumento de triple cuadrupolo. En resumen, en el caso de extractos de carne los LODs en el intrumento de trampa de iones han sido de 370-4700 pg inyectados (2-10 ng g^{-1} de muestra) en modo *fullscan MS* y de 70-500 pg inyectados (0,4-2 ng g^{-1} de muestra) en modo *product ion scan*. Con el instrumento de triple cuadrupolo, los LODs para esta muestra han sido de 200-1300 pg inyectados (1-12 ng g^{-1} de muestra) en modo SIM y de 10-100 pg inyectados (0,1-0,9 ng g^{-1} de muestra) en modo MRM. Para la ternera a la plancha, las cantidades mínimas detectadas han sido en el instrumento de trampa de iones de 60-700 pg inyectados (0,1-1 ng g^{-1} de muestra) en modo *fullscan MS* y de 30-300 pg inyectados (0,05-0,8 ng g^{-1} de muestra) en modo *product ion scan*, mientras que los valores para el instrumento cuadrupolar fueron de 50-800 pg inyectados (0,1-1,9 ng g^{-1} de muestra) en modo SIM y de 10-40 pg inyectados (0,02-0,09 ng g^{-1} de muestra) en modo MRM. Para DMIP, el límite de detección expresado por gramo de muestra fue muy superior al de las demás HAs por su menor recuperación en el proceso de tratamiento de muestra. Por otro lado, al igual que en el estudio de disoluciones patrón se observó una interferencia importante en el análisis de MeIQx utilizando el instrumento de triple cuadrupolo en modo SIM, con lo que el límite de detección calculado era de ~7000 pg inyectados (~35 ng g^{-1}) para las dos muestras. En el caso de AαC, la interferencia observada en el análisis de disoluciones estándar fue de escasa importancia en el análisis de muestras, ya que los LODs calculados fueron comparables a los de los analitos que eluyen a tiempos de retención parecidos.

En general, los límites de detección en muestra obtenidos en esta memoria no difieren de los valores publicados en la bibliografía, tal y como se puede observar en la Tabla 3.9 donde se han incluido para algunos analitos nuestros resultados y los de algunas referencias. La variabilidad existente entre los valores incluidos en esta tabla es atribuible al tipo de muestra, a la instrumentación utilizada y al tratamiento de muestra aplicado.

Tabla 3.9.- Comparación de los límites de detección en alimentos obtenidos con los métodos LC-MS desarrollados en la memoria y los publicados en la literatura.

Analito	**Límites de detección (ng g^{-1})**					
	Bilbiografía				**Memoria**	
	MS		MS/MS		MS	MS/MS
	ESI	*APCI*	*ESI*	*APCI*		
IQ	3 [1]; 0,2 [2]	0,2 [3]; 1-3 [4]; 0,6 [5]	0,025 [6]	0,1 [7]; 0,015 [8]	0,8-6	0,05-1,4
MeIQx	1,1 [2]	1,0 [3]; 1-3 [4]; 0,6 [5]	0,01 [6]	0,1 [7]; 0,015 [8]	0,5-10	0,09-1,1
4,8-DiMeIQx	0,2 [2]	0,4 [3]	0,05 [6]	0,015 [8]	0,6-5	0,03-0,7
PhIP	3 [1]; 0,3 [2]	1,4 [3]; 1-3 [4]; 0,6 [5]	0,05 [6]	0,1 [7]; 0,015 [8]	0,5-4	0,03-0,4
AαC	6 [1]; 0,1 [2]	0,3 [3]		0,1 [7]	0,2-5	0,02-0,3
Trp-P-1	4 [1]; 0,2 [2]	0,4 [3]; 1-3 [4]; 1,1 [5]			0,7-8	0,09-1,3
Glu-P-1	2,3 [2]	1,4 [3]	0,01 [6]		0,9-8	0,1-3

Artículos incluidos en la Tabla:
[1] (Galceran *et al.*, 1996) [2] (Pais *et al.*, 1997b) [3] (Pais *et al.*, 1997a)
[4] (Stavric *et al.*, 1997b) [5] (Stavric *et al.*, 1997a) [6] (Richling *et al.*, 1998)
[7] (Holder *et al.*, 1997) [8] (Guy *et al.*, 2000)

La comparación de los LODs obtenidos con patrones con los correspondientes a las muestras ha permitido estimar el efecto que ejerce la matriz sobre la señal de los analitos. La Tabla 3.10, donde se recoge la relación entre los LODs obtenidos en muestra con respecto a los correspondientes a disoluciones estándar, indica que la matriz alimentaria produce un incremento en los LODs de hasta 30 veces, dependiendo de la muestra, del analito, del modo de adquisición y del instrumento. Este efecto es más importante para el extracto de carne que para la ternera, debido a su mayor complejidad. Así, por ejemplo, en el instrumento de trampa de iones los LODs para el extracto de carne han aumentado con respecto a los patrones un promedio de 15 veces en el modo *fullscan MS* y 10 veces en el modo *product ion scan*, mientras que para la ternera a la plancha los LODs se han incrementado tan sólo un promedio de 3 veces para el mismo instrumento. También puede observarse que, sobretodo para el extracto de carne, el incremento es mayor en el modo de trabajo MS, debido a su menor selectividad comparado con el modo tándem.

Como se acaba de comentar y como se explicó para disoluciones estándar, la mayor selectividad del modo de trabajo en tándem permite una disminución de los límites de detección con respecto al modo MS. En la Tabla 3.11 se recoge la magnitud de esa mejora para los dos instrumentos utilizados y las dos muestras estudiadas. Como se puede observar, el instrumento de trampa de iones ha permitido una disminución de los LODs entre 3 y 7 veces en función de la muestra, mientras que en el instrumento de triple cuadrupolo la sustitución de la adquisición en SIM por MRM ha supuesto una mejora de entre 5 y 35 veces.

Tabla 3.10.- Incremento de los LODs en muestra con respecto a los calculados para disoluciones estándar.

Analitos	Extracto de carne				Ternera a la plancha			
	Trampa de iones		Triple cuadrupolo		Trampa de iones		Triple cuadrupolo	
	Fullscan MS	*Product ion scan*	*SIM*	*MRM*	*Fullscan MS*	*Product ion scan*	*SIM*	*MRM*
DMIP	13	12	6	12	2	4	3	3
Glu-P-2	12	10	7	10	2	6	4	3
IQ	12	9	9	3	2	6	8	2
MeIQ	15	9	8	4	2	4	12	2
Glu-P-1	15	13	13	12	1	5	9	4
MeIQx	13	14	-[a]	5	1	8	-[a]	4
7,8-DiMeIQx	16	8	10	5	3	5	7	2
4,8-DiMeIQx	19	8	10	4	4	5	6	2
Norharman	7	5	18	3	1	3	11	3
Harman	9	11	16	4	1	3	10	4
Trp-P-2	19	11	18	4	4	4	4	2
PhIP	30	12	24	5	6	2	11	3
Trp-P-1	19	20	16	8	6	3	4	3
AαC	12	7	-[a]	3	2	3	-[a]	3
MeAαC	8	7	11	5	1	3	3	3

[a] Presencia de un ion interferente.

Tabla 3.11.- Relación entre los LODs calculados en modo MS y MS/MS para los dos espectrómetros de masas empleados.

Analitos	Extracto de carne		Ternera a la plancha	
	IT	QqQ	IT	QqQ
DMIP	9	13	4	27
Glu-P-2	7	13	1	23
IQ	7	20	2	25
MeIQ	6	13	3	35
Glu-P-1	5	6	2	13
MeIQx	7	-[a]	1	-[a]
7,8-DiMeIQx	7	18	2	25
4,8-DiMeIQx	7	23	2	20
Norharman	5	23	1	13
Harman	4	18	1	10
Trp-P-2	7	13	3	5
PhIP	10	35	7	30
Trp-P-1	5	10	8	5
AαC	11	30	2	20
MeAαC	7	10	2	5

[a] Presencia de un ion interferente en el modo de adquisición SIM.

Por otro lado, si comparamos los valores obtenidos utilizando los dos instrumentos (Tabla 3.12) se puede constatar que, tanto para el extracto de carne como para la ternera a la plancha, los LODs en modo MS son similares. En cambio, el trabajar en modo tándem

en el triple cuadrupolo supone con respecto al instrumento de trampa de iones una mejora que puede llegar a ser de 7 veces para el extracto de carne y de hasta 12 veces para la ternera a la plancha. Así, los menores LODs han sido proporcionados por el método LC-MS/MS utilizando el instrumento de triple cuadrupolo, pudiéndose detectar niveles de hasta 10 pg inyectados (0,2 ng g^{-1}). Por lo tanto, esta metodología es la más indicada para la determinación de HAs a niveles de concentración muy bajos. Sin embargo, si la concentración lo permite, el uso de un instrumento de tampa de iones tiene la ventaja de confirmar la identidad de los analitos sin pérdida de señal, como se mostró en la Figura 6 del artículo incluido en el apartado 3.2.2.4 para las HAs cercanas al su límite de detección.

Tabla 3.12.- Relación entre los LODs calculados con el instrumento de trampa iónica y el de triple cuadrupolo para las dos muestras analizadas.

Analitos	**Extracto de carne**		**Ternera a la plancha**	
	MS	MS/MS	MS	MS/MS
DMIP	2	3	1	7
Glu-P-2	1	3	1	7
IQ	2	7	1	12
MeIQ	1	4	1	8
Glu-P-1	1	3	1	5
MeIQx	1	4	-[a]	5
7,8-DiMeIQx	1	3	1	8
4,8-DiMeIQx	1	4	1	10
Norharman	0,5	3	0,5	5
Harman	0,5	2	0,5	4
Trp-P-2	1	3	3	5
PhIP	1	4	1	2
Trp-P-1	1	2	2	2
AαC	2	3	0,3	2
MeAαC	2	3	1	3

[a] Presencia de un ion interferente en el instrumento de triple cuadrupolo.

3.4.2. Comparación de los métodos LC-UV y LC-MS

En este capítulo de la memoria, se ha utilizado la metodología LC-MS para analizar un extracto de carne, muestra que había sido utilizada a su vez en el Capítulo 2 para evaluar el método LC-UV presentado en ese capítulo. Esta muestra, que contiene IQ, MeIQx, 4,8-DiMeIQx y PhIP a un nivel de concentración de 10-40 ng g^{-1}, se ha purificado en ambos casos utilizando el método de tratamiento de muestra desarrollado en el Capítulo 2, que mediante el uso de un cartucho de intercambio iónico en forma ácida consigue

reunir todos los analitos en un único extracto. En la Figura 3.9 se muestran los resultados del análisis empleando los métodos LC-MS y LC-MS/MS en el instrumento de trampa de iones (Apartados 3.2.2.2 y 3.2.2.4, respectivamente). Además, se han incluido en esta figura los resultados obtenidos en el Capítulo 2 de esta memoria utilizando LC-UV para la determinación (Apartado 2.2.2.3).

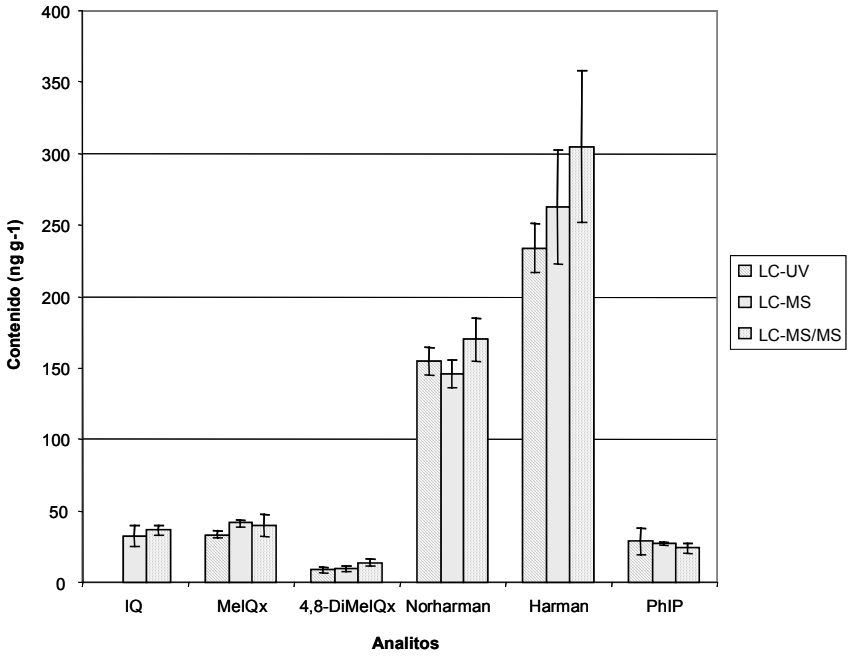

Figura 3.9.- Comparación de los resultados obtenidos en la cuantificación de un extracto de carne liofilizado utilizando algunos de los métodos establecidos en la memoria. Las condiciones experimentales del sistema LC-UV se encuentran en el apartado 2.2.2.3, las del método LC-MS en el apartado 3.2.2.2 y las de LC-MS/MS en el apartado 3.2.2.4.

Como puede observarse en la figura anterior, tanto las desviaciones estándar como las concentraciones de las HAs en la muestra obtenidas con los diferentes métodos de determinación son equivalentes. Sin embargo, hay que destacar que dada la menor selectividad del sistema de detección por UV los límites de detección de esta técnica son considerablemente superiores a los de los métodos LC-MS. Además, no se ha podido cuantificar IQ con el método LC-UV debido a la coelución con una interferencia, y se han cuantificado algunas HAs cuya identidad no ha podido ser confirmada. En cambio, los métodos LC-MS han permitido determinar el contenido de IQ en la muestra y han confirmado la ausencia de MeIQ y Glu-P-1 en la muestra a valores de concentración superiores al límite de detección. Además, se ha detectado la Trp-P-1 a un nivel cercano al límite de detección del método LC-MS/MS(IT) (~ 1 ng g^{-1}).

3.4.3. Estudios de fragmentación de las HAs

Con el objetivo de poder identificar nuevas HAs en muestras de alimentos, en este capítulo se han intentado establecer los modelos de fragmentación característicos de estos compuestos, utilizando para ello un analizador de trampa de iones que permite llevar a cabo experimentos de espectrometría de masas en tándem múltiple (MS^n). Así, en primer lugar se han estudiado los espectros MS/MS, y gracias a la información complementaria proporcionada por algunos analitos marcados isotópicamente se ha identificado el origen de los principales iones producto. Se ha observado una fragmentación diferente para las dos familias de HAs. Así, los aminoimidazoazaarenos (AIAs) presentan un pico base derivado de la pérdida del metilo unido a uno de los nitrógenos del anillo aminoimidazólico, aunque se ha observado también la pérdida del grupo amino primario y la ruptura de la estructura imidazólica, lo que ha originado pérdidas de C_2NH_3, CN_2H_2 y $C_3N_2H_4$. Las quinoxalinas también se rompen por la pirazina, con pérdidas de HCN o CH_3CN según el compuesto. En cambio, la fragmentación de las carbolinas está caracterizada por la pérdida del grupo amino primario para α-, γ- y δ-carbolinas. El carbocatión generado es altamente electrodeficiente, ya que la carga positiva queda localizada en la posición α del nitrógeno piridínico. Por este motivo, se produce un ataque nucleófilo por parte de moléculas neutras presentes en la trampa de iones, como agua o acetonitrilo, como se demostró en el trabajo incluido en el apartado 3.2.2.3. Otros fragmentos importantes en los espectros MS/MS de las carbolinas son los derivados de la pérdida de un grupo metilo para MeAαC, harman y Glu-P-1, y de la ruptura de los heterociclos con pérdidas de HCN.

Posteriormente y a fin de comparar los procesos de fragmentación se realizaron experimentos MS/MS utilizando un instrumento con un analizador de triple cuadrupolo. En general, la fragmentación observada ha sido similar en los dos instrumentos empleados en el estudio. En la Figura 3.10 se resumen algunas de las fragmentaciones más típicas observadas en los espectros MS/MS de las HAs en los instrumentos de trampa de iones y de triple cuadrupolo.

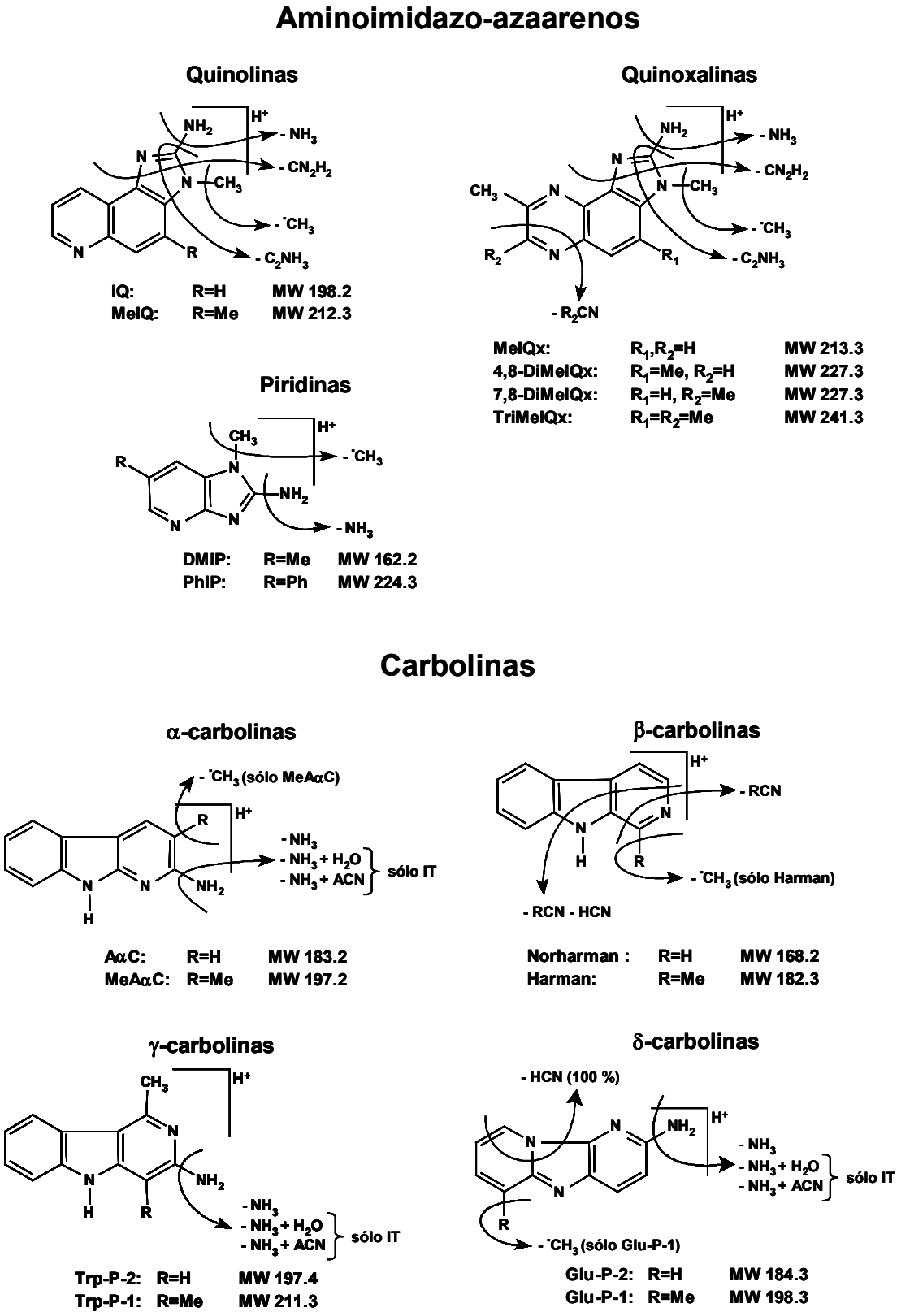

Figura 3.10.- Origen de los principales iones producto existentes en los espectros MS/MS de las HAs.

A pesar de la similitud de los espectros MS/MS obtenidos con los dos instrumentos estudiados, el diferente mecanismo de fragmentación en la trampa de iones y en la cámara de colisión del triple cuadrupolo ha originado algunas diferencias destacables. Por ejemplo, se ha observado un aumento en la abundancia de algunos iones en los espectros de masas obtenidos con el triple cuadrupolo, o incluso en algunos casos han aparecido iones no observados en el instrumento de trampa de iones. El estudio de los espectros de masas en tándem múltiple proporcionados por la trampa de iones y de las curvas de energía de colisión correspondientes al triple cuadrupolo ha revelado que el aumento de la abundancia de algunos iones producto en los espectros MS/MS de las HAs en el triple cuadrupolo se debe a la existencia de colisiones múltiples en la cámara de colisión, lo que provoca la fragmentación secuencial del ion precursor antes de llegar al tercer cuadrupolo. En la Figura 3.11 se muestran a modo de ejemplo los espectros MS/MS obtenidos en la trampa de iones y en el triple cuadrupolo para la 4,8-DiMeIQx. Puede observarse que las principales diferencias entre los dos espectros son la menor abundancia en el triple cuadrupolo de los iones derivados de la pérdida de NH_3 y de C_2NH_3 (*m/z* 211 y 187, respectivamente), el incremento en el mismo instrumento de la abundancia del ion m/z 160 ($-C_3N_2H_4$) así como la aparición de un ion a *m/z* 212 en el espectro MS/MS del triple cuadrupolo. Los estudios de tándem múltiple realizados con el instrumento de trampa de iones indican que este último ion está originado por la perdida de un radical hidrógeno a partir del ion *m/z* 213. Esta afirmación se puede corroborar si se estudian las curvas de energía de colisión obtenidas en el triple cuadrupolo para la 4,8-DiMeIQx, ya que la diferente posición de los máximos de las curvas de los iones *m/z* 213 y *m/z* 212 sugieren que este último ion puede provenir de la ruptura del primero. De igual manera, el incremento de la abundancia del ion m/z 160 en el espectro MS/MS del triple cuadrupolo podría explicarse por la fragmentación del ion m/z 187, lo que también justificaría la menor abundancia de este ion.

Otra de las diferencias destacables entre los espectros de masas obtenidos en los dos instrumentos es que en el triple cuadrupolo no se ha observado la formación de los aductos de los iones $[M+H-NH_3]^+$ de las carbolinas con moléculas neutras. Estos aductos, formados en la trampa de iones, son tan importantes que incluso constituyen el pico base en los espectros MS/MS de algunos analitos, tal y como se aprecia en la Figura 3.12 donde se muestran los espectros MS/MS de la MeAαC.

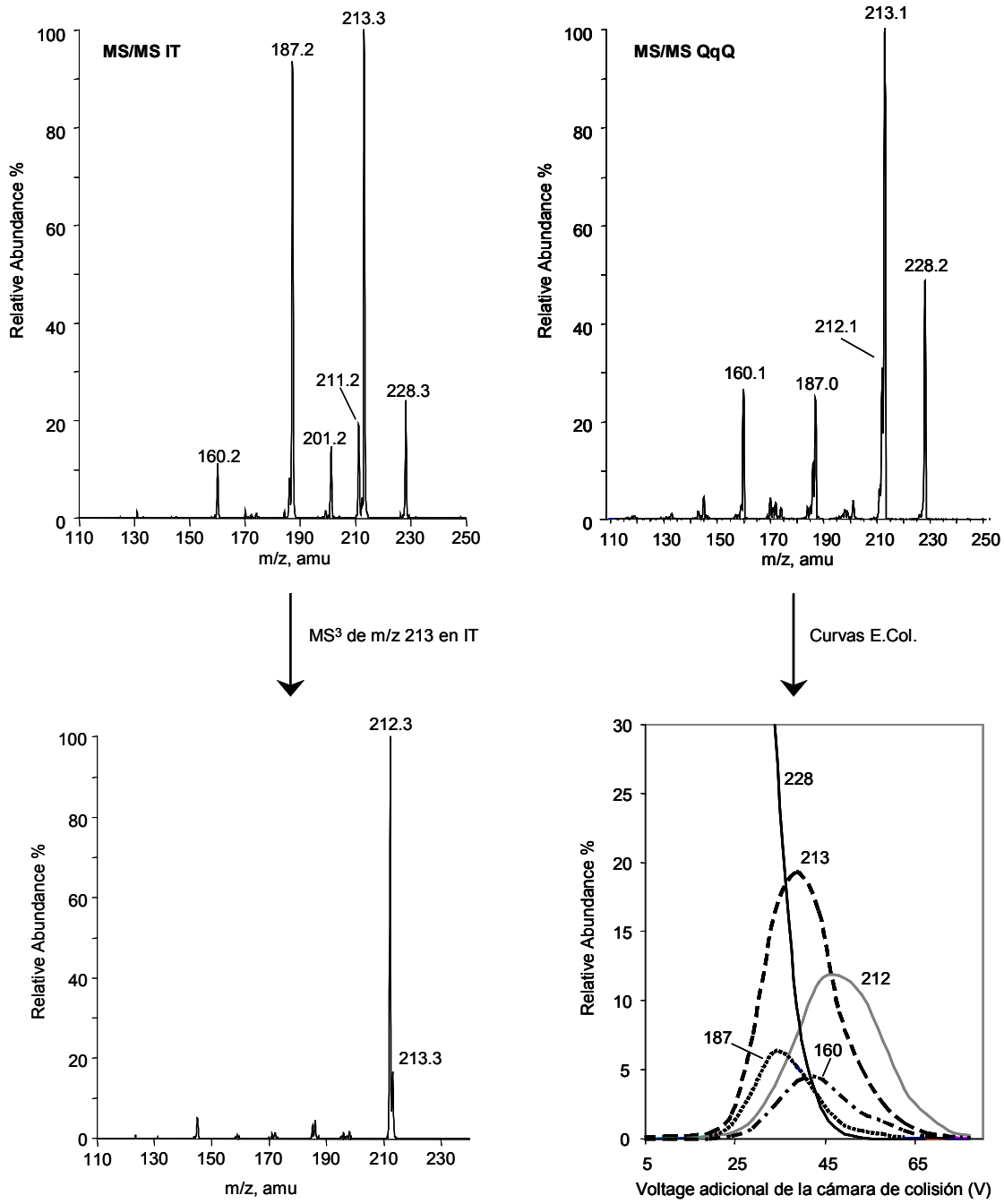

Figura 3.11.- Espectros MS/MS de la 4,8-DiMeIQx obtenidos con los instrumentos de trampa de iones y de triple cuadrupolo. Justificación de la aparición del ion *m/z* 212 en el espectro obtenido con el triple cuadrupolo a partir de la fragmentación del ion *m/z* 213.

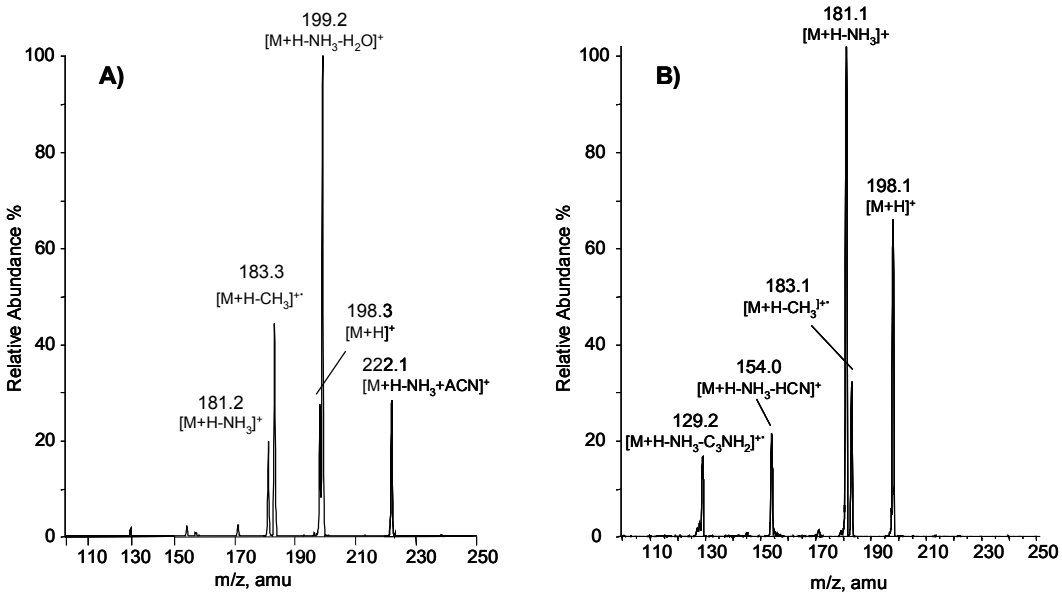

Figura 3.12.- Espectros en tándem de MeAαC en el instrumento de A) trampa de iones y B) triple cuadrupolo.

Una vez conocidas las fragmentaciones típicas de las HAs en MS/MS, se han estudiado las rutas de fragmentación seguidas por cada uno de los analitos. Para ello, se ha utilizado principalmente la información obtenida por espectrometría de masas en tándem múltiple (MS^n) en el instrumento de trampa de iones, información que se ha complementado con el estudio de analitos marcados isotópicamente. Además, se ha utilizado la espectrometría de masas en tándem con fragmentación en la fuente en un triple cuadrupolo con el fin de obtener resultados complementarios a los obtenidos en el instrumento de trampa de iones. Como resultado de la interpretación de toda la información disponible, se han podido establecer las principales rutas de fragmentación de los analitos, las cuales se muestran en las Figuras 3.13 y 3.14. En el caso de los AIAs (Figura 3.13), la ruta comienza principalmente con la pérdida de CH_3 o de C_2NH_3 provenientes del anillo aminoimidazólico. A continuación, se produce la rotura del heterociclo piridina para las quinolinas o pirazina para las quinoxalinas, lo que da lugar a pérdidas de HCN o CH_3CN. En el caso de DMIP o de las quinolinas y quinoxalinas con un grupo metilo unido al carbono 4 de la molécula (MeIQ, 4,8-DiMeIQx, TriMeIQx) se observa seguidamente la pérdida de un radical hidrógeno. Como se muestra además en la figura, las principales diferencias entre los dos instrumentos utilizados están relacionadas con la abundancia relativa de algunos fragmentos.

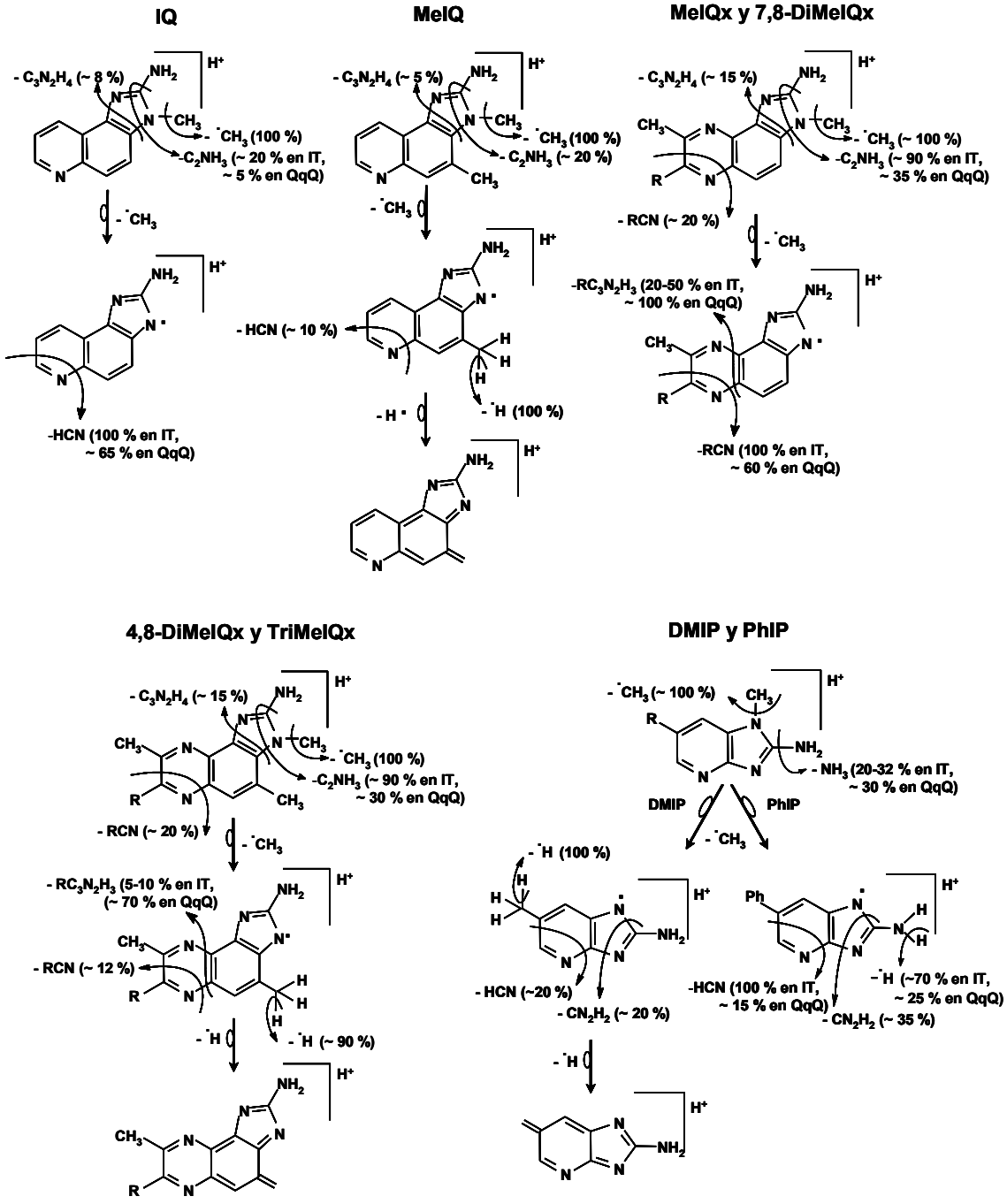

Figura 3.13.- Principales rutas de fragmentación seguidas por los AIAs en un analizador de trampa de iones y otro de triple cuadrupolo.

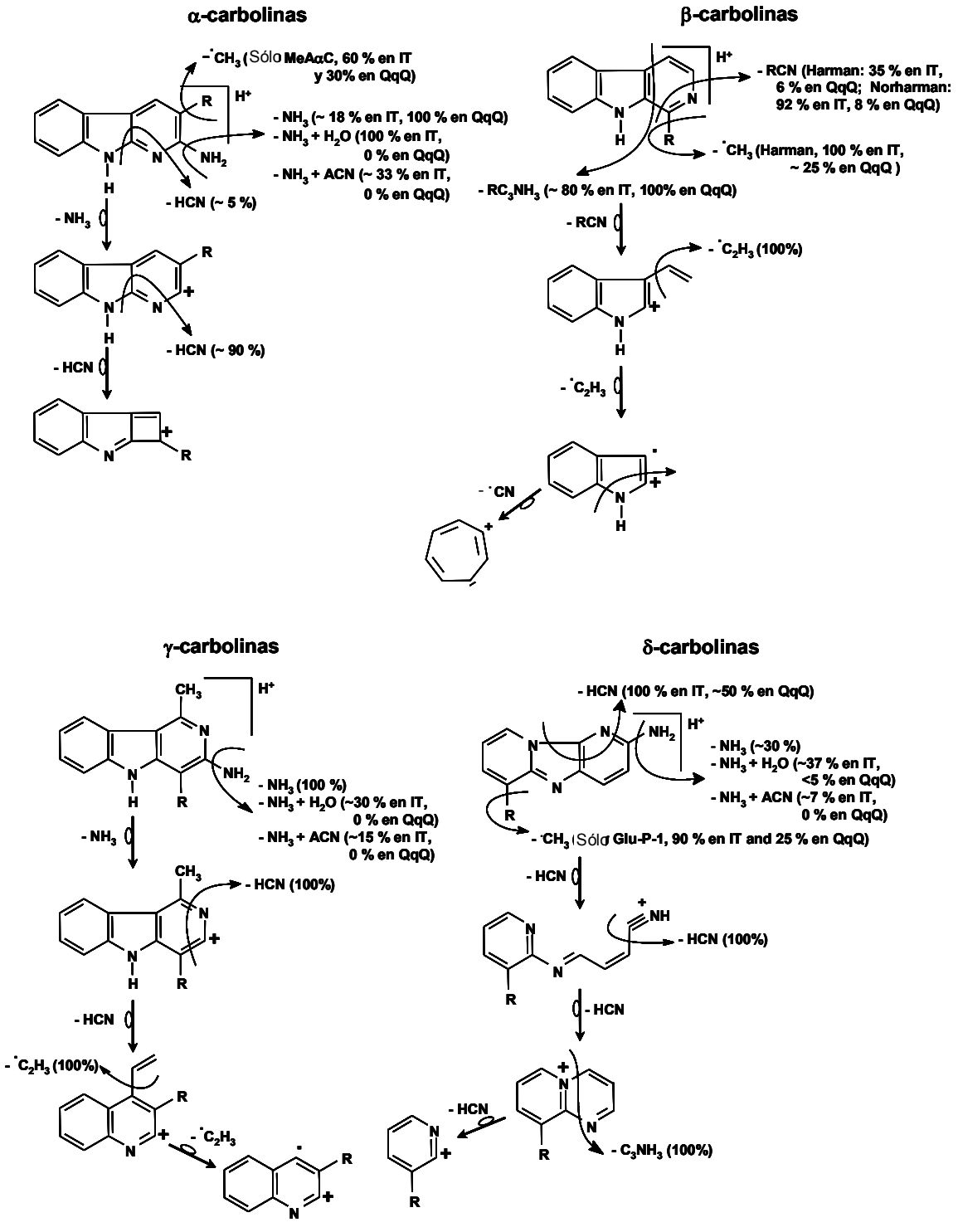

Figura 3.14.- Principales rutas de fragmentación propuestas para las carbolinas en un analizador de trampa de iones y otro de triple cuadrupolo.

En el caso de las β-carbolinas, la ruta de fragmentación consiste principalmente en pérdidas de radicales hidrógeno y en la ruptura de los heterociclos piridina y pirrol, tal como se muestra en la Figura 3.14. Para las α-, γ- y δ-carbolinas, la ruta de fragmentación se inicia con la pérdida del grupo amino primario del anillo piridínico. A continuación, en el analizador de trampa de iones se forman aductos del ion $[M+H-NH_3]^+$ con moléculas de disolvente (agua o acetonitrilo). La formación de estos aductos dificulta el seguimiento del proceso de fragmentación, ya que en los experimentos de MS^3 y MS^4 se observan mayoritariamente intercambios o pérdidas de moléculas de disolvente (Figura 6 del Artículo V). En cambio, la realización de experimentos de masas en tándem con fragmentación en la fuente en el triple cuadrupolo ha permitido obtener información adicional. Así, tras la pérdida del grupo amino primario, las α-, γ- y δ-carbolinas presentan la ruptura de los heterociclos, con pérdidas de ácido cianhídrico principalmente.

3.5. CONCLUSIONES

El trabajo experimental incluido en el Capítulo 3 de la memoria nos ha permitido llegar a las siguientes conclusiones:

- Ha sido necesario adaptar las características de separación cromatográfica utilizada con anterioridad a los requerimientos del sistema de detección por espectrometría de masas.
  - Las condiciones óptimas de separación han consistido en un sistema de elución por gradiente en fase invertida utilizando dos tampones acuosos de ácido fórmico/formiato de amonio a pH 3,25 y pH 3,7 y acetonitrilo como modificador orgánico y una columna de C18. Se ha eliminado la trietilamina de la fase móvil debido al importante efecto de supresión iónica producido en la fuente de ionización en modo positivo.
  - Además de proporcionar resultados cuantitativos equivalentes a los obtenidos con tampones ácido fosfórico/fosfato tradicionalmente utilizados en la bibliografía para métodos LC-UV, el tampón basado en ácido fórmico posee una mayor capacidad reguladora en el pH de trabajo.

- El uso de un espectrómetro de masas con analizador de trampa de iones ha permitido el establecimiento de un método LC-MS con características adecuadas para el análisis de HAs en muestras de alimentos.
  - La utilización de una fuente de ionización química a presión atmosférica ha posibilitado el acoplamiento directo entre una columna de LC convencional que trabaja a 1 mL min^{-1} y el sistema espectrométrico.
  - La formación de los iones en la fuente de ionización ha sido óptima en las siguientes condiciones: potencial aplicado a la aguja 5 kV, temperatura del *heated capillary* 150ºC y de vaporización 450ºC. Se ha utilizado nitrógeno como gas envolvente (72 L h^{-1}) y auxiliar (360 L h^{-1}).
  - La estable estructura de las HAs y sus propiedades básicas han posibilitado una elevada abundancia de iones $[M+H]^+$, que son adecuados para la cuantificación

por LC-MS. Con el fin cuantificar todas las HAs, se han registrado los iones entre *m/z* 150 y 250.

- La precisión presentada del método ha sido aceptable, ya que para el cálculo de concentración los valores de RSD han sido siempre inferiores al 11 %.
- Los límites de detección calculados para disoluciones patrón han sido de 27-360 pg inyectados (1,8-24 ng mL^{-1}), valores que son hasta 43 veces inferiores a los calculados para LC-UV. Los valores son similares a los descritos en la bibliografía para otros métodos LC-MS y para LC-ED.
- La matriz de las muestras alimentarias ha mostrado un fuerte efecto sobre los límites de detección, los cuales han aumentado hasta 60-4700 pg inyectados (0,1-10 ng g^{-1} de alimento). El aumento ha sido mayor cuanto más compleja ha sido la muestra.
- Los bajos LODs en muestra alcanzados con la detección MS han permitido cuantificar las HAs presentes en un extracto de carne liofilizado utilizando para su purificación el método simplificado desarrollado en el Capítulo 2 de la memoria.

- Se han establecido los modelos de fragmentación de las HAs mediante espectrometría de masas en tándem múltiple (MS^n) en un analizador de trampa de iones y se ha observado un diferente comportamiento entre AIAs y carbolinas.
  - Al utilizar el ion $[M+H]^+$ de los AIAs como ion precursor se ha obtenido como principal ion producto el derivado de la pérdida del grupo metilo unido a nitrógeno. Otros iones producto en el espectro MS/MS característicos de los AIAs han sido los derivados de la pérdida de NH_3, de C_2NH_3, de CN_2H_2 y de $C_3N_2H_4$ del anillo imidazólico. Las quinoxalinas han presentado también en el espectro MS/MS una elevada abundancia de iones originados por la pérdida de HCN y CH_3CN entre otros, provenientes de la fragmentación de la pirazina. Al realizar experimentos de MS^3 utilizando el ion $[M+H-CH_3]^{+\bullet}$ como precursor se ha observado principalmente la rotura de los heterociclos, con pérdidas de HCN y/o CH_3CN. Para los compuestos con un grupo metilo unido al carbono 4 u 8 de la molécula, se ha observado también la pérdida de un radical hidrógeno.

- El estudio de los espectros MS/MS de IQ y MeIQx trideuteradas ha permitido observar la existencia de un proceso de intercambio hidrógeno-deuterio, explicable por un proceso reversible de ciclación que incluye el metilo en un anillo de seis átomos.
- Los iones producto principales de las carbolinas han sido los derivados de la pérdida del grupo amino primario, excepto para las β-carbolinas. Debido a la elevada reactividad del ion $[M+H-NH_3]^+$, se ha observado a continuación el ataque nucleófilo de moléculas neutras presentes en el analizador, como agua o acetonitrilo. Las carbolinas metiladas (MeAαC, harman y Glu-P-1) han presentado además la pérdida del grupo metilo, y se ha observado también en los espectros MS/MS iones productos originados por la ruptura de los heterociclos. Los experimentos de mayor orden de fragmentación indican la continuación de la ruptura de los heterociclos, con pérdidas entre otros de HCN y/o CH_3CN.

▪ El espectrómetro de masas con analizador de trampa de iones ha sido utilizado para establecer un método LC-MS/MS, el cual ha demostrado poseer una elevada selectividad.

- Aunque las condiciones cromatográficas y las de la fuente de ionización han sido las mismas que las del método LC-MS, ha sido necesario optimizar los parámetros que influyen en la fragmentación de los iones precursor y en el análisis de los iones producto originados. Se ha fijado el parámetro Q de activación en 0,45, el tiempo de activación en 30 ms y se ha utilizado una energía de colisión normalizada de 36,3-43,6 %. Se ha realizado el registro de los iones producto de cada analito, y la cuantificación se ha llevado a cabo utilizando los más intensos. En el caso de las carbolinas que presentan reacciones ion-molécula, la robustez de la cuantificación se ha aumentado empleando tanto el ion $[M+H-NH_3]^+$ como sus aductos con agua o acetonitrilo, independientemente de su abundancia.
- Aunque los valores de precisión obtenidos en LC-MS/MS han sido muy similares a los correspondientes al método LC-MS, la mayor selectividad de la espectrometría de masas en tándem ha permitido disminuir los límites de detección. En el caso de disoluciones patrón, se han detectado las HAs en

MS/MS a partir de 10-64 pg inyectados (0,7-4 ng mL^{-1}), lo que supone una reducción de hasta 8 veces con respecto a MS.

- Aunque el efecto de la matriz es algo menor en la espectrometría de masas en tándem, los límites de detección en muestra obtenidos en el análisis de alimentos mediante LC-MS/MS han sido un promedio de 10 veces superiores a los calculados para disoluciones estándar. Así, se han detectado las HAs en muestras a partir de 30-500 pg inyectados (0,05-2 ng g^{-1}), valores que son hasta 11 veces más pequeños que los calculados con el método LC-MS.
- Como el espectro MS de las HAs consiste básicamente en el ion $[M+H]^+$, una ventaja adicional del método LC-MS/MS radica en la posibilidad de obtener el espectro de masas de iones producto para cada pico cromatográfico. La comparación de este espectro con el correspondiente a un patrón permite la identificación de los analitos, lo cual es fundamental en el análisis de muestras tan complejas como las alimentarias.

▪ El uso de un espectrómetro de masas con analizador de triple cuadrupolo para desarrollar métodos LC-MS ha permitido detectar los analitos a niveles más bajos que con el instrumento de trampa de iones.

- Las condiciones cromatográficas utilizadas para separar las HAs han sido las mismas que con el instrumenmto de trampa de iones. En cambio, ha sido necesario establecer las condiciones óptimas de formación y fragmentación de los iones. Se ha utilizado nitrógeno como gas de nebulización y como gas cortina a 11 y 14 unidades arbitrarias, respectivamente. La corriente aplicada al electrodo de aguja ha sido de 3,5 μA, la temperatura de vaporización ha sido de 460ºC y el potencial de desolvatación (*declustering potential*) se ha fijado en 30 V. La fragmentación de los iones ha tenido lugar en la cámara de colisión utilizando como gas de colisión nitrógeno a una presión de 6 unidades arbitrarias y fijando un potencial adicional de 35-49 V dependiendo del compuesto.
- En el método LC-MS, la cuantificación se ha realizando registrando únicamente los iones $[M+H]^+$ (modo SIM), durante 0,5 s por cada analito. En el análisis por LC-MS/MS, se han monitorizado las transiciones entre el ion $[M+H]^+$ y el ion producto más abundante (modo MRM), durante 0,5 s para cada compuesto. Para

los AIAs, el pico base de los espectros MS/MS ha sido el ion $[M+H-CH_3]^{+\bullet}$, mientras que para las α-, γ- y δ-carbolinas ha sido el ion $[M+H-NH_3]^+$. En el caso de las β-carbolinas, el ion producto elegido ha sido el *m/z* 115.

- Aunque en términos de precisión el instrumento de triple cuadrupolo ha proporcionado resultados equivalentes a los del instrumento de trampa de iones, los límites de detección alcanzados han sido mejores. Así, en el modo SIM los LODs para disoluciones estándar han sido de 15-240 pg inyectados (1-16 ng mL^{-1}) y en el modo MRM de 3-12 pg inyectados (0,2-0,8 ng mL^{-1}). Al igual que en el instrumento de trampa de iones, los LODs en muestra han sido algo mayores. En modo SIM los analitos se han detectado por encima de 47-1300 pg inyectados (0,1-12 n g^{-1}), mientras que en el modo MRM los LODs han sido de 10-120 pg inyectados (0,02-0,9 n g^{-1}). A pesar de los menores límites de detección alcanzados con el instrumento de triple cuadrupolo, este instrumento únicamente permite confirmar la identidad de un compuesto mediante el registro de más de un ion producto, lo que supone una pérdida en la señal.

▪ El estudio de los espectros de masas originados en un triple cuadrupolo ha permitido obtener información relacionada con la fragmentación de las HAs comparable a la correspondiente a un instrumento de trampa de iones.

- El estudio de los espectros MS, MS/MS y MS/MS con colisión inducida en la fuente ha permitido establecer los patrones de fragmentación típicos en el analizador de triple cuadrupolo. El comportamiento de las HAs en este sistema ha sido muy similar al observado en el instrumento de trampa de iones, ya que en general los iones producto obtenidos fueron los mismos. Sin embargo, hay que tener presente que los espectros generados mediante experimentos MS/MS con colisión inducida en la fuente son más difíciles de interpretar que los espectros MS^n en un analizador de trampa de iones, ya que los fragmentos pueden haber sido originados por diversos mecanismos.
- Se ha observado en ciertos casos un aumento de la abundancia relativa de algunos fragmentos o incluso la aparición de iones producto no observados previamente en el analizador de trampa de iones. Esta mayor fragmentación en

el analizador de triple cuadrupolo es atribuible al diferente mecanismo de fragmentación utilizado en los dos instrumentos.

- Otra diferencia destacable entre los espectros de masas obtenidos con los dos instrumentos fue la ausencia de aductos de las carbolinas con moléculas neutras al emplear el analizador cuadrupolar. De esta manera ha sido posible la obtención de información adicional a la de la trampa de iones, ya que la abundancia relativa de los demás iones producto ha aumentado. Sin embargo, al no disponerse de carbolinas marcadas isotópicamente no ha sido posible la confirmación de las rutas de fragmentación propuestas.

ELSEVIER

Journal of Chromatography A, 869 (2000) 307–317

JOURNAL OF CHROMATOGRAPHY A

www.elsevier.com/locate/chroma

Determination of heterocyclic aromatic amines in meat extracts by liquid chromatography–ion-trap atmospheric pressure chemical ionization mass spectrometry

F. Toribio, E. Moyano, L. Puignou*, M.T. Galceran

Departament de Química Analítica, Universitat de Barcelona, Diagonal 647, 08028 Barcelona, Spain

Abstract

When protein-rich foods are processed under normal cooking conditions, heterocyclic aromatic amines (HAAs) can be generated at a few parts per billion level. In this work, we have analyzed the HAAs present in a lyophilized meat extract by means of a simplified solid-phase extraction procedure. All the analytes were collected in a single extract with recoveries in the range of 45.6–75.2%, so the analysis time has been greatly reduced. Problems derived from the less exhaustive purification of the extract have been solved by using MS(ion trap) detection. The RSD for quantification ranged from 2.1% to 5.1% for run-to-run precision and from 5.2% to 11% for day-to-day precision. The limits of detection for standard solutions ranged from 20 to 150 pg injected. For the meat extract analyzed limits of detection from 0.9 to 11.2 ng g^{-1} were obtained. Results of the quantification are in agreement with those obtained using different clean-up procedures.

Keywords: Food analysis; Amines; Heterocyclic aromatic compounds

1. Introduction

Heterocyclic aromatic amines (HAAs) are a group of basic compounds to which humans are regularly exposed from diet, since they are produced in trace quantities (ng g^{-1} level) when proteinaceous foods, such as meat and fish, are processed by typical cooking practices [1–3]. Previous studies have shown that meat extracts, some beef flavours [4–6] and other matrices including wine, beer and environmental samples also contain HAAs [7–9].

These chemicals constitute a major health risk due to their potent mutagenic activity [10,11]. To date, more than 20 HAAs have been isolated as mutagens, and the structure of 19 of them have been elucidated [12]. The ten HAAs so far examined in animals have proved to be tumourigenic in standard animal experiments, with target organs including lung, liver, mammary gland, colon and skin [13,14]. In addition, several epidemiological studies have revealed a positive association between consumption of cooked meat and fish and risk of colorectal cancer development [15,16], and they also suggest a relationship between methods of cooking meat and various cancers [17,18].

To assess potential health risks associated with the consumption of HAAs, it is of vital importance that their occurrence should be monitored by reliable quantitative methods. A major drawback in the analysis of these mutagens from foods is their very low level of concentration (0.1–50 ng g^{-1}) and the high number of matrix interferences. So, many purification techniques based on liquid–liquid

*Corresponding author. Fax: +34-3-402-1233.
E-mail address: puignou@zeus.qui.ub.es (L. Puignou)

0021-9673/00/$ – see front matter
PII: S0021-9673(99)01091-2

[19,20] or solid-phase extraction [21,22] can be found in the literature, mainly followed by different separation techniques: liquid chromatography (LC) [23–25], gas chromatography (GC) [26–28] or capillary electrophoresis (CE) [29–31]. The degree of selectivity in the detection depends on the efficiency of the clean-up procedure. The use of poor specific detectors such as UV detectors [32,33] requires exhaustive purification processes, but this often leads to a decrease in analyte recovery and therefore in the accuracy of the results. This is the reason why some authors use more specific detectors like diode array detection (DAD) [34,35], fluorescence [36,37], electrochemical detection (ED) [38,39], mass spectrometry (MS) [40,41] or even tandem mass spectrometry (MS–MS) [42,43]. Since MS offers very selective detection and on-line identification, in this work we used this technique to analyze the heterocyclic aromatic amines present in a lyophilized meat extract in order to prove the applicability of a clean-up procedure described in a previous work [44], which is easier than the usual ones [45,46]. In addition, since all the amines are recovered in a single extract, the analysis time is reduced by 40%. The determination of the amines was achieved by means of liquid chromatography coupled to mass spectrometry via an atmospheric pressure chemical ionization source and an ion trap as analyzer (LC–APCI-MS(IT)). The separation of the analytes was performed in a C_{18} column using a suitable mobile phase compatible with mass spectrometry. The parameters that influence the ion formation and detection were optimized, and repeatability, medium term precision and limits of detection have been studied in order to establish the quality parameters of the system. The proposed method was applied to the determination of heterocyclic amines in a lyophilized meat extract, proposed as a reference material [47].

2. Experimental

2.1. Chemicals

Methanol and acetonitrile were gradient grade (Merck, Darmstadt, Germany), water was purified in an Elix-Milli Q system (Millipore, Bedford, MA, USA) and dichloromethane was HPLC grade (Fisher, Leicestershire, UK). Both ammonia solution and formic acid were analytical grade (Merck), as was ammonium acetate (Fluka, Buchs, Switzerland). Caffeine, MRFA (L–Met–Arg–Phe–Ala acetate·H_2O) and Ultramark 1621 (polyethylene glycol mixture) were purchased from Sigma (Steinheim, Germany). He and N_2 were N50 quality, and all the solutions were passed through a 0.45 μm filter before injection into the LC system.

The compounds studied, which are shown in Fig. 1, were 2-amino-3-methylimidazo[4,5-*f*]quinoline (IQ), 2-amino-3,4-dimethylimidazo[4,5-*f*]quinoline (MeIQ), 2-amino-3,8-dimethylimidazo[4,5-*f*]quinoxaline (MeIQx), 2-amino-3,4,8-trimethylimidazo[4,5-*f*]quinoxaline (4,8-DiMeIQx), 2-amino-3,7,8-trimethylimidazo[4,5-*f*]quinoxaline (7,8-DiMeIQx), 2-amino-3,4,7,8-tetramethylimidazo[4, 5-*f*]quinoxaline (TriMeIQx), 3-amino-1,4-dimethyl-5*H*-pyrido[4,3-*b*]indole (Trp-P-1), 3-amino-1-methyl-5*H*-pyrido-[4,3-*b*]indole (Trp-P-2), 2-amino-6-methyldipyrido-[1,2-*a*:3′,2′-*d*]imidazole (Glu-P-1), 2-aminodipyrido[1,2-*a*:3′,2′-*d*]imidazole (Glu-P-2), 2-amino-9*H*-pyrido[2,3-*b*]indole (AαC), 2-amino-3-methyl-9*H*-pyrido[2,3-*b*]indole (MeAαC) and 2-amino-1-methyl-6-phenylimidazo[4,5-*b*]pyridine (PhIP), purchased from Toronto Research Chemicals Inc. (Toronto, Canada), and 1-methyl-9*H*-pyrido[3,4-*b*]indole (Harman) and 9*H*-pyrido[3,4-*b*]indole (Norharman), which were from Sigma. Stock standard solutions of 100 μg ml^{-1} in methanol were prepared and used for further dilutions. TriMeIQx was used as internal standard (2 μg ml^{-1} methanolic solution).

Diatomaceous earth extraction cartridges (Extrelut-20) and refill material were provided by Merck; PRS sodium form (500 mg) and endcapped C_{18} (100 mg) Bond-Elut cartridges, as well as coupling pieces and stopcocks were from Varian Associates (Harbor City, CA, USA). These cartridges were preconditioned with dichloromethane (7 ml) for PRS and methanol (5 ml) and water (5 ml) for C_{18}. A lyophilized meat extract [47] was used for the analysis.

2.2. Instruments

The separation of the amines was optimized using a Beckman System Gold 168 (Fullerton, CA, USA)

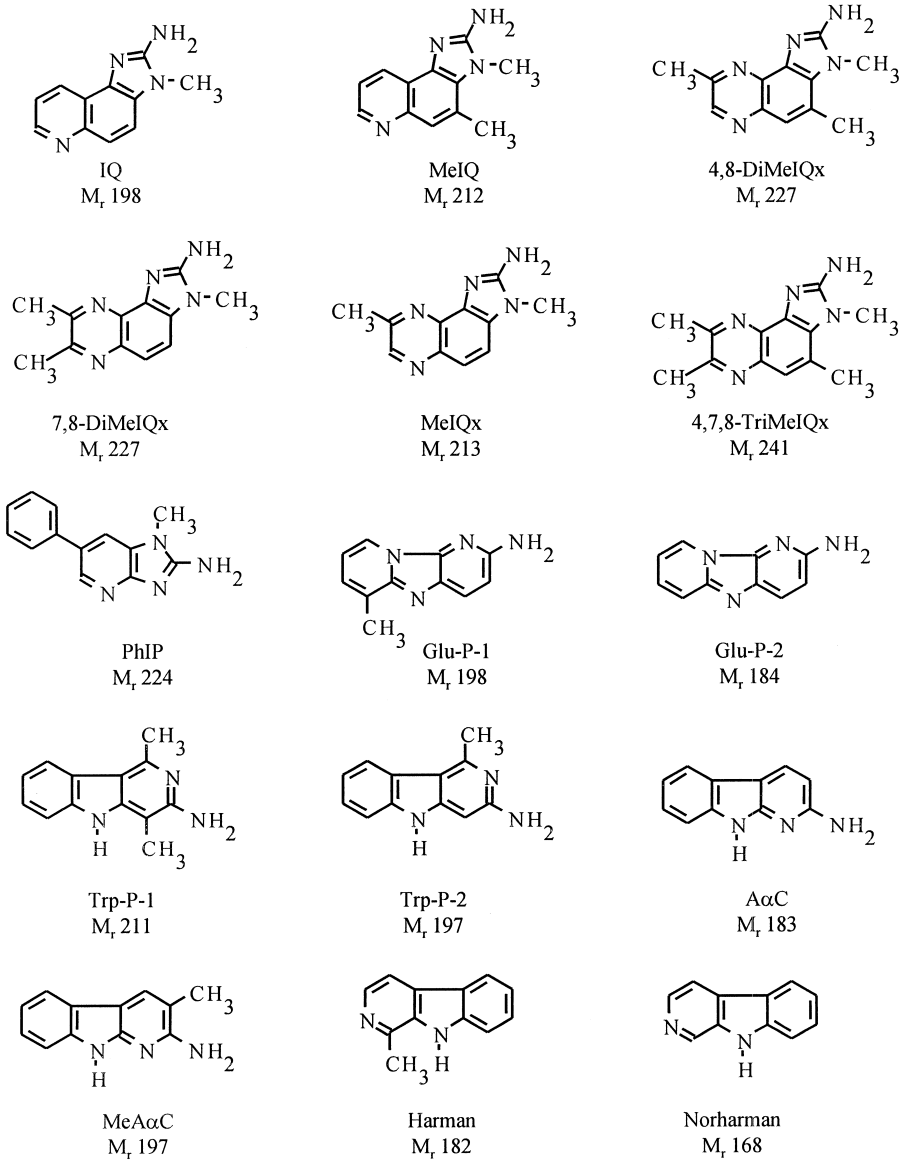

Fig. 1. Structures of the studied aromatic amines together with their abbreviation and isotopical molecular mass.

photodiode-array UV detector, which acquired spectra of peaks from 200 to 300 nm. In this case, the pumping system was a Pharmacia LKB HPLC system (Uppsala, Sweden) equipped with a high-pressure mixer, a low-pressure mixer and a Rheodyne 7125 injector (Cotati, CA, USA).

For mass spectrometry analysis, reversed-phase LC analyses were performed by means of a Waters 2690 Separations Module (Milford, MA, USA), and determination and identification of the peaks in the sample were carried out with an LCQ (Finnigan MAT, San Jose, CA, USA) provided with an APCI interface and an ion trap mass analyzer. Source working conditions to record positive ions were optimized by varying the parameters influencing the ionization. Discharge voltage was varied between 3 and 7 kV; heated capillary and vaporizer temperatures were tested in the range of 100–250°C and

300–500°C respectively, and nitrogen was used as drying gas (0–144 l h^{-1}) and as nebulizing gas (270–450 l h^{-1}). For data acquisition in full scan mode, the mass spectrometer operated over a range of m/z 150–250 in the centroid mode with a maximum injection time, which was varied from 200 to 1000 ms, 1 microscan, automatic gain control (AGC) ON and inject waveform off. Efficiency of ion transference from source to the ion trap was automatically optimized by infusing methanolic solutions of IQ, 4,8-DiMeIQx and Trp-P-1. To prevent MS contamination when running LC–MS, a divert valve was used. MS calibration was carried out with the infusion of a mixture containing caffeine, MRFA and Ultramark 1621 into the APCI source.

A Supelco Visiprep and a Visidry SPE vacuum manifold (Supelco, Gland, Switzerland) were used for manipulations with solid-phase extraction cartridges and solvent evaporation, respectively.

2.3. Chromatographic conditions

In all cases, the amines were separated using a TSK-Gel ODS 80T column (5 μm, 25.0×4.6 mm I.D.) (TosoHaas, Stuttgart, Germany) equipped with a Supelguard LC-8-DB precolumn (Supelco, Bellefonte, PA, USA).

Optimal separation was achieved with a ternary mobile phase at a flow-rate of 1 ml min^{-1}. Solvent A: 30 m*M* formic acid in water adjusted with ammonia solution to pH 3.25; solvent B: 30 m*M* formic acid in water adjusted with ammonia solution to pH 3.7; solvent C: acetonitrile. For LC–MS analysis, the gradient program was: 5–23% C in A, 0–18 min; 23% C in A, 18–21 min; 23% C in B, 21–25 min; 23–60% C in B, 25–33 min; 60% C in B, 33–40 min; return to the initial conditions, 40–50 min; 5 min post-run delay. For UV detection 7 m*M* triethylamine was used, but with MS detection it was discarded due to the strong ionization suppression observed. In all cases the amount injected was 15 μl.

2.4. Sample analysis

To extract the analytes from a lyophilized meat extract a previously described purification method [44] was used. Briefly, 1 g beef extract sample was dissolved in 12 ml 1 *M* NaOH with sonication and shaking until homogenization for 3 h. The alkaline solution was mixed with Extrelut refill material (12.9 g) and used to fill an empty Extrelut column. A Bond-Elut PRS (500 mg) column was preconditioned with 5 ml 0.1 *M* HCl, 10 ml water and 5 ml methanol. After drying the cartridge under vacuum, 7 ml dichloromethane were passed, and then the PRS column was coupled on-line with the Extrelut column. To extract the analytes from diatomaceous earth, 75 ml dichloromethane were passed through the tandem, and the PRS cartridge was then dried and successively rinsed with 15 ml methanol–water (4:6, v/v) and 2 ml water. The cationic exchanger column was then coupled to a preconditioned C_{18} (100 mg) column, and this tandem was eluted with 20 ml of 0.5 *M* ammonium acetate at pH 8.0. The adsorbed HAAs were finally eluted from C_{18}, after rinsing with 5 ml water, using 0.8 ml of methanol–ammonia (9:1, v/v). The solvent was evaporated with a stream of nitrogen and the analytes were redissolved with 50 μl of the internal standard in methanol. The final extract was analyzed using the LC–MS method described above.

Quantification and recovery calculation of the amines in the beef extract was carried out by standard addition method. The meat extract was spiked with all the analyzed compounds at three levels (80, 160 and 320 ng g^{-1}) by adding different volumes of a methanolic solution of the analytes to the sample. The solvent was allowed to evaporate before the addition of NaOH.

3. Results and discussion

3.1. LC–MS

As it was described in the experimental section, the chromatographic separation of the HAAs was performed in a C_{18} column with a volatile mobile phase, based in ammonium formate and acetonitrile, to be compatible with the mass spectrometric system. APCI involves a soft ionization process, therefore studied HAAs readily provide unfragmented protonated-molecular ions $[M+H]^+$ as the base peak. In order to optimize the ionization, various parameters were studied, and the best results were obtained with the following conditions: discharge voltage and

current 5 kV and 5 μA respectively; the capillary was heated to 150°C, and the vaporizer temperature was 450°C; nitrogen was introduced as drying gas at a flow-rate of 72 l h^{-1}, and used for nebulization at a flow-rate of 360 l h^{-1}.

The chromatogram (Fig. 2) can be divided in three regions where the amines 1 to 5, 6 to 10 and 11 to 15 were eluted. These regions corresponded to different mobile phase composition according to the gradient program mentioned in the experimental section.

The parameters which influence ionization, desolvatation and ion transference from source to analyzer, including capillary voltage, tube lens voltage and optics, were automatically optimized for each segment using a methanolic solution of the amines (1 μg ml^{-1} concentration level) chosen as model. For the first segment (0–18 min) IQ was used, segment two (18–24.7 min) was tuned using 4,8-DiMeIQx and for segment three (24.7–40 min) Trp-P-1 was chosen. The amine solutions were introduced into the system by infusion at a flow-rate of 9 ml min^{-1} using a syringe pump and a tee piece for mixture with the mobile phase at the eluting conditions for each analyte.

Fig. 2 shows the total ion chromatogram (TIC) and the traces for each m/z corresponding to $[M+H]^+$ for a standard solution of 3.7 μg ml^{-1}. This chromatogram, where it can be seen that resolution between all the traces is acceptable, was acquired under the optimal conditions.

3.2. Quality parameters

Calibration curves for the amines were performed at six concentration levels in the range of 0.15–7.30 μg ml^{-1}. Calibration curves were calculated daily from the representation of the peak area of the analytes in relation to the peak area of the internal standard (TriMeIQx) vs. the concentration of each compound. The curves were fitted to a quadratic function using a $1/x^2$ weighting, which gave regression coefficients better than 0.994 for all the analytes.

The quality parameters repeatability or run-to-run precision, medium term or day-to-day precision and limit of detection were calculated. To determine both repeatability and medium term precision, five daily replicate injections of a methanolic solution of all the analytes at an approximate level of 0.8 μg ml^{-1} were carried out on three successive days. A study of the variance of one factor for both concentration and retention time was then performed [48]. The target value for the concentration of each analyte and the mean values for retention time and concentration are shown in Table 1, together with the relative standard deviations for run-to-run and day-to-day precision obtained with the variance analysis study. It can be observed that the range of variability for concentration is 2.1–5.1% for run-to-run precision, and 4.6–11.0 for day-to-day precision. For retention times, run-to-run precision is comprised between 0.04 and 0.4, and the day-to-day between 0.07 and 0.7. The good figures of merit obtained are better than those calculated when the conventional phosphoric acid/dihydrogenphosphate is used as mobile phase with UV detection [49].

Detection limits for standard solutions, which are based on a signal-to-noise ratio of 3:1, ranged from 27 pg to 150 pg injected (1.8 ng ml^{-1}–10 ng ml^{-1}), as it can be seen in Table 1. These full scan values are comparable to those obtained using electrospray [40] and APCI sources [41] with selected ion monitoring (SIM). In addition, they are similar to the limits of detection obtained with electrochemical detection [38,39] and at least 10 times lower than those obtained with UV detection [4,50].

3.3. Analysis of a beef extract

The main objective of this work was to demonstrate the applicability of the simplified SPE method, using MS detection, to the analysis of a real sample. For this reason it has been applied to a lyophilized meat extract proposed as a reference material [47]. As it can be seen in Fig. 3, the quantification with UV detection is difficult due to the complexity of the matrix. For instance, IQ coeluted with an interfering compound, and the internal standard TriMeIQx had to be replaced by 7,8-DiMeIQx due to matrix interferences. By using MS detection and due to its high selectivity and specificity, the low resolution and the interferences coextracted from the matrix can be compensated by selecting adequate masses to monitor. In Fig. 4 the ion trace chromatogram for each amine is given and the compounds IQ, MeIQx, 4,8-DiMeIQx, norharman, harman and PhIP were

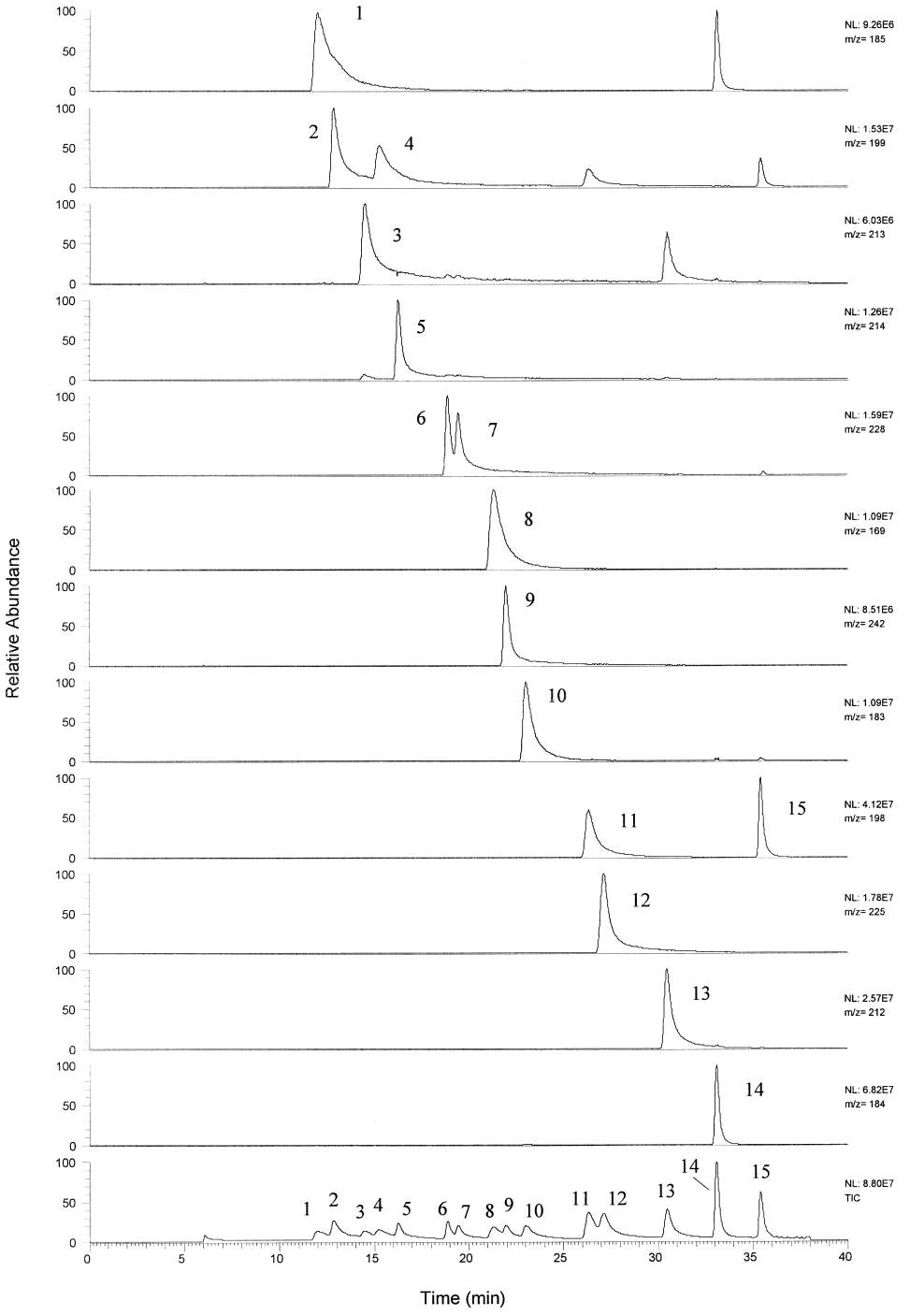

Fig. 2. Total ion chromatogram and chromatogram for each mass of a standard solution (3.7 μg ml^{-1}). Peak identification: 1. Glu-P-2; 2. IQ; 3. MeIQ; 4. Glu-P-1; 5. MeIQx; 6. 7,8-DiMeIQx; 7. 4,8-DiMeIQx; 8. Norharman; 9. TriMeIQx (IS); 10. Harman; 11. Trp-P-2; 12. PhIP; 13. Trp-P-1; 14. AαC; 15. MeAαC. Chromatographic conditions as given in experimental section.

Table 1
Quality parameters: run-to-run precision, day-to-day precision and limit of detection

Compound	Target value ($\mu g\ ml^{-1}$)	Mean values ($n=15$)		Precision RSD% ($n=15$, $\alpha=0.05$)				Limit of detection			
		Conc. ($\mu g\ ml^{-1}$)	t_R (min)	Conc.		t_R		Standards		Sample	
				run-to-run	day-to-day	run-to-run	day-to-day	ng ml^{-1}[a]	pg injected	pg injected	ng g^{-1}
Glu-P-2	0.78	0.80	12.2	2.2	8.2	0.4	0.5	6.0	90	1300	7.9
IQ	1.16	1.14	13.1	2.7	7.1	0.3	0.6	6.2	93	1000	4.9
MeIQ	0.61	0.63	14.8	4.2	11.0	0.2	0.7	10.0	150	3100	10.1
Glu-P-1	0.70	0.67	15.4	3.8	7.3	0.2	0.5	4.8	72	1500	9.0
MeIQx	0.78	0.78	16.4	3.1	8.2	0.1	0.3	5.6	84	1100	5.3
7,8-DiMeIQx	0.85	0.84	19.0	3.3	4.6	0.1	0.4	6.9	103	710	2.9
4,8-DiMeIQx	0.62	0.63	19.6	4.8	10.1	0.2	0.3	6.1	91	400	2.7
Norharman	0.84	0.82	21.5	2.1	7.0	0.2	0.3	7.4	111	370	2.3
Harman	0.78	0.75	23.2	3.5	7.5	0.2	0.3	5.6	84	390	2.7
Trp-P-2	0.99	0.97	26.6	2.5	7.0	0.2	0.2	2.7	40	300	1.9
PhIP	0.82	0.83	27.4	2.9	5.2	0.1	0.3	6.0	90	380	1.5
Trp-P-1	0.82	0.81	30.6	2.2	6.8	0.08	0.1	1.8	27	175	1.7
AαC	1.27	1.22	33.2	5.1	8.1	0.04	0.1	2.0	30	100	0.8
MeAαC	0.82	0.78	35.5	4.7	5.8	0.04	0.07	3.0	45	200	1.0

[a] 15 μl were injected.

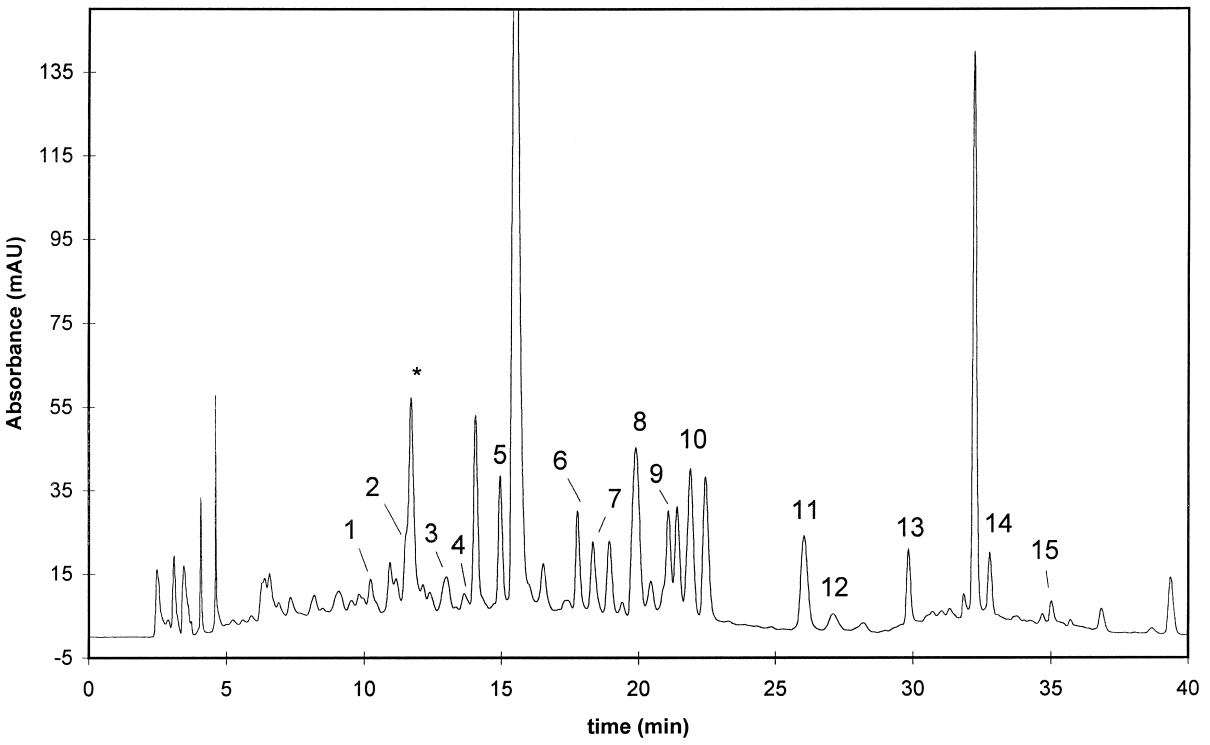

Fig. 3. Chromatogram of a meat extract spiked with 80 ng of each analyte (UV detection, at $\lambda=263$ nm). Peak identification: 1. Glu-P-2; 2. IQ; 3. MeIQ; 4. Glu-P-1; 5. MeIQx; 6. 7,8-DiMeIQx (IS_1); 7. 4,8-DiMeIQx; 8. Includes Norharman; 9. TriMeIQx (IS_2); 10. Harman; 11. Trp-P-2; 12. PhIP; 13. Trp-P-1; 14. AαC; 15. MeAαC; * interfering compound. Chromatographic conditions as given in experimental section.

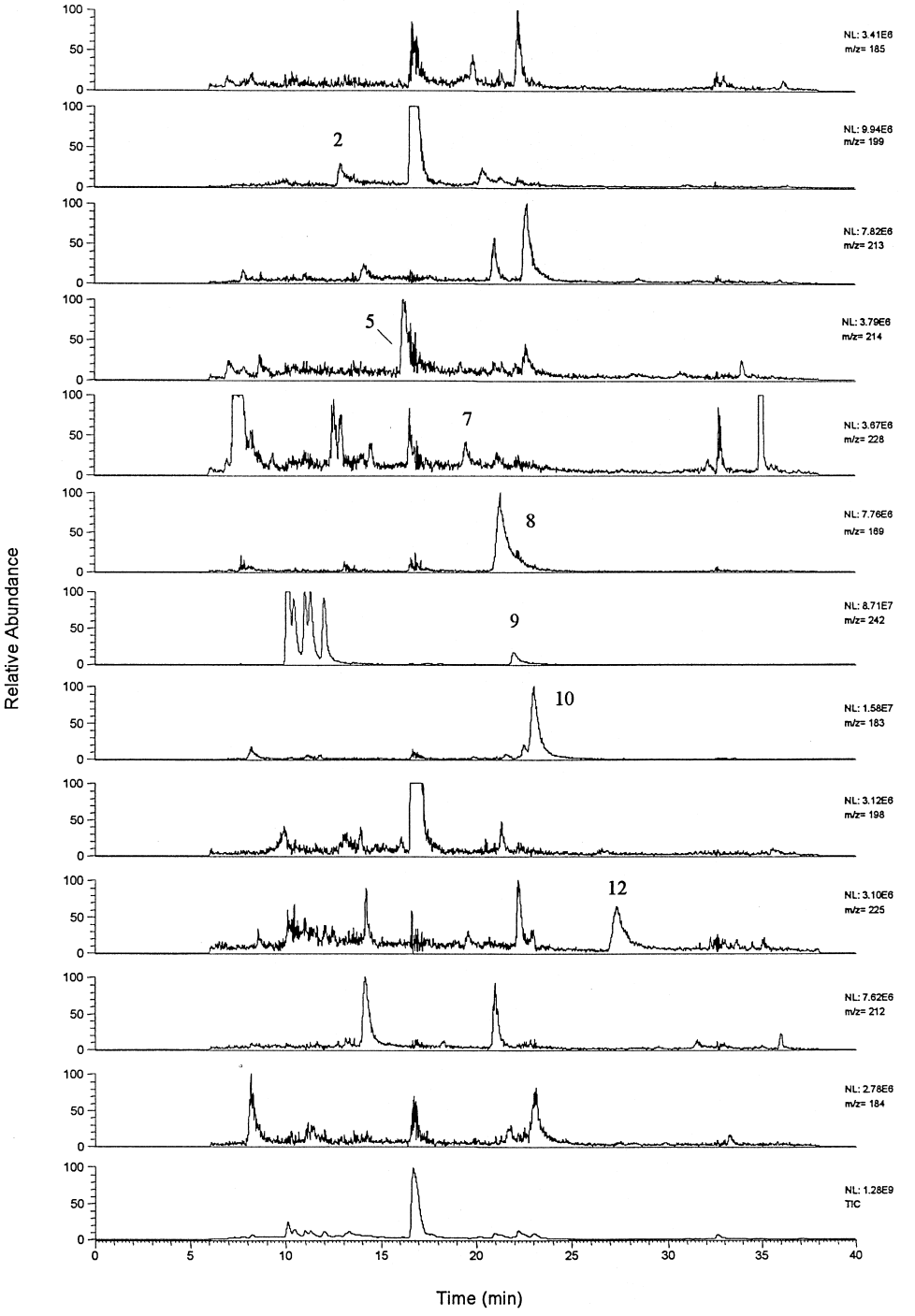

Fig. 4. Chromatogram of the non-spiked meat extract, which includes the signal obtained in the mass correspondent to each analyte and the total ion current (TIC). Identification of the peaks: 2. IQ; 5. MeIQx; 7. 4,8-DiMeIQx; 8. Norharman; 9. TriMeIQx (IS); 10. Harman; 12. PhIP. Chromatographic conditions as in Fig. 2.

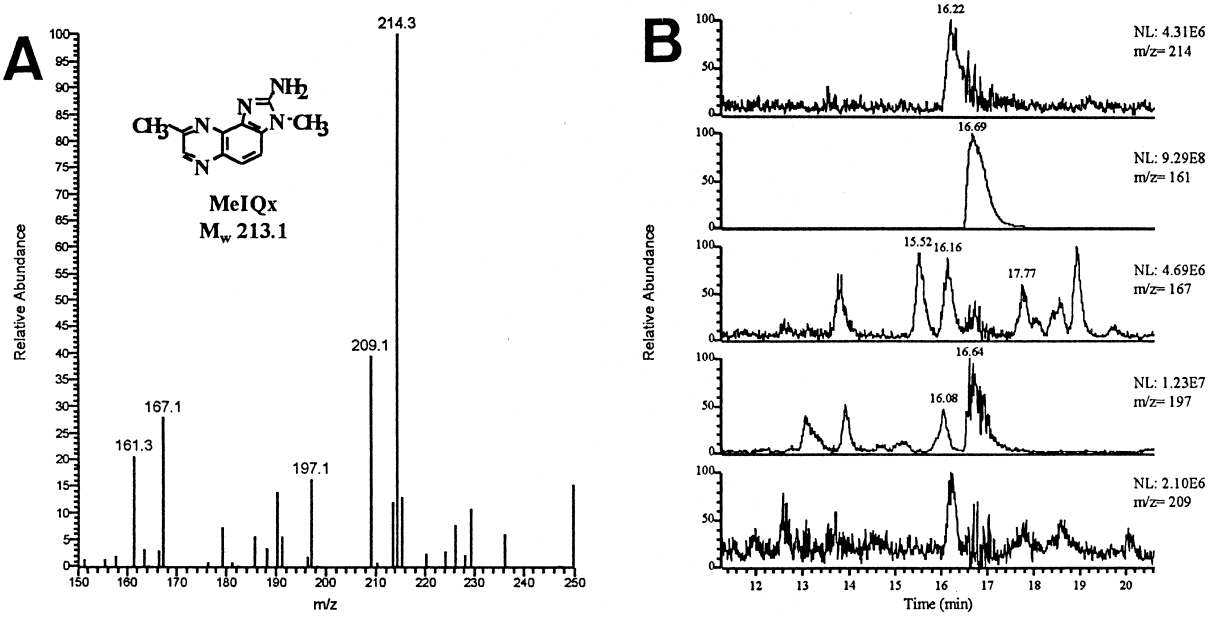

Fig. 5. (A) Full scan mass spectra of the peak eluted at the retention time of MeIQx. (B) Ion trace chromatograms of the most intense m/z shown in (A). Chromatographic conditions as in Fig. 2.

clearly identified. Nevertheless an important noise was observed for some of the compounds, for instance MeIQx. The Fig. 5A shows the full scan spectra of the eluted peak corresponding to this analyte, there it can be seen that an important number of interfering ions in addition to the molecular protonated ion were present. From the trace ion chromatogram (Fig. 5B) it can be deduced that the noise in the target compound is due to the coelution of the interferences. Moreover, when this coelution occurred the ionization of the target compounds may be affected by a suppression phenomenon, giving a lower signal-to-noise ratio. As a consequence, detection limits in the meat extract were higher than expected, as it can be seen in Table 1. This effect was more pronounced for the compounds eluted in the first zone of the chromatogram which is the less exhaustively purified.

Nevertheless, as it can be seen in Table 2, the results obtained in the analysis of the lyophilized meat extract are in agreement with those when UV detection was used for the analysis of the meat extract [44], avoiding the problems originated in the UV detection. For instance, it was impossible to quantify IQ using UV–DAD and, in addition, the identity of some peaks could not be confirmed using UV spectra, as in the case of MeIQ, Glu-P-2 or Trp-P-1. Selectivity of MS detection has permitted more reliable quantification, providing results similar to those obtained previously with other clean-up procedures [47,51].

Furthermore, it must be mentioned that some differences were observed between recoveries obtained with both LC–MS and LC–UV, as it can be seen in Table 2, that can be attributed to differences in cartridges batches or to the matrix interferences which occur when UV detection was used. This suggested that standard addition is mandatory to guarantee accurate quantification of the analytes, but if the analytes were strongly retained by the matrix components, an overestimation of the recoveries could be introduced.

4. Conclusions

The SPE method applied in this work has been shown to be suitable for the analysis of heterocyclic aromatic amines in proteinaceous matrices when it is used in conjunction with a sensitive, specific and

Table 2
Analysis of a lyophilized meat extract

Analytes	UV detection				MS detection			
	Recovery (%)	SD	ng g^{-1}	RSD (%)	Recovery (%)	SD	ng g^{-1}	RSD (%)
Glu-P-2	71.0	7.8	n.d.	–	57.6	1.9	n.d.	–
IQ	[b]	–	[b]	–	69.5	3.2	32.5	22.4
MeIQ	79.31	3.1	17.3[a]	55.5	73.2	4.4	n.d.	–
Glu-P-1	78.1	2.5	16.6[a]	27.1	57.2	1.1	n.d.	–
MeIQx	80.8	2.0	33.4	7.5	70.3	3.9	41.4	6.3
7,8-DiMeIQx	IS	–	IS	–	75.2	1.8	n.d.	–
4,8-DiMeIQx	88.1	8.0	8.9	24.2	52.3	1.9	9.7	17.5
Norharman	65.0	5.7	155	6.2	54.1	3.3	146	6.8
Harman	61.2	4.8	234	7.3	49.6	5.2	263	15.2
Trp-P-2	43.6	2	n.d.	–	49.8	1.0	n.d.	–
PhIP	57.2	3	28.8	31.9	74.3	2.7	27.1	3.7
Trp-P-1	50.8	3	9.0[a]	80.0	45.6	2.0	n.d.	–
AαC	65.8	3.7	n.d.	–	49.4	1.5	n.q.	–
MeAαC	–	–	–	–	51.1	1.4	n.q.	–

[a] Identity not confirmed with UV spectra.
[b] Coelution with a major interference prevented quantification.
n.d.: non detected compounds in the meat extract.
n.q.: analyte nearly its limit of detection.

selective LC detection technique, such as MS. This purification and preconcentration method allowed a reduction in analysis time and in materials, therefore it can be recommended for the analysis of heterocyclic amines in different matrices. However, in the case of complex samples such as meat extracts, where a high number of coeluting compounds are present, detection limits were found to be higher than those obtained with standard solutions. It was observed that an increase between 3 and 20 times occurred, showing that a compromise has to be achieved between limits of detection and clean-up efficiency, that depends on the food sample to be analyzed and the HAAs concentration levels.

Acknowledgements

The authors gratefully acknowledge the receipt of financial support from the C.I.C.Y.T. for research project ALI96-0863.

References

[1] G.N. Wogan, Environ. Health Perspect. 98 (1992) 167.
[2] D.W. Layton, K.T. Bogen, M.G. Knize, F.T. Hatch, V.M. Johnson, J.S. Felton, Carcinogenesis 16 (1995) 39.
[3] K. Skog, K. Augustsson, G. Steineck, M. Stenberg, M. Jägerstad, Food Chem. Toxicol. 35 (1997) 555.
[4] R. Schwarzenbach, D. Gubler, J. Chromatogr. 624 (1992) 491.
[5] L.S. Jackson, W.A. Hargraves, W.H. Stroup, G.W. Diachenko, Mutation Res. 320 (1994) 113.
[6] B. Stavric, B.P.-Y. Lau, T.I. Matula, R. Klassen, D. Lewis, R.H. Downie, Food Chem. Toxicol. 35 (1997) 185.
[7] E. Richling, C. Decker, D. Häring, M. Herderich, P. Schreier, J. Chromatogr. A 791 (1997) 71.
[8] H. Kataoka, J. Chomatogr. A 774 (1997) 121.
[9] H. Kataoka, K. Kijima, G. Maruo, Bull. Environ. Contam. Toxicol. 60 (1998) 60.
[10] H. Bartsch, C. Malaveille, M. Friesen, F.F. Kadlubar, P. Vineis, Eur. J. Cancer 29 (1993) 1199.
[11] T. Sugimura, M. Nagao, K. Wakabayashi, Environ. Health Perspect. 104 (1996) 429.
[12] T. Sugimura, Mutation Res. 376 (1997) 211.
[13] C.D. Davis, E.J. Dacquel, H.A.J. Schut, S.S. Thorgeirsson, E.G. Snyderwine, Mutation Res. 356 (1996) 287.
[14] H. Ohgaki, S. Takayama, T. Sugimura, Mutation Res. 259 (1991) 399.
[15] M.R. Welfare, J. Cooper, M.F. Bassendine, A.K. Daly, Carcinogenesis 18 (1997) 1351.
[16] R. Sinha, N. Rothman, Mutation Res. 376 (1997) 195.
[17] J.S. Felton, M.A. Malfatti, M.G. Knize, C.P. Salmon, Mutation Res. 376 (1997) 37.
[18] M.H. Ward, R. Sinha, E.F. Heineman, N. Rothman, R. Markin, D.D. Weisenburger, P. Correa, S.H. Zahm, Int. J. Cancer 71 (1997) 14.

[19] H. Lee, S.J. Tsai, Food Chem. Toxicol. 29 (1991) 517.
[20] K.R. Grose, J.L. Grant, L.F. Bjeldanes, B.D. Andresen, S.K. Healy, P.R. Lewis, J.S. Felton, F.T. Hatch, J. Agric. Food Chem. 34 (1986) 201.
[21] G.A. Gross, G. Philipposian, H.U. Aeschbacher, Carcinogenesis 10 (1989) 1175.
[22] G.A. Gross, A. Grüter, J. Chromatogr. 592 (1992) 271.
[23] M.G. Knize, R. Sinha, N. Rothman, E.D. Brown, C.P. salmon, O.A. Levander, P.L. Cunningham, J.S. Felton, Food Chem. Toxicol. 33 (1995) 545.
[24] Ch. Bross, S. Springer, G. Sontag, Deut. Lebensm.-Rundsch. 93 (1997) 384.
[25] M.G. Knize, C.P. Salmon, E.C. Hopmans, J.S. Felton, J. Chromatogr. A 763 (1997) 179.
[26] S. Murray, A.M. Lynch, M.G. Knize, N.J. Gooderham, J. Chromatogr. 616 (1993) 211.
[27] H. Kataoka, K. Kijima, J. Chromatogr. A 767 (1997) 187.
[28] K. Skog, A. Solyakov, P. Arvidsson, M. Jägerstad, J. Chromatogr. A 803 (1998) 227.
[29] J. Wu, M.-K. Wong, H.-K. Lee, B.-L. Lee, C.-Y. Shi, C.-N. Ong, Food Addit. Contam. 13 (1996) 851.
[30] L. Puignou, J. Casal, F.J. Santos, M.T. Galceran, J. Chromatogr. A 769 (1997) 293.
[31] Y. Zhao, M. Schelfaut, P. Sandra, F. Banks, Electrophoresis 19 (1998) 2213.
[32] G.A. Gross, A. Grüter, S. Heyland, Food Chem. Toxicol. 30 (1992) 491.
[33] G.A. Perfetti, J. AOAC Int. 79 (1996) 813.
[34] G.A. Gross, Carcinogenesis 11 (1990) 1597.
[35] M.G. Knize, J.S. Felton, G.A. Gross, J. Chromatogr. 624 (1992) 253.
[36] H. Ushiyama, K. Wakabayashi, M. Hirose, H. Itoh, T. Sugimura, M. Nagao, Carcinogenesis 12 (1991) 1417.
[37] M.T. Galceran, P. Pais, L. Puignou, J. Chromatogr. A 719 (1996) 203.
[38] S.M. Billedeau, M.S. Bryant, C.L. Holder, LC·GC 4 (1991) 38.
[39] M.M.C. Van Dyck, B. Rollman, C. De Meester, J. Chromatogr. A 697 (1995) 377.
[40] P. Pais, E. Moyano, L. Puignou, M.T. Galceran, J. Chromatogr. A 775 (1997) 125.
[41] P. Pais, E. Moyano, L. Puignou, M.T. Galceran, J. Chromatogr. A 778 (1997) 207.
[42] C.L. Holder, S.W. Preece, S.C. Conway, Y.M. Pu, D.R. Doerge, Rapid Commun. Mass Spectrom. 11 (1997) 1667.
[43] E. Richling, D. Häring, M. Herderich, P. Schreier, Chromatographia 48 (1998) 258.
[44] F. Toribio, L. Puignou, M.T. Galceran, J. Chromatogr. A 836 (1999) 223.
[45] M.T. Galceran, E. Moyano, L. Puignou, P. Pais, J. Chromatogr. A 730 (1996) 185.
[46] L.B. Fay, S. Ali, G.A. Gross, Mutation Res. 376 (1997) 29.
[47] C. de Meester, M.T. Galceran, M. Rabache, Report EUR 17652 EN, BCR Information, 1997.
[48] D.L. Massart, B.G.M. Vandeginste, L.M.C. Buydens, S. de Jong, P.J. Lewi, J. Smeyers-Verbeke, in: Data Handling in Science and Technology, Handbook of Chemometrics and Qualimetrics: Part A, Vol. 20A, Elsevier, Amsterdam, 1997.
[49] F. Toribio, L. Puignou, M.T. Galceran, in preparation.
[50] M.G. Knize, F.A. Dolbeare, K.L. Carrol, D.H. Moore II, J.S. Felton, Food Chem. Toxicol. 32 (1994) 595.
[51] P. Pais, Doctoral Thesis, Barcelona, 1996.

JOURNAL OF MASS SPECTROMETRY
J. Mass Spectrom. 2002; **37**: 812–828
Published online 28 June 2002 in Wiley InterScience (www.interscience.wiley.com). DOI: 10.1002/jms.340

JMS

Multistep mass spectrometry of heterocyclic amines in a quadrupole ion trap mass analyser

Francisca Toribio, Encarnación Moyano,* Lluís Puignou and Maria Teresa Galceran

Analytical Chemistry Department, University of Barcelona, Martí i Franquès 1–11, 08028 Barcelona, Spain

Received 8 January 2002; Accepted 2 May 2002

The fragmentation of heterocyclic amines (HAs) in an ion trap was studied by means of the infusion of methanolic solutions containing the compounds under assay, and using an atmospheric pressure chemical ionization (APCI) as ion source. The MS^n spectra obtained for compounds included in the same family, either aminoimidazoazaarenes (AIAs) or carbolines, were compared in order to propose fragmentation pathways for each HA. Moreover, labelled AIAs were used to establish the mechanisms. The protonated molecule was always obtained, but subsequent fragmentation was different for both families. In the case of AIAs, major product ions came from the fragmentation of the aminoimidazole moiety, thus the base peak in MS^2 corresponded to the loss of the methyl group, and losses of C_2NH_3 and CN_2H_2 were also observed. Further fragmentation occurred in the heterocyclic rings, mainly with losses of HCN and CH_3CN. For carbolines, the most important product ions came from the loss of ammonia, except for harman and norharman, the loss of a methyl group for methylated carbolines or the loss of diverse fragments from the heterocyclic rings. In some cases, ion–molecule reactions into the ion trap were observed. For instance, for AαC or MeAαC one ion originating from these reactions corresponded to the base peak. Copyright © 2002 John Wiley & Sons, Ltd.

KEYWORDS: heterocyclic amines; aminoimidazoazaarenes; carbolines; multistep mass spectrometry; ion trap

INTRODUCTION

Some of the compounds responsible for the mutagenic activity found in food samples have been identified as heterocyclic amines (HAs). These microcontaminants are generated when protein-rich foods, such as meat or fish, are thermally processed.[1] Depending on their chemical structure and their mechanism of formation, HAs can be grouped into two main families, aminoimidazoazaarenes (AIAs), generated at ordinary cooking temperatures, and carbolines, formed at temperatures above 300 °C.[2] To date, more than 20 HAs have been isolated and identified;[3] all of them, except harman and norharman, are potent mutagens,[4] and some of them have also been shown to be carcinogenic in animals.[5] Moreover, several epidemiological studies suggest a relationship between the consumption of meat and an increased risk of tumour generation in humans, especially colorectal cancers.[6] In order to evaluate the significance of HAs in human cancer development, an accurate determination of their dietary intake is necessary.[7] The low level of concentration of these analytes and the complexity of the food matrix make necessary the availability of selective and sensitive analytical methods. Many purification techniques have been described,[3] mainly followed by chromatographic methods[8] including liquid chromatography with ultraviolet (LC/UV), electrochemical (LC/ECD) or fluorescence detection, capillary electrophoresis with ultraviolet detection (CE/UV) or gas chromatography with nitrogen–phosphorus selective detection (GC/NPD). However, in recent years a large number of works based on the use of either liquid chromatography or gas chromatography in combination with mass spectrometry (MS) have been published.

In earlier work, mass spectrometry was used to characterize mutagenic compounds isolated from different food samples or to confirm their identity.[9–13] After several steps of purification and isolation of the mutagenic substances, the extracts obtained were directly introduced into the mass spectrometric system and electron ionization was used as ion source.

As mentioned above, the use of mass spectrometry in combination with gas chromatography for the analysis of HAs has also been described. Some of the main GC/MS methods published include a derivatization step and use electron ionization[14] or negative ion chemical ionization[15–18] followed by a quadrupole analyser. Since the analysis of HAs by using GC requires a derivatization step, LC is a more appropriate separation method. On the other hand, the improvements introduced during the last decade in the coupling of liquid chromatography with mass spectrometry (LC/MS) have allowed this hyphenated technique to

*Correspondence to: Encarnación Moyano, Analytical Chemistry Department, University of Barcelona, Martí i Franquès 1–11, 08028 Barcelona, Spain. E-mail: encarna.moyano@apolo.qui.ub.es
Contract/grant sponsor: Commission of the European Community;
Contract/grant number: QLK1-CT99-01197.
Contract/grant sponsor: Ministerio de Ciencia y Tecnología;
Contract/grant number: AGL2000-0948.

be broadly used in recent years. The first studies based on LC / MS used a thermospray (TSP) interface and quadrupole instruments.[19–21] Later, TSP ionization was substituted by the more robust atmospheric pressure ionization (API) sources, namely electrospray (ES)[22–29] and atmospheric pressure chemical ionization (APCI).[30–34] Most cases involved the use of either single-quadrupole[26,34] or triple-quadrupole[24,30] instruments operating in the MS mode or triple-quadrupole instruments working in the MS / MS mode.[22,25,29] Only a few groups reported the use of ion trap instruments in the MS[32] or MS / MS mode.[27,28,35] A small number of studies based on CE / MS have been described.[36]

In most of the studies that used MS, only applications, such as confirmation or quantification of the analytes, were described. Only a few studies have examined the fragmentation patterns for some heterocyclic amines and fragment ions were tentatively assigned. For example, electron ionization mass spectra were used to elucidate the structure of mutagens found in cooked food.[9,13] In other cases, the mass spectra obtained using LC coupled to single quadrupole instruments with in-source collision[24,34] and triple-quadrupole instruments operating in the MS / MS mode[22] were studied to provide a tentative assignment of the fragments. In other work, a triple-quadrupole instrument with in-source collision was used to obtain the MS^3 spectra in order to study the fragmentation of several HAs and to postulate a fragmentation pathway for the major product ions observed from MeIQx.[33] The assignment of the fragments was established using complementary information obtained from the corresponding labelled compound.

This paper describes the application of multistep ion trap mass spectrometry (MS^n) in the study of the fragmentation pathway of heterocyclic amines. The establishment of the characteristic fragmentation pathway for each family of HAs, namely AIAs and carbolines, could make possible the screening of unknown mutagens belonging to these families. Multistep ion trap mass spectrometry was performed by infusing methanolic solutions of the analytes in the mobile phase flow using an APCI ion source. Labelled compounds (^{13}C or D_3) were used to establish the fragmentation pathways.

EXPERIMENTAL

Chemicals

Organic solvents (methanol and acetonitrile) were of gradient grade (Merck, Darmstadt, Germany) and water was purified in an Elix-Milli Q system (Millipore, Bedford, MA, USA). Both ammonia solution and formic acid (Merck), used for the preparation of the aqueous mobile phase, were of analytical grade. He of high purity and N_2 (N1) from Air Liquide (Madrid, Spain) were used. The compounds studied were 2-amino-3-methylimidazo[4,5-*f*]quinoline (IQ), 2-amino-3-trideuteromethylimidazo[4,5-*f*]quinoline (D_3-IQ), [2-^{13}C]-2-amino-3-methylimidazo[4,5-*f*]quinoline (2-^{13}C-IQ), 2-amino-3,4-dimethylimidazo[4,5-*f*]quinoline (MeIQ), 2-amino-3,8-dimethylimidazo[4,5-*f*]quinoxaline (MeIQx), 2-amino-8-methyl-3-trideuteromethylimidazo[4,5-*f*]quinoxaline (D_3-MeIQx), [2-^{13}C]-2-amino-3,8-dimethylimidazo[4,5-*f*]quinoxaline (2-^{13}C-MeIQx), 2-amino-3,4,8-trimethylimidazo [4,5-*f*]quinoxaline (4,8-DiMeIQx), 2-amino-3,7,8-trimethylimidazo[4,5-*f*]quinoxaline (7,8-DiMeIQx), 2-amino-3,4,7,8-dimethylimidazo[4,5-*f*]quinoxaline (TriMeIQx), 2-amino-1,6-dimethylimidazo[4,5-*b*]pyridine (DMIP), 2-amino-1-methyl-6-phenylimidazo[4,5-*b*]pyridine (PhIP), 2-amino-9*H*-pyrido[2,3-*b*]indole (AαC), 2-amino-3-methyl-9*H*-pyrido[2,3-*b*]indole (MeAαC), 3-amino-1,4-dimethyl-5*H*-pyrido[4,3-*b*]indole (Trp-P-1), 3-amino-1-methyl-5*H*-pyrido[4,3-*b*]indole (Trp-P-2), 2-amino-6-methyldipyrido[1,2-*a*:3′,2′-*d*]imidazole (Glu-P-1) and 2-aminodipyrido[1,2-*a*:3′,2′-*d*]imidazole (Glu-P-2), which were obtained from Toronto Research Chemicals (Toronto, Canada), 1-methyl-9*H*-pyrido[4,3-*b*]indole (harman) and 9*H*-pyrido[4,3-*b*]indole (norharman), which were from Sigma (St. Louis, MO, USA). Individual methanolic stock standard solutions (10 μg g^{-1}) were used for the infusion of each analyte into the LC / MS system. All the solutions were passed through a 0.45 μm filter before their use. A 30 mM formic acid–ammonium formate buffer (pH 3.25 or pH 3.7) and acetonitrile from 15 to 60% was used as mobile phase. Each compound was infused with the mobile phase composition corresponding to their previously optimized[32] chromatographic conditions. The infusion of DMIP, Glu-P-2, IQ, MeIQ, Glu-P-1 and MeIQx was performed at pH 3.25 and with 15% acetonitrile. In the case of 7,8-DiMeIQx, 4,8-DiMeIQx, norharman, TriMeIQx and harman, the pH was also 3.25 but the proportion of acetonitrile in the mobile phase was 30%. For the study of Trp-P-2, PhIP, Trp-P-1, AαC and MeAαC, the pH was 3.7 and 30% acetonitrile was used.

Instrumentation and MS^n conditions

The mobile phase pumping system was an Alliance 2690 Separations Module (Waters, Milford, MA, USA). A 10 μg g^{-1}stock standard solution of each compound was infused at a flow-rate of 3 μl min^{-1} using the syringe pump included in the mass spectrometer, and it was mixed with the mobile phase (1 ml min^{-1}) by means a Valco zero dead volume tee piece (Supelco, Alcobendas, Spain). The mass spectrometric experiments were performed using a Finnigan LCQ mass spectrometer (Finnigan MAT, San Jose, CA, USA) provided with an APCI ion source and an ion trap as mass analyser. Xcalibur version 1.0 software was used for instrument control and acquisition of the mass spectrometric data. Ion source working conditions in positive mode were optimized in previous work[32] by varying the parameters influencing the ionization. The discharge voltage was set at 5 kV and the spray current was 5 μA; the capillary was heated to 150 °C and the vaporiser temperature was 450 °C; nitrogen was used as sheath gas at a flow-rate of 80 arbitrary units (72 l h^{-1}), and as auxiliary gas at a flow-rate of 20 arbitrary units (360 l h^{-1}). The ion transference efficiency from the ion source to the ion trap was automatically optimized before carrying out the MS^n study. For MS^n experiments, protonated molecular ions were isolated in the ion trap as precursor ions, and product ion full scan spectra were recorded after fragmentation by collision-induced dissociation (CID). The following parameters were used: the isolation width was fixed at m/z 1.5 to avoid interferences from isotopic species, five microscans were carried out with a maximum injection time of 200 ms and the activation time

JMS

value (AT, duration of the voltage applied to the endcap electrodes) was 30 ms. Moreover, helium damping gas was introduced into the ion trap according to the manufacturer's recommendations. In MS^2 experiments, the remaining variables controlling CID in the ion trap, namely activation Q (AQ, magnitude of the voltage applied to the ring electrode) and normalized collision energy (NCE %, amplitude of the voltage applied to the endcap electrodes), were optimized for the normal mass range.[35] An optimum AQ value of 0.45 was chosen to maximize the intensity of product ions. In the case of NCE, the optimum values ranged from 26.0 to 42.0% for the different HAs in order to provide a maximum intensity of the product ion keeping a significant signal for the precursor ion. For higher order MS studies, the selected product ion was isolated and fragmented similarly to the case of MS^2 experiments.

RESULTS AND DISCUSSION

In this work, the two families of HAs, namely aminoimidazoazaarenes (AIAs, Fig. 1) and carbolines (Fig. 2), were studied by MS^n. To obtain additional information, labelled IQ and MeIQx were also studied. These analytes had either a ^{13}C in position 2 or a trideuterated methyl group bonded

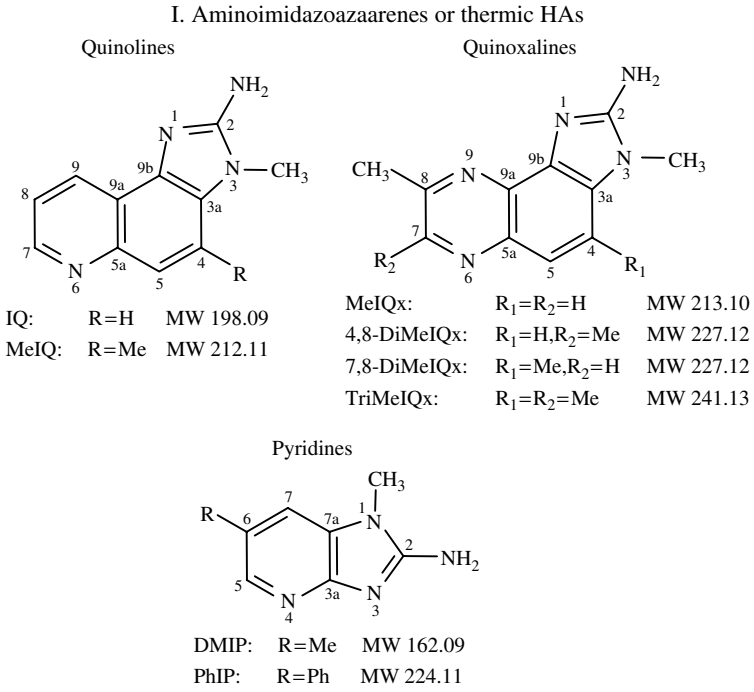

Figure 1. Structures of the AIAs used in this work.

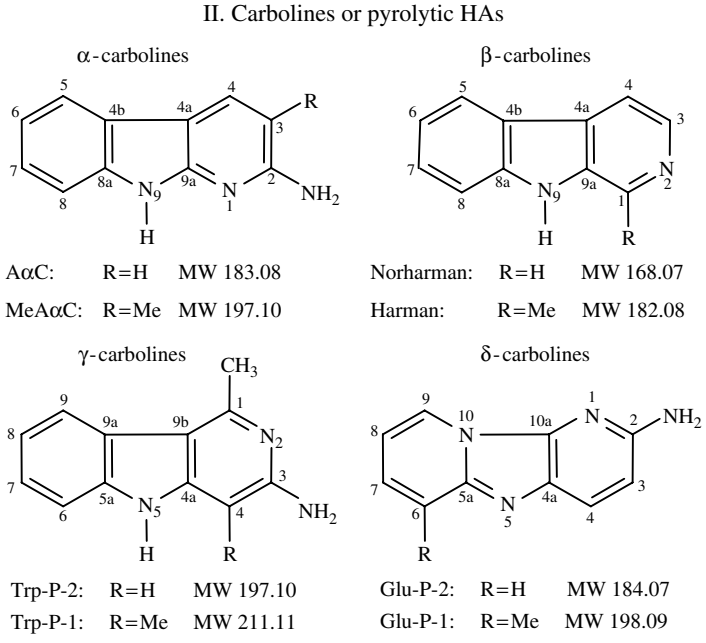

Figure 2. Structures of the carbolines used in this work.

to the nitrogen in position 3 (see Fig. 1). In all cases, the unfragmented quasi molecular ion $[M + H]^+$ was exclusively obtained in the MS mode, therefore these ions were used as primary precursor ions. In higher order MS^n experiments, AIAs and carbolines showed a different fragmentation pattern.

Aminoimidazoazaarenes

In Table 1, the CID working conditions, the main product ions and their assignment obtained in MS^2 and MS^3 for IQ and its corresponding labelled compounds are given. In Fig. 3, the corresponding MS^2 spectra of IQ (m/z 199.2 as precursor ion), D_3-IQ (m/z 202.2 as precursor ion) and ^{13}C-IQ (m/z 200.2 as precursor ion) are shown, together with higher order fragmentation spectra of some of the most abundant product ions. The base peak in the MS^2 spectrum of IQ (m/z 184.2) originated from the loss of $^{\bullet}CH_3$ (−15 Da) from the protonated molecular ion. The same base peak could be observed in the MS^2 spectrum of D_3-IQ, which indicated that the trideuterated methyl group was lost, and this was also supported by the fact that the base peak in the MS^2 spectrum of ^{13}C-IQ, at m/z 185.3, was shifted in mass according to the ^{13}C. In order to obtain more information, higher order MS^n experiments were performed. Thus, the ion $[M + H - CH_3]^{+\bullet}$ was conveniently isolated and fragmented. For both IQ and D_3-IQ, the main product ion was generated by the loss of HCN (−27 Da), which might arise from the aminoimidazo or the pyridine moieties. In the case of ^{13}C-IQ, two simultaneous fragmentations of the ion at m/z 185.3 led to two main peaks. One of them, at m/z 157.2, corresponded to the base peak, and was derived from the loss of $H^{13}CN$ (−28 Da) from the aminoimidazo moiety. The other (m/z 158.2), with a relative abundance of 82%, probably arose from the breaking of the pyridine ring, with the loss of HCN (−27 Da).

The MS^2 spectra of both IQ and ^{13}C-IQ also showed a peak at m/z 182.3 and 183.3 respectively, with relative abundances of 8–9%. These fragment ions could originate from the loss of NH_3 (−17 Da) from the respective precursor ion. However, in the case of D_3-IQ, the relative abundance of the peak derived from the loss of 17 mass units, located at m/z 185.2, had a relative abundance of 20%. This can be explained if $^{\bullet}CD_2H$ is lost in addition to the loss of NH_3, which would mean that a deuterium atom could remain in the molecule. To confirm this hypothesis, the MS^3 spectra of the ions at m/z 182.2 for IQ, m/z 185.2 for D_3-IQ and m/z 183.3 for ^{13}C-IQ were studied. Whereas IQ showed the loss of HCN (−27 Da) leading to an ion at m/z 155.1, in the case of ^{13}C-IQ two product ions were observed at m/z 155.1 and 156.2. The first ion could originate from the loss of $H^{13}CN$ (−28 Da) from the aminoimidazo moiety, and the second ion may arise from the loss of HCN (−27 Da) probably from the pyridine ring. For D_3-IQ, two main fragments were observed at m/z 158.2 (−27 Da) and 157.2 (−28 Da). The ion with the higher mass arose from the loss of HCN from the pyridine ring or the aminoimidazo moiety, as discussed above. However, the other ion can be due to an intramolecular hydrogen–deuterium exchange,[37] which could be explained by a reversible ring expansion that would include the methyl group in a six-atom ring.

Another abundant fragment in the MS^2 spectrum of IQ, at m/z 158.1, could be produced by the loss of C_2NH_3 from the aminoimidazole moiety of the protonated molecular ion. This was supported by the fact that ^{13}C-IQ showed the loss of $^{13}CCNH_3$ (m/z 158.2) and D_3-IQ the loss of C_2ND_3 (m/z 158.1). For the trideuterated compound, an additional fragment at m/z 159.1 was observed, which could be justified if a deuterium atom persisted in the molecule and C_2ND_2H was lost. The MS^3 spectra of the ion at m/z 158.1 were identical for the three compounds, showing the loss of HCN. In the case of D_3-IQ, the ion at m/z 159.1 gave two different product ions at m/z 132.1 and 131.1 (Table 1), which could arise from the loss of HCN and DCN, respectively.

IQ also showed the loss of CN_2H_2 from the aminoimidazole moiety, leading to an ion at m/z 157.1. The same product ion was observed in the MS^2 spectrum of ^{13}C-IQ, but for D_3-IQ the product ion was shifted in mass according to the deuterium atoms (m/z 160.1). Moreover, a fragment at m/z 131.1, with a relative abundance of 5–7%, was observed in the MS^2 spectra of the three compounds. This ion also arose from the cleavage of the aminoimidazolic ring with the subsequent loss of $C_3N_2H_4$ for IQ, $C_3N_2D_3H$ for D_3-IQ and $^{13}CC_2N_2H_4$ for ^{13}C-IQ.

The product ion mass spectra of MeIQx (m/z 214.3 as precursor ion), D_3-MeIQx (m/z 217.3 as precursor ion) and ^{13}C-MeIQx (m/z 215.3 as precursor ion) are shown in Fig. 4, together with mass spectra of higher order fragmentation of some of the most abundant product ions. In general, the fragmentation pattern of MeIQx was very similar to that of IQ. Thus, the base peak was derived from the loss of the 3-methyl group (m/z 199.2), and product ions arising from the breaking of the aminoimidazole ring with the loss of C_2NH_3 (m/z 173.2), CN_2H_2 (m/z 172.1) and $C_3N_2H_4$ (m/z 146.1) were also observed. Moreover, as in the case of D_3-IQ, two fragment ions proceeding from the loss of C_2ND_3 (m/z 173.1) and C_2ND_2H (m/z 174.1) were detected in the MS^2 spectrum of D_3-MeIQx (Fig. 4).

However, some significant differences occurred. For example, when the ion at m/z 199.2 was used as a precursor in MS^3 experiments, the loss of $^{\bullet}H$ (m/z 198.3) was observed in addition to that of HCN (m/z 172.1), which can be favoured by the presence of the methyl group in position 8 of the pyrazine ring. This would contribute to the stabilization of the product ion. In addition, the ion at m/z 199.2 showed the breaking of the pyrazine ring, with the loss of $C_3N_2H_4$ (m/z 131.1, relative abundance 20%). Guy *et al*., using a triple quadrupole instrument,[33] proposed that the ion at m/z 131.1 was one of the main fragmentation products of the ion at m/z 172.1. In contrast with these results, we observed that in the MS^4 spectrum of this last ion (Fig. 4), the fragment ion at m/z 131.1 represents only a minor peak (relative abundance ~5%).

MeIQx, D_3-MeIQx and ^{13}C-MeIQx also showed the loss of 27 u (m/z 187.1, 190.2 and 188.2, respectively), which indicated the breaking of the pyrazine ring with the loss of HCN. MS^3 experiments using these ions as precursors gave main fragments arising from the loss of the 3-methyl group (m/z 172.1 for MeIQx and D_3-MeIQx, m/z 173.2 for ^{13}C-MeIQx) or the cleavage of the aminoimidazole moiety with

Table 1. Optimized CID conditions in MS^2 and MS^3 and main product ions obtained for IQ and the corresponding labelled compounds[a]

	MS spectra		MS^2 CID conditions		MS^2 spectra		MS^3 CID conditions		MS^3 spectra	
Compound	*m/z* (rel. ab., %)	Tent. assign.	NCE (%)	AQ	*m/z* (rel. ab.,%)	Tent. assign.	NCE (%)	AQ	*m/z* (rel. ab.,%)	Tent. assign.
IQ	199.2 (100)	$[M+H]^+$	40.0	0.45	199.2 (9)	$[M+H]^+$				
					184.2 (100)	$[M+H-CH_3]^{+\bullet}$	39.8	0.45	184.2 (16)	$[M+H-CH_3]^{+\bullet}$
									157.1 (100)	$[M+H-CH_3-HCN]^{+\bullet}$
									156.1 (20)	$[M+H-CH_3-HCN-H]^+$
					182.2 (9)	$[M+H-NH_3]^+$	38.5	0.45	182.2 (47)	$[M+H-NH_3]^+$
									155.1 (100)	$[M+H-NH_3\text{-}HCN]^+$
					158.1 (22)	$[M+H-C_2NH_3]^+$	33.0	0.45	158.1 (15)	$[M+H-C_2NH_3]^+$
									131.1 (100)	$[M+H-C_2NH_3-HCN]^+$
					157.1 (8)	$[M+H-CN_2H_2]^+$				
					131.1 (7)	$[M+H-C_3N_2H_4]^+$				
D_3-IQ	202.2 (100)	$[M+H]^+$	40.0	0.45	202.2 (9)	$[M+H]^+$				
					185.2 (21)	$[M+H-NH_3]^+$	38.5	0.45	185.2 (21)	$[M+H-NH_3]^+$
						$[M+H-CD_2H]^{+\bullet}$				$[M+H-CD_2H]^{+\bullet}$
									158.2 (100)	$[M+H-NH_3-HCN]^+$
										$[M+H-CD_2H-HCN]^{+\bullet}$
									157.2 (30)	$[M+H-NH_3-DCN]^+$
										$[M+H-CD_2H-DCN]^{+\bullet}$
										$[M+H-CD_2H-HCN-H]^+$
					184.2 (100)	$[M+H-CD_3]^{+\bullet}$	39.8	0.45	184.2 (12)	$[M+H-CD_3]^{+\bullet}$
									157.1 (100)	$[M+H-CD_3-HCN]^{+\bullet}$
									156.1 (18)	$[M+H-CD_3-HCN-H]^{+\bullet}$
					160.1 (8)	$[M+H-CN_2H_2]^+$				
					159.1 (8)	$[M+H-C_2ND_2H]^+$	33.0	0.45	159.1 (27)	$[M+H-C_2ND_2H]^+$
									132.1 (100)	$[M+H-C_2ND_2H-HCN]^+$
									131.1 (50)	$[M+H-C_2ND_2H-DCN]^+$
					158.1 (16)	$[M+H-C_2ND_3]^+$	33.0	0.45	158.1 (18)	$[M+H-C_2ND_3]^+$
									131.1 (100)	$[M+H-C_2ND_3-HCN]^+$
					131.1 (5)	$[M+H-C_3N_2D_3H]^+$				
^{13}C-IQ	200.2 (100)	$[M+H]^+$	40.0	0.45	200.2 (8)	$[M+H]^+$				
					185.3 (100)	$[M+H-CH_3]^{+\bullet}$	37.0	0.45	185.3 (74)	$[M+H-CH_3]^{+\bullet}$
									158.2 (82)	$[M+H-CH_3-HCN]^{+\bullet}$
									157.2 (100)	$[M+H-CH_3-H^{13}CN]^{+\bullet}$
										$[M+H-CH_3-HCN-H]^+$
									156.1 (20)	$[M+H-CH_3-H^{13}CN-H]^{+\bullet}$
					183.3 (8)	$[M+H-NH_3]^+$	36.0	0.45	183.3 (100)	$[M+H-NH_3]^+$
									156.2 (50)	$[M+H-NH_3-HCN]^+$
									155.1 (38)	$[M+H-NH_3-H^{13}CN]^+$
					158.2 (23)	$[M+H-{}^{13}CCNH_3]^+$	33.0	0.45	158.2 (24)	$[M+H-{}^{13}CCNH_3]^+$
									131.1 (100)	$[M+H-{}^{13}CCNH_3-HCN]^+$
					157.2 (8)	$[M+H-{}^{13}CN_2H_2]^+$				
					131.1 (6)	$[M+H-{}^{13}CC_2N_2H_4]^+$				

[a] rel. ab. = relative abundance; Tent. assign. = tentative assignment; NCE = normalized collision energy.

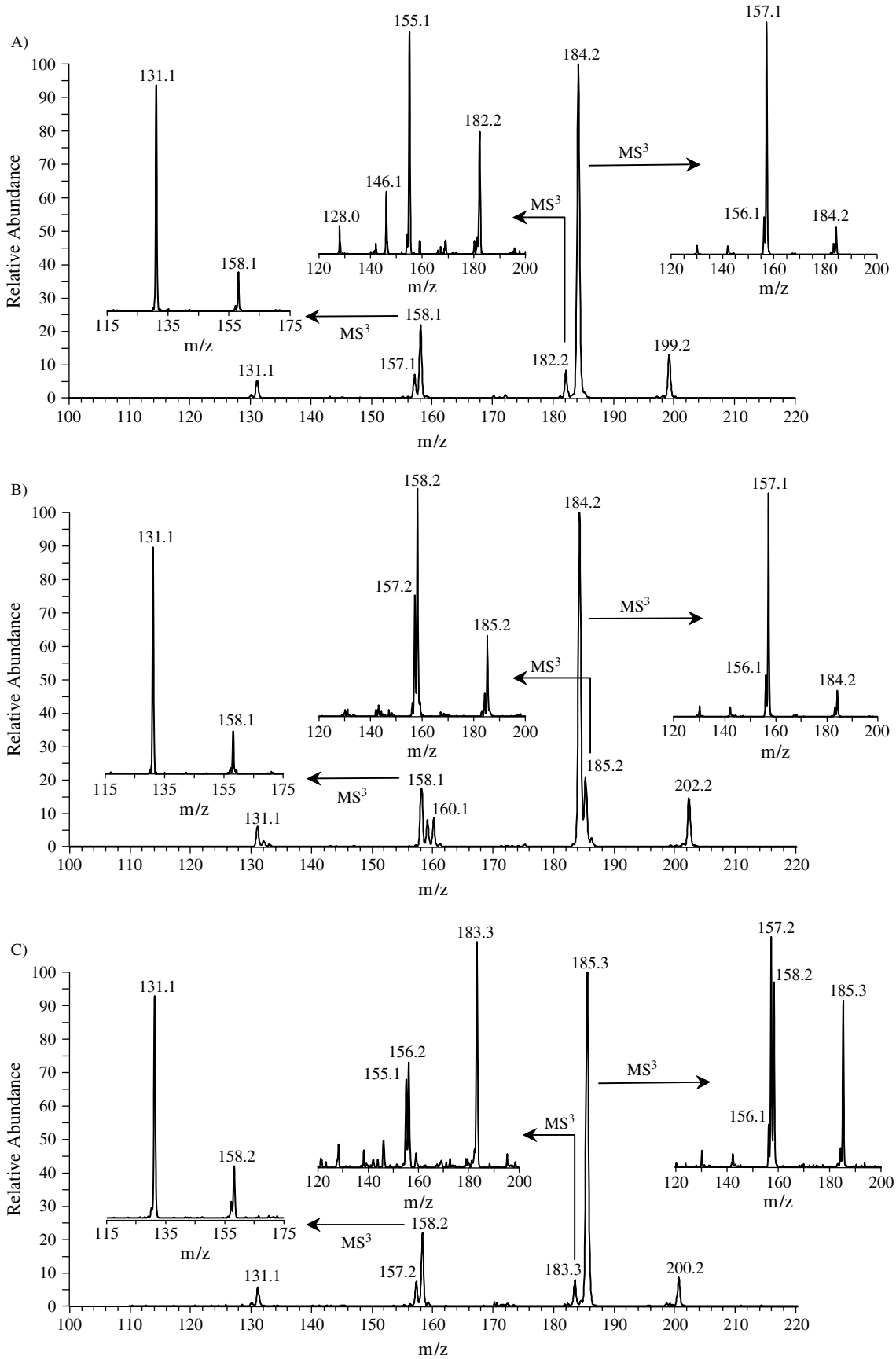

Figure 3. MS^2 spectra of (A) IQ, (B) D_3-IQ and (C) ^{13}C-IQ, and higher order mass spectra of some of the most important product ions. Working conditions as described in the Experimental section; CID conditions as given in Table 1.

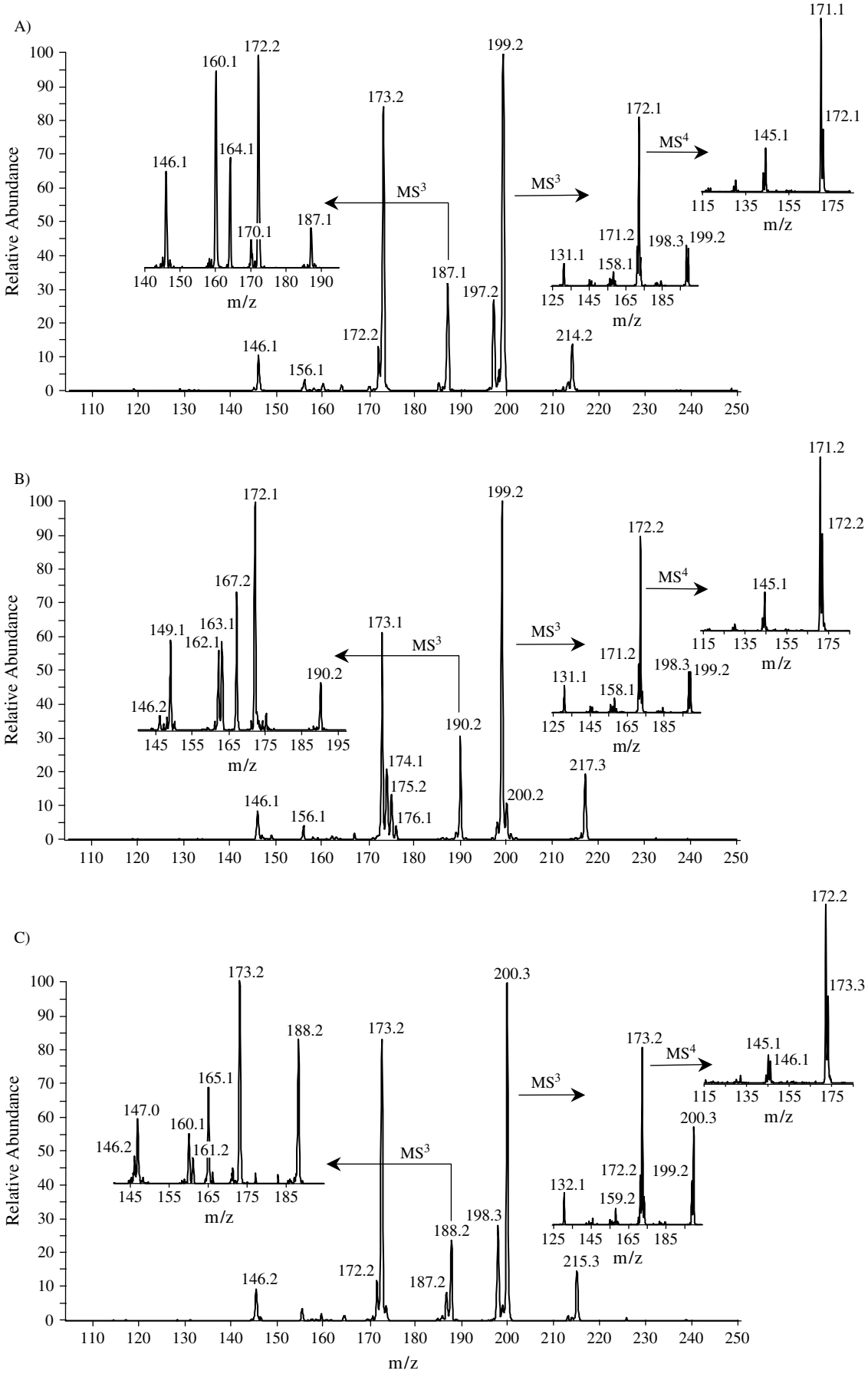

Figure 4. MS^2 spectra of (A) MeIQx, (B) D_3-MeIQx and (C) ^{13}C-MeIQx and higher order mass spectra of some of the most important product ions. Working conditions as described in the Experimental section; CID conditions as given in Table 1.

the loss of HCN or C_2NH_3 either with or without labelled atoms in the case of D_3-MeIQx and ^{13}C-MeIQx (Table 2).

Another marked difference between the MS^2 spectra of IQ and MeIQx was the increase in the relative abundance of the ion derived from the loss of C_2NH_3. Whereas for IQ the relative abundance of this ion at m/z 158.1 was 22%, for MeIQx the value for the ion at m/z 173.2 was 90%. This dissimilarity could be due to stabilization of the product ion, with the nitrogen in position 9 of the molecule playing an important role. To obtain more information, higher order MS experiments were carried out (Table 2). In addition to the loss of HCN (m/z 146.2), the loss of NH_3 was observed (m/z 156.1), with a relative abundance of 50%.

The other aminoimidazoazaarenes studied agreed in general with the fragmentation patterns of IQ and MeIQx (Table 3). Thus, the characteristic losses in MS^2 arising from the loss of the 3-methyl group (relative abundance 89–100%), the loss of ammonia (5–32%) and the breaking of the aminoimidazole ring, with the losses of C_2NH_3 (relative abundance 16–22% for quinolines, 87–100% for quinoxalines and 7% for DMIP), CN_2H_2 (relative abundance 5–10% for quinolines, quinoxalines and DMIP) and $C_3N_2H_4$ (relative abundance 5–12% for quinolines and quinoxalines), were observed. Moreover, in MS^2 quinoxalines showed the cleavage of the pyrazine moiety, with losses of HCN for MeIQx and 4,8-DiMeIQx (relative abundance 14–31%) and CH_3CN for the analytes with a methyl group in position 7 of the molecule, namely 7,8-DiMeIQx and TriMeIQx (relative abundance 97–100%).

In addition, when the ion derived from the loss of the 3-methyl group was used to carry out MS^3 experiments, a significant difference was observed. Whereas for quinolines and quinoxalines having a 4-methyl group (MeIQ, 4,8-DiMeIQx and TriMeIQx) the base peak arose from the loss of $^{\bullet}H$, for the other compounds the main fragmentation was produced in the pyridine ring for IQ ($-$HCN) or the pyrazine ring for MeIQx ($-$HCN) and 7,8-DiMeIQx ($-CH_3CN$). By way of summary, Fig. 5 shows a tentative fragmentation pathway proposal for some of the most important product ions from quinolines and quinoxalines.

All these results are consistent with those obtained with triple quadrupole instruments[22,33] or single quadrupoles and in-source collision,[34,24] which observed that the main fragmentation for AIAs was derived from the loss of a methyl group ($-$15 Da) and breaking of the aminoimidazil group. For quinoxalines, the breaking of the pyrazine ring was also observed.[33]

Carbolines

In the case of carbolines (α-carbolines; AαC and MeAαC; β-carbolines, H and NH; γ-carbolines, Trp-P-1 and Trp-P-2; δ-carbolines, Glu-P-1 and Glu-P-2), the CID conditions and the main product ions obtained in MS^2 and MS^3 experiments are given in Table 4. For this family of compounds, major fragment ions were derived from the loss of a methyl group for the methylated carbolines (relative abundances ranging from 52 to 100% for MeAαC, harman and Glu-P-1), from the loss of NH_3 for the primary amines (100% of relative abundance for γ-carbolines and in the range 13–40% for α- and δ-carbolines) and from the loss of HCN for α-, β- and δ-carbolines (92–100% for δ-carbolines and norharman and from 5 to 16% for α-carbolines and harman). Other important fragment ions in the MS^2 spectra of harman and norharman corresponded to the loss of hydrogen radicals and, in the case of harman and Trp-P-2, to the loss of CH_3CN from the cleavage of the pyridine ring. All these results are generally in agreement with those of previous work using quadrupole instruments,[22,24,34] which found that main product ions for carbolines, except harman and norharman, arose from the loss of NH_3 and HCN. For harman and norharman, the breaking of the pyridil group was observed.

However, a significant difference between quadrupole and ion trap instruments was observed. When using the ion trap analyser, peaks at $[M + H + 1]^+$ and $[M + H + 24]^+$ were observed in some cases. These product ions were so abundant that, for instance, for α-carbolines the base peak corresponded to m/z $[M + H + 1]^+$, and for γ-carbolines and δ-carbolines the relative abundance of this ion ranged from 29 to 38%. As an example, in Fig. 6 the mass spectra of Trp-P-2 are shown (precursor ion at m/z 198.2). Figure 6(A), which corresponds to the infusion of this analyte with a mobile phase containing acetonitrile, shows that the base peak in MS^2 is located at m/z 181.2. This fragment ion could be formed due to the loss of ammonia ($-$17 Da) from the protonated molecular ion. Other important fragments appeared at m/z 157.2 ($-$41 Da), arising from the loss of CH_3CN from the protonated molecular ion, and m/z 154.2, due to the loss of HCN ($-$27 Da) from the ion at m/z 181.2, as shown by MS^3 experiments. Moreover, two abundant ions at m/z higher than the precursor ion (m/z 199.2 and 222.1) can be observed in the MS^2 spectrum. Further experiments showed that these ions were easily broken to provide ions at m/z 181.2, 199.2 and 222.1, which suggested that an ion–molecule[38] association reaction between the ion $[M + H - NH_3]^+$ (m/z 181.2) and neutral molecules present in the ion trap, such as water (18 Da) or acetonitrile (41 Da), occurred. This was also supported by the fact that these fragments were present when simply isolating the ion at m/z 181.2 (NCE 0%). The ion at m/z 199.2 could be a water adduct, and the ion at m/z 222.1 might correspond to the acetonitrile adduct. Spectra of higher order fragmentation showed that these neutral molecules could be lost, leading to a product ion at m/z 181.2. Moreover, an interchange between water and acetonitrile was always observed. In order to ensure that the ions at m/z 199.2 and 222.1 corresponded to adducts with neutral molecules arising from the mobile phase, infusion of Trp-P-2 with a mobile phase containing methanol instead of acetonitrile was carried out. Some of the multistep mass spectra obtained are shown in Fig. 6(B), where it can be observed that the corresponding methanol adduct, at m/z 213.2, was formed instead of the previously observed adduct with acetonitrile, at m/z 222.1. However, the ion at m/z 213.2 showed a different behaviour in the MS^3 spectrum. Instead of an interchange between neutral molecules, the loss of a methyl group ($-$15 Da, m/z 198.2) was observed, which suggested that in this case a condensation reaction occurred. In the MS^4 spectrum of the ion m/z 198.2 the loss of CO ($-$28 Da), typical of the carbonyl group, appeared.

Table 2. Optimized CID conditions in MS^2 and MS^3 and main product ions obtained for MeIQx and the corresponding labelled compounds[a]

	MS spectra		MS^2 CID conditions		MS^2 spectra		MS^3 CID conditions		MS^3 spectra	
Compound	*m/z* (rel. ab.,%)	Tent. assign.	NCE (%)	AQ	*m/z* (rel. ab.,%)	Tent. assign.	NCE (%)	AQ	*m/z* (rel. ab.,%)	Tent. assign.
MeIQx	214.3 (100)	$[M+H]^+$	40.7	0.45	214.2 (19)	$[M+H]^+$				
					199.2 (100)	$[M+H-CH_3]^{+\bullet}$	38.5	0.45	199.2 (22)	$[M+H-CH_3]^{+\bullet}$
									198.3 (30)	$[M+H-CH_3-H]^+$
									172.1 (100)	$[M+H-CH_3-HCN]^{+\bullet}$
									131.1 (20)	$[M+H-CH_3-C_3N_2H_4]^{+\bullet}$
					197.2 (29)	$[M+H-NH_3]^+$				
					187.1 (31)	$[M+H-HCN]^+$	37.3	0.45	187.1 (27)	$[M+H-HCN]^+$
									172.1 (100)	$[M+H-HCN-CH_3]^{+\bullet}$
									164.1 (45)	$[M+H-HCN-C_2NH_3+H_2O]^+$
									160.1 (95)	$[M+H-HCN-HCN]^+$
									146.1 (50)	$[M+H-HCN-C_2NH_3]^+$
					173.2 (87)	$[M+H-C_2NH_3]^+$	35.5	0.45	173.2 (17)	$[M+H-C_2NH_3]^+$
									156.1 (50)	$[M+H-C_2NH_3-NH_3]^+$
									146.2 (100)	$[M+H-C_2NH_3-HCN]^+$
					172.2 (12)	$[M+H-CN_2H_2]^+$				
					146.1 (11)	$[M+H-C_3N_2H_4]^+$				
D_3-MeIQx	217.3 (100)	$[M+H]^+$	40.7	0.45	217.3 (20)	$[M+H]^+$				
					200.2 (13)	$[M+H-NH_3]^+$				
						$[M+H-CD_2H]^{+\bullet}$				
					199.2 (100)	$[M+H-CD_3]^{+\bullet}$	38.5	0.45	199.2 (24)	$[M+H-CD_3]^{+\bullet}$
									198.3 (20)	$[M+H-CD_3-H]^+$
									172.2 (100)	$[M+H-CD_3-HCN]^{+\bullet}$
									131.1 (20)	$[M+H-CD_3-C_3N_2H_4]^{+\bullet}$
					190.2 (30)	$[M+H-HCN]^+$	37.3	0.45	190.2 (15)	$[M+H-HCN]^+$
									172.1 (100)	$[M+H-HCN-CD_3]^{+\bullet}$
									167.2 (65)	$[M+H-HCN-C_2NH_3+H_2O]^+$
									163.1 (25)	$[M+H-HCN-HCN]^+$
									162.1 (28)	$[M+H-HCN-DCN]^+$
									149.1 (40)	$[M+H-HCN-C_2NH_3]^+$

					175.2 (13)	$[M+H-CN_2H_2]^+$		
					174.1 (24)	$[M+H-C_2ND_2H]^+$	35.5	0.45
					173.1 (64)	$[M+H-C_2ND_3]^+$	35.5	0.45
					146.1 (9)	$[M+H-C_3N_2D_3H]^+$		
					215.3 (15)	$[M+H]^+$		
$^{13}C-$MeIQx	215.3 (100)	$[M+H]^+$	40.7	0.45	200.3 (100)	$[M+H-CH_3]^{+\bullet}$	37.0	0.45
					198.3 (28)	$[M+H-NH_3]^+$		
					188.2 (24)	$[M+H-HCN]^+$	35.0	0.45
					187.2 (8)	$[M+H-H^{13}CN]^+$		
					173.2 (83)	$[M+H-{}^{13}CCNH_3]^+$	35.5	0.45
					172.2 (12)	$[M+H-{}^{13}CN_2H_2]^+$		
					146.2 (10)	$[M+H-{}^{13}CC_2N_2H_4]^+$		

$[M+H-C_2ND_2H]^+$	174.1 (50)	
$[M+H-C_2ND_2H-NH_2D]^{+\bullet}$	156.1 (90)	
$[M+H-C_2ND_2H-HCN]^+$	147.1 (60)	
$[M+H-C_2ND_2H-DCN]^+$	146.1 (100)	
$[M+H-C_2ND_3]^+$	173.1 (20)	0.45
$[M+H-C_2ND_3-NH_3]^+$	156.1 (50)	
$[M+H-C_2ND_3-HCN]^+$	146.1 (100)	
$[M+H-CH_3]^{+\bullet}$	200.3 (55)	0.45
$[M+H-CH_3-H]^+$	199.2 (22)	
$[M+H-CH_3-HCN]^{+\bullet}$	173.2 (100)	
$[M+H-CH_3-H^{13}CN]^{+\bullet}$	172.2 (26)	
$[M+H-CH_3-C_3N_2H_4]^{+\bullet}$	132.1 (18)	
$[M+H-HCN]^+$	188.2 (72)	0.45
$[M+H-HCN-CH_3]^{+\bullet}$	173.2 (100)	
$[M+H-HCN-C_2NH_3+H_2O]^+$	165.1 (48)	
$[M+H-HCN-HCN]^+$	161.2 (10)	
$[M+H-HCN-H^{13}CN]^+$	160.1 (22)	
$[M+H-HCN-C_2NH_3]^+$	147.0 (30)	
$[M+H-HCN-{}^{12}CCNH_3]^+$	146.2 (12)	
$[M+H-{}^{13}CCNH_3]^+$	173.2 (20)	0.45
$[M+H-{}^{13}CCNH_3-NH_3]^+$	156.1 (50)	
$[M+H-{}^{13}CCNH_3-HCN]^+$	146.2 (100)	

[a] See Table 1.

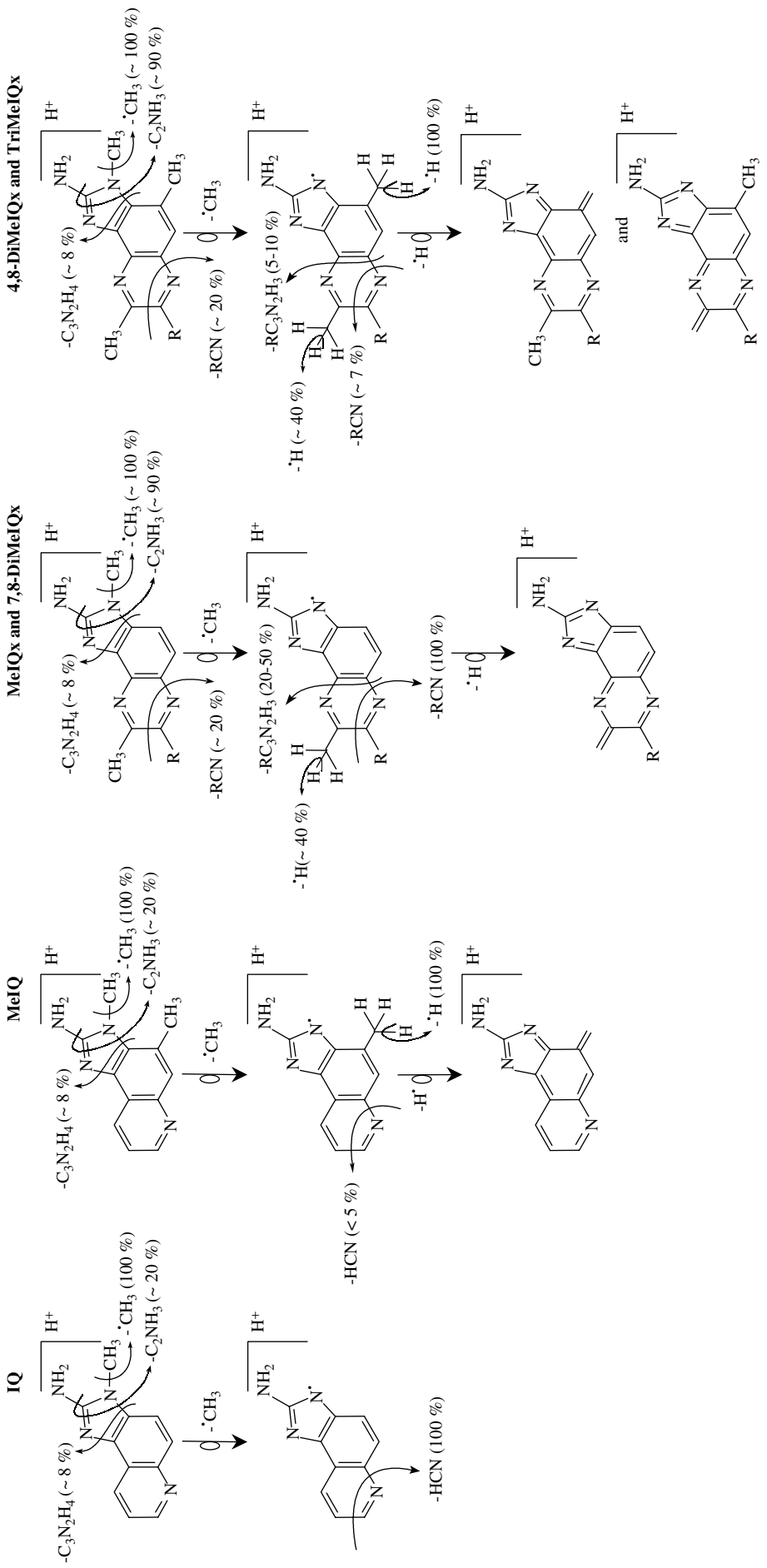

Figure 5. Tentative fragmentation pathway for some of the most important product ions obtained from quinolines and quinoxalines.

Table 3. Optimized CID conditions in MS^2 and MS^3 and main product ions obtained for the rest of AIAs[a]

	MS spectra		MS^2 CID conditions		MS^2 spectra		MS^3 CID conditions		MS^3 spectra	
Compound	*m/z* (rel. ab.,%)	Tent. assign.	NCE (%)	AQ	*m/z* (rel. ab.,%)	Tent. assign.	NCE (%)	AQ	*m/z* (rel. ab.,%)	Tent. assign.
MeIQ	213.3 (100)	$[M+H]^+$	39.0	0.45	213.3 (10)	$[M+H]^+$				
					198.2 (100)	$[M+H-CH_3]^{+\bullet}$	36.5	0.40	198.2 (50)	$[M+H-CH_3]^{+\bullet}$
									197.3 (100)	$[M+H-CH_3-H]^+$
									170.2 (25)	$[M+H-CH_3-H-HCN]^+$
					196.2 (5)	$[M+H-NH_3]^+$	35.0	0.40	196.2 (100)	$[M+H-NH_3]^+$
									169.2 (30)	$[M+H-NH_3-HCN]^+$
					172.1 (16)	$[M+H-C_2NH_3]^+$	30.5	0.30	172.1 (34)	$[M+H-C_2NH_3]^+$
									145.2 (100)	$[M+H-C_2NH_3-HCN]^+$
					171.1 (5)	$[M+H-CN_2H_2]^+$				
					145.2 (5)	$[M+H-C_3N_2H_4]^+$				
4,8-DiMeIQx	228.3 (100)	$[M+H]^+$	40.5	0.45	228.3 (11)	$[M+H]^+$				
					213.3 (100)	$[M+H-CH_3]^{+\bullet}$	35.0	0.45	213.3 (23)	$[M+H-CH_3]^{+\bullet}$
									212.3 (100)	$[M+H-CH_3-H]^{+\bullet}$
					211.3 (17)	$[M+H-NH_3]^+$	38.0	0.45	211.3 (73)	$[M+H-NH_3]^+$
									184.2 (100)	$[M+H-NH_3-H]^+$
					201.1 (14)	$[M+H-HCN]^+$	33.0	0.45	201.1 (100)	$[M+H-HCN]^+$
									186.2 (40)	$[M+H-HCN-CH_3]^{+\bullet}$
									174.2 (70)	$[M+H-HCN-HCN]^+$
									160.1 (35)	$[M+H-HCN-C_2NH_3]^+$
					187.2 (89)	$[M+H-C_2NH_3]^+$	36.0	0.45	187.2 (17)	$[M+H-C_2NH_3]^+$
									170.1 (20)	$[M+H-C_2NH_3-NH_3]^+$
									160.1 (100)	$[M+H-C_2NH_3-HCN]^+$
					186.2 (8)	$[M+H-CN_2H_2]^+$				
					160.2 (13)	$[M+H-C_3N_2H_4]^+$				
7,8-DiMeIQx	228.3 (100)	$[M+H]^+$	41.6	0.45	228.3 (12)	$[M+H]^+$				
					213.2 (89)	$[M+H-CH_3]^{+\bullet}$	36.0	0.50	213.2 (95)	$[M+H-CH_3]^{+\bullet}$
									212.2 (90)	$[M+H-CH_3-H]^+$
									187.2 (20)	$[M+H-CH_3-CN]^+$
									172.1 (100)	$[M+H-CH_3-C_2NH_3]^{+\bullet}$
									131.1 (50)	$[M+H-CH_3-C_4N_2H_6]^{+\bullet}$
					211.2 (28)	$[M+H-NH_3]^+$	38.0	0.45	211.2 (75)	$[M+H-NH_3]^+$
									184.1 (100)	$[M+H-NH_3-HCN]^+$
									170.2 (30)	$[M+H-NH_3-C_2NH_3]^+$

(*continued overleaf*)

Table 3. (*Continued*)

Compound	MS spectra		MS^2 CID conditions		MS^2 spectra		MS^3 CID conditions		MS^3 spectra	
	m/z (rel. ab.,%)	Tent. assign.	NCE (%)	AQ	*m/z* (rel. ab.,%)	Tent. assign.	NCE (%)	AQ	*m/z* (rel. ab.,%)	Tent. assign.
					187.2 (100)	$[M+H-C_2NH_3]^+$	36.5	0.45	187.2 (25)	$[M+H-C_2NH_3]^+$
									172.2 (40)	$[M+H-C_2NH_3-CH_3]^{+\bullet}$
									170.0 (55)	$[M+H-C_2NH_3-NH_3]^+$
									164.2 (20)	$[M+H-C_2NH_3-C_2NH_3+H_2O]^+$
									160.2 (100)	$[M+H-C_2NH_3-HCN]^+$
									146.1 (20)	$[M+H-C_2NH_3-C_2NH_3]^+$
					186.2 (6)	$[M+H-CN_2H_2]^+$				
					160.2 (8)	$[M+H-C_3N_2H_4]^+$				
TriMeIQx	242.3 (100)	$[M+H]^+$	40.7	0.45	242.2 (10)	$[M+H]^+$				
					227.2 (100)	$[M+H-CH_3]^{+\bullet}$	35.0	0.35	227.2 (40)	$[M+H-CH_3]^{+\bullet}$
									226.3 (100)	$[M+H-CH_3-H]^+$
									186.2 (10)	$[M+H-CH_3-C_2NH_3]^{+\bullet}$
									145.1 (10)	$[M+H-CH_3-C_4N_2H_6]^{+\bullet}$
					225.2 (17)	$[M+H-NH_3]^+$	36.5	0.40	225.2 (100)	$[M+H-NH_3]^+$
									210.3 (10)	$[M+H-NH_3-CH_3]^{+\bullet}$
									198.3 (50)	$[M+H-NH_3-HCN]^+$
									184.1 (20)	$[M+H-NH_3-C_2NH_3]^+$
					201.2 (97)	$[M+H-C_2NH_3]^+$	36.0	0.40	201.2 (35)	$[M+H-C_2NH_3]^+$
									186.1 (18)	$[M+H-C_2NH_3-CH_3]^{+\bullet}$
									184.1 (20)	$[M+H-C_2NH_3-NH_3]^+$
									174.2 (100)	$[M+H-C_2NH_3-HCN]^+$
									160.2 (8)	$[M+H-C_2NH_3-C_2NH_3]^+$
					200.2 (5)	$[M+H-CN_2H_2]^+$				
					174.2 (5)	$[M+H-C_3N_2H_4]^+$				
DMIP	163.2 (100)	$[M+H]^+$	40.7	0.45	163.2 (25)	$[M+H]^+$				
					148.2 (100)	$[M+H-CH_3]^{+\bullet}$	34.5	0.45	148.2 (62)	$[M+H-CH_3]^{+\bullet}$
									147.2 (100)	$[M+H-CH_3-H]^+$
									121.2 (31)	$[M+H-CH_3-HCN]^{+\bullet}$
									120.2 (34)	$[M+H-CH_3-H-HCN]^+$
									106.1 (24)	$[M+H-CH_3-CN_2H_2]^{+\bullet}$
									105.1 (25)	$[M+H-CH_3-CN_2H_2-H]^+$
					146.1 (32)	$[M+H-NH_3]^+$	34.0	0.45	146.1 (60)	$[M+H-NH_3]^+$
									119.2 (100)	$[M+H-NH_3-HCN]^+$
									105.2 (57)	$[M+H-NH_3-C_2NH_3]^+$
					136.2 (5)	$[M+H-HCN]^+$				
					122.1 (7)	$[M+H-C_2NH_3]^+$				
					121.1 (7)	$[M+H-CN_2H_2]^+$				
PhIP	225.3 (100)	$[M+H]^+$	42.7	0.45	225.3 (18)	$[M+H]^+$				
					210.2 (100)	$[M+H-CH_3]^{+\bullet}$	39.0	0.45	210.2 (66)	$[M+H-CH_3]^{+\bullet}$
									209.2 (70)	$[M+H-CH_3-H]^+$
									183.2 (100)	$[M+H-CH_3-HCN]^{+\bullet}$
									168.1 (50)	$[M+H-CH_3-CN_2H_2]^{+\bullet}$
					208.2 (20)	$[M+H-NH_3]^+$	37.0	0.45	208.2 (100)	$[M+H-NH_3]^+$
									181.2 (85)	$[M+H-NH_3-HCN]^+$
									167.1 (60)	$[M+H-NH_3-C_2NH_3]^+$

[a] See Table 1.

Table 4. Optimized CID conditions in MS^2 and MS^3 and main product ions obtained for carbolines[a]

	MS spectra		MS^2 CID conditions		MS^2 spectra		MS^3 CID conditions		MS^3 spectra	
Compound	m/z (rel. Ab%)	Tent. assign.	NCE (%)	AQ	m/z (rel. Ab%)	Tent. assign.	NCE (%)	AQ	m/z (rel. Ab%)	Tent. assign.
AαC	184.2 (100)	$[M+H]^+$	37.6	0.45	208.1 (34)	$[M+H-NH_3+ACN]^+$	27.0	0.45	208.1 (20)	$[M+H-NH_3+ACN]^+$
									185.2 (100)	$[M+H-NH_3+H_2O]^+$
					185.2 (100)	$[M+H-NH_3+H_2O]^+$	42.0	0.45	208.1 (60)	$[M+H-NH_3+ACN]^+$
									185.2 (100)	$[M+H-NH_3+H_2O]^+$
									167.1 (15)	$[M+H-NH_3]^+$
					184.2 (18)	$[M+H]^+$				
					167.1 (13)	$[M+H-NH_3]^+$	30.0	0.45	185.2 (100)	$[M+H-NH_3+H_2O]^+$
									167.1 (85)	$[M+H-NH_3]^+$
									140.2 (70)	$[M+H-NH_3-HCN]^+$
					157.2 (9)	$[M+H-HCN]^+$				
MeAαC	198.2 (100)	$[M+H]^+$	36.3	0.45	222.0 (20)	$[M+H-NH_3+ACN]^+$	35.0	0.45	222.0 (80)	$[M+H-NH_3+ACN]^+$
									199.2 (100)	$[M+H-NH_3+H_2O]^+$
					199.2 (100)	$[M+H-NH_3+H_2O]^+$	42.0	0.45	222.0 (60)	$[M+H-NH_3+ACN]^+$
									199.2 (100)	$[M+H-NH_3+H_2O]^+$
									181.2 (30)	$[M+H-NH_3]^+$
					198.2 (32)	$[M+H]^+$				
					183.2 (52)	$[M+H-CH_3]^{+\bullet}$	38.0	0.45	183.2 (34)	$[M+H-CH_3]^{+\bullet}$
									156.2 (100)	$[M+H-CH_3-HCN]^{+\bullet}$
					181.2 (20)	$[M+H-NH_3]^+$	32.5	0.45	199.2 (70)	$[M+H-NH_3+H_2O]^+$
									181.2 (100)	$[M+H-NH_3]^+$
									154.1 (60)	$[M+H-NH_3-HCN]^+$
					171.2 (5)	$[M+H-HCN]^+$				
Harman	183.3 (100)	$[M+H]^+$	43.0	0.45	183.3 (31)	$[M+H]^+$				
					182.2 (17)	$[M+H-H]^{+\bullet}$				
					181.2 (35)	$[M+H-2H]^+$	41.0	0.45	181.2 (35)	$[M+H-2H]^+$
									154.2 (100)	$[M+H-2H-HCN]^+$
					168.2 (100)	$[M+H-CH_3]^{+\bullet}$	39.0	0.45	168.2 (67)	$[M+H-CH_3]^{+\bullet}$
									167.2 (65)	$[M+H-CH_3-H]^+$
									141.2 (100)	$[M+H-CH_3-HCN]^{+\bullet}$
									140.2 (50)	$[M+H-CH_3-HCN-H]^+$
					167.2 (24)	$[M+H-CH_3-H]^+$	36.0	0.45	167.2 (90)	$[M+H-CH_3-H]^+$
									140.1 (100)	$[M+H-CH_3-H-HCN]^+$
					156.1 (16)	$[M+H-HCN]^+$				
					142.1 (24)	$[M+H-CH_3CN]^+$	30.0	0.45	142.1 (53)	$[M+H-CH_3CN]^+$
									115.2 (100)	$[M+H-CH_3CN-HCN]^+$
					115.1 (48)	$[M+H-C_3H_4N_2]^+$	41.0	0.45	115.1 (50)	$[M+H-C_3H_4N_2]^+$
									89.1 (100)	$[M+H-CH_3CN-HCN-C_2H_2]^+$
Norharman	169.2 (100)	$[M+H]^+$	43.6	0.45	169.2 (51)	$[M+H]^+$				
					168.2 (45)	$[M+H-H]^{+\bullet}$	36.5	0.45	168.2 (100)	$[M+H-H]^{+\bullet}$
									167.2 (40)	$[M+H-H-H]^+$
									141.2 (30)	$[M+H-H-HCN]^{+\bullet}$
					167.2 (72)	$[M+H-2H]^+$	36.0	0.45	181.1 (12)	$[M+H-2H-HCN+ACN]^+$
									167.2 (25)	$[M+H-2H]^+$
									140.2 (100)	$[M+H-2H]^+-HCN]^+$
					142.1 (92)	$[M+H-HCN]^+$	32.0	0.40	160.2 (5)	$[M+H-HCN+H_2O]^+$
									142.1 (40)	$[M+H-HCN]^+$
									115.2 (100)	$[M+H-HCN-HCN]^+$
					141.2 (43)	$[M+H-HCN-H]^{+\bullet}$	34.0	0.40	141.2 (100)	$[M+H-HCN-H]^{+\bullet}$
									140.1 (50)	$[M+H-HCN-H-H]^+$
									114.2 (60)	$[M+H-HCN-H-HCN]^{+\bullet}$
					140.1 (16)	$[M+H-HCN-2H]^+$				

(*continued overleaf*)

Table 4. (*Continued*)

Compound	MS spectra		MS² CID conditions		MS² spectra		MS³ CID conditions		MS³ spectra	
	m/z (rel. Ab%)	Tent. assign.	NCE (%)	AQ	*m/z* (rel. Ab%)	Tent. assign.	NCE (%)	AQ	*m/z* (rel. Ab%)	Tent. assign.
					115.1 (100)	$[M+H-2HCN]^+$	42.0	0.45	115.1 (40)	$[M+H-2HCN]^+$
									89.1 (100)	$[M+H-2HCN-C_2H_2]^+$
Trp-P-1	212.3 (100)	$[M+H]^+$	39.6	0.45	236.0 (15)	$[M+H-NH_3+ACN]^+$	26.0	0.45	236.0 (25)	$[M+H-NH_3+ACN]^+$
									213.2 (100)	$[M+H-NH_3+H_2O]^+$
					213.2 (35)	$[M+H-NH_3+H_2O]^+$	40.0	0.45	236.2 (35)	$[M+H-NH_3+ACN]^+$
									213.2 (50)	$[M+H-NH_3+H_2O]^+$
									195.2 (100)	$[M+H-NH_3]^+$
					212.3 (10)	$[M+H]^+$				
					197.2 (7)	$[M+H-CH_3]^{+\bullet}$				
					195.2 (100)	$[M+H-NH_3]^+$	35.0	0.45	213.2 (5)	$[M+H-NH_3+H_2O]^+$
									195.2 (35)	$[M+H-NH_3]^+$
									168.2 (100)	$[M+H-NH_3-HCN]^+$
					168.2 (5)	$[M+H-CN_2H_4]^+$				
Trp-P-2	198.4 (100)	$[M+H]^+$	39.6	0.45	222.1 (11)	$[M+H-NH_3+ACN]^+$	26.0	0.45	222.1 (47)	$[M+H-NH_3+ACN]^+$
									199.2 (100)	$[M+H-NH_3+H_2O]^+$
					199.2 (29)	$[M+H-NH_3+H_2O]^+$	39.0	0.45	222.1 (40)	$[M+H-NH_3+ACN]^+$
									199.2 (53)	$[M+H-NH_3+H_2O]^+$
									181.2 (100)	$[M+H-NH_3]^+$
					198.2 (12)	$[M+H]^+$				
					181.2 (100)	$[M+H-NH_3]^+$	31.0	0.45	199.2 (5)	$[M+H-NH_3+H_2O]^+$
									181.2 (60)	$[M+H-NH_3]^+$
									154.2 (100)	$[M+H-NH_3-HCN]^+$
					157.2 (17)	$[M+H-CH_3CN]^+$	33.0	0.45	157.2 (75)	$[M+H-CH_3CN]^+$
									130.2 (100)	$[M+H-CH_3CN-HCN]^+$
					154.1 (13)	$[M+H-CN_2H_4]^+$				
					130.1 (12)	$[M+H-C_3H_4N_2]^+$				
Glu-P-1	199.3 (100)	$[M+H]^+$	42.6	0.45	223.1 (7)	$[M+H-NH_3+ACN]^+$				
					200.2 (38)	$[M+H-NH_3+H_2O]^+$	40.5	0.45	223.1 (15)	$[M+H-NH_3+ACN]^+$
									200.2 (100)	$[M+H-NH_3+H_2O]^+$
									182.2 (30)	$[M+H-NH_3]^+$
					199.3 (18)	$[M+H]^+$				
					184.2 (89)	$[M+H-CH_3]^{+\bullet}$	38.0	0.45	184.2 (45)	$[M+H-CH_3]^{+\bullet}$
									157.2 (98)	$[M+H-CH_3-HCN]^{+\bullet}$
									144.1 (100)	$[M+H-CH_3-C_2NH_2]^+$
					182.2 (40)	$[M+H-NH_3]^+$	36.5	0.45	182.2 (100)	$[M+H-NH_3]^+$
									155.2 (35)	$[M+H-NH_3-HCN]^+$
					172.2 (100)	$[M+H-HCN]^+$	35.0	0.45	172.2 (33)	$[M+H-HCN]^+$
									145.1 (100)	$[M+H-HCN-HCN]^+$
					145.1 (16)	$[M+H-2HCN]^+$				
Glu-P-2	185.3 (100)	$[M+H]^+$	42.0	0.45	209.0 (8)	$[M+H-NH_3+ACN]^+$				
					186.2 (35)	$[M+H-NH_3+H_2O]^+$	40.0	0.35	209.0 (20)	$[M+H-NH_3+ACN]^+$
									186.2 (100)	$[M+H-NH_3+H_2O]^+$
									168.2 (10)	$[M+H-NH_3]^+$
					185.2 (9)	$[M+H]^+$				
					168.2 (18)	$[M+H-NH_3]^+$	37.0	0.45	186.2 (20)	$[M+H-NH_3+H_2O]^+$
									168.2 (75)	$[M+H-NH_3]^+$
									159.2 (100)	$[M+H-NH_3-HCN+H_2O]^+$
									141.2 (20)	$[M+H-NH_3-HCN]^+$
					158.1 (100)	$[M+H-HCN]^+$	32.5	0.45	158.1 (73)	$[M+H-HCN]^+$
									131.2 (100)	$[M+H-HCN-HCN]^+$
					131.0 (16)	$[M+H-2HCN]^+$				

[a] See Table 1.

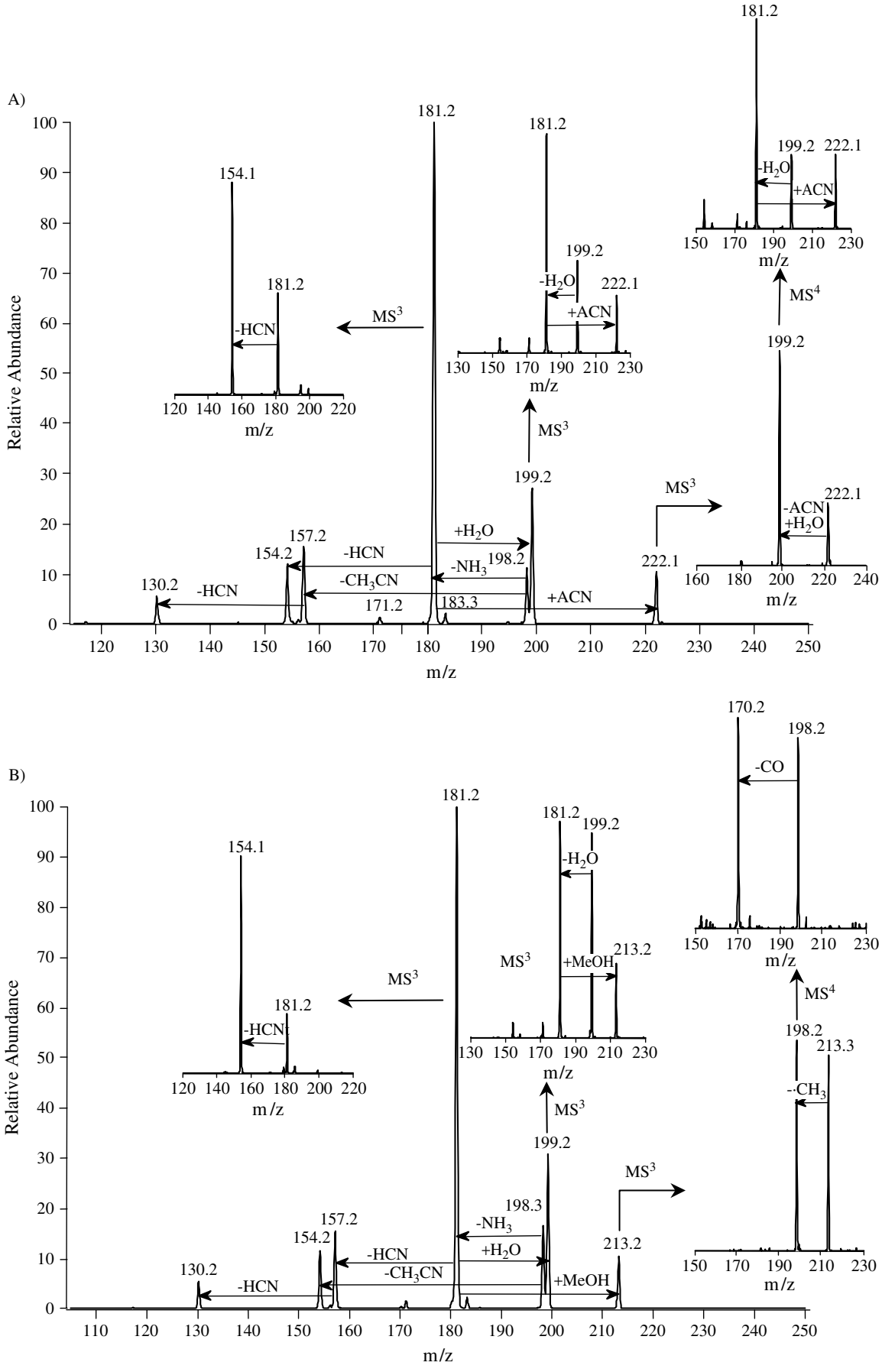

Figure 6. MS^2 spectra of Trp-P-2 and higher order mass spectra of some of the most important product ions. The infusion was carried out with mobile phase containing (A) acetonitrile and (B) methanol.

CONCLUSIONS

The use of multistep mass spectrometry in combination with the study of labelled compounds allowed the establishment of a fragmentation pattern for AIAs. The main fragmentation was produced in the aminoimidazole ring, thus the base peak in the MS^2 spectra arose from the loss of the methyl group, although quinoxalines also showed an intense peak corresponding to the loss of C_2NH_3 from the aminoimidazo moiety. Further fragmentation was mainly produced in the heterocyclic rings, and losses of $^{\bullet}H$ or HCN were observed, among others.

In the case of carbolines, the most abundant product ions arose from the loss of a methyl $[M + H - CH_3]^{+\bullet}$ for the methylated carbolines (MeAαC, harman and Glu-P-1), from the loss of ammonia $[M - NH_3]^+$ in the case of primary amines, and from the loss of HCN and/or CH_3CN from the heterocyclic rings for all the carbolines. Moreover, the study of the MS^n spectra of carbolines revealed the occurrence of ion–molecule reactions into the ion trap, which sometimes led to the base peak.

Acknowledgements

This work was carried out with financial support from the Commission of the European Community, specific RTD programme 'Quality of Life and Management of Living Resources,' project QLK1-CT99-01197 'Heterocyclic Amines in Cooked Foods—Role in Human Health.' Financial support was also provided by the Ministerio de Ciencia y Tecnología, project AGL2000-0948.

REFERENCES

1. Skog K, Johansson M, Jägerstad M. *Food and Chemical Toxicology* 1998; **36**: 879.
2. Jägerstad M, Skog K, Arvidsson P, Solyakov A. *Food Research and Technology* 1998; **207**: 419.
3. Toribio F, Puignou L, Galceran MT. *Journal of Chromatography B* 2000; **747**: 171.
4. Sugimura T, Nagao M, Wakabayashi K. *Mutation Research* 2000; **447**: 15.
5. Shirai T, Sano M, Tamano S, Takahashi S, Hirose M, Futakuchi M, Hasegawa R, Imaida K, Matsumoto K, Wakabayashi K, Sugimura T, Ito N. *Cancer Research* 1997; **57**: 195.
6. Slattery ML, Boucher KM, Caan BJ, Potter JD, Ma K-N. *American Journal of Epidemiology* 1998; **148**: 4.
7. Keating GA, Layton DW, Felton JS. *Mutation Research* 1999; **443**: 149.
8. Pais P, Knize MG. *Journal of Chromatography B* 2000; **747**: 139.
9. Felton JS, Knize MG, Shen NH, Andresen BD, Bjeldanes LF, Hatch FT. *Environmental Health Perspectives* 1986; **67**: 17.
10. Grose KR, Grant JL, Bjeldanes LF, Andresen BD, Healy SK, Lewis PR, Felton JS, Hatch FT. *Journal of Agricultural and Food Chemistry* 1986; **34**: 201.
11. Johansson M, Skog K, Jägerstad M. *Carcinogenesis* 1993; **14**: 89.
12. Manabe S, Kurihara N, Wada O, Izumikawa S, Asakuno K, Morita M. *Environmental Pollution* 1993; **80**: 281.
13. Hargraves WA, Pariza MW. *Cancer Research* 1983; **43**: 1467.
14. Vainiotalo S, Matveinen K, Reunanen A. *Fresenius' Journal of Analytical Chemistry* 1993; **345**: 462.
15. Murray S, Gooderham NJ, Barnes UF, Boobis AR, Davies DS. *Carcinogenesis* 1987; **8**: 937.
16. Lynch AM, Knize MG, Boobis AR, Gooderham NJ, Davies DS, Murray S. *Cancer Research* 1992; **52**: 6216.
17. Tikkanen LM, Latva-Kala KJ, Heiniö RL. *Food and Chemical Toxicology* 1996; **34**: 725.
18. Stillwell WG, Turesky RJ, Sinha R, Skipper PL, Tannenbaum SR. *Cancer Letters* 1999; **143**: 145.
19. Turesky RJ, Bur H, Huynh-Ba T, Aeschbacher HU, Milon H. *Food and Chemical Toxicology* 1988; **26**: 501.
20. Gross GA, Turesky RJ, Fay LB, Stillwell WG, Skipper PL, Tannenbaum SR. *Carcinogenesis* 1993; **14**: 2313.
21. Edmons CG, Sethi SK, Yamaizumi Z, Kasai H, Nishimura S, McCloskey JA. *Environmental Health Perspectives* 1986; **67**: 35.
22. Richling E, Herderich M, Schreier P. *Chromatographia* 1996; **42**: 7.
23. Fay LB, Ali S, Gross GA. *Mutation Research* 1997; **376**: 29.
24. Pais P, Moyano E, Puignou L, Galceran MT. *Journal of Chromatography A* 1997; **775**: 125.
25. Stillwell WG, Kidd LCR, Wishnok JS, Tannenbaum SR, Sinha R. *Cancer Research* 1997; **57**: 3457.
26. Kataoka H, Pawliszyn J. *Chromatographia* 1999; **50**: 532.
27. Pais P, Tanga MJ, Salmon CP, Knize MG. *Journal of Agricultural and Food Chemistry* 2000; **48**: 1721.
28. Knize MG, Kulp KS, Malfatti MA, Salmon CP, Felton JS. *Journal of Chromatography A* 2001; **914**: 95.
29. Gangl ET, Turesky RJ, Vouros P. *Analytical Chemistry* 2001; **73**: 2397.
30. Stavric B, Lau BPY, Matula TI, Klassen R, Lewis D, Downie RH. *Food and Chemical Toxicology* 1997; **35**: 185.
31. Holder CL, Preece SW, Conway SC, Pu YM, Doerge DR. *Rapid Communications in Mass Spectrometry* 1997; **11**: 1667.
32. Toribio F, Moyano E, Puignou L, Galceran MT. *Journal of Chromatography A* 2000; **869**: 307.
33. Guy PA, Gremaud E, Richoz J, Turesky RJ. *Journal of Chromatography A* 2000; **883**: 89.
34. Pais P, Moyano E, Puignou L, Galceran MT. *Journal of Chromatography A* 1997; **778**: 207.
35. Toribio F, Moyano E, Puignou L, Galceran MT. *Journal of Chromatography A* 2002; **948**: 267.
36. Zhao YI, Schelfaut M, Sandra P, Banks F. *Electrophoresis* 1998; **19**: 2213.
37. Reed DR, Kass SR. *Journal of the American Society for Mass Spectrometry* 2001; **12**: 1163.
38. Harrison AG. *Chemical Ionization Mass Spectrometry*. CRC Press: Boca Raton, FL, 1992.

ELSEVIER

Journal of Chromatography A, 948 (2002) 267–281

JOURNAL OF CHROMATOGRAPHY A

www.elsevier.com/locate/chroma

Ion-trap tandem mass spectrometry for the determination of heterocyclic amines in food

F. Toribio, E. Moyano, L. Puignou, M.T. Galceran*

Departament de Química Analítica, Universitat de Barcelona, Martí i Franquès 1-11, E-08028 Barcelona, Spain

Abstract

Heterocyclic amines (HAs) are mutagenic compounds to which humans are regularly exposed through diet. Due to the high complexity of the sample matrix and the low level of concentration of HAs, sensitive and selective analytical methodologies are required. Here we describe a methodology based on liquid chromatography–atmospheric pressure chemical ionisation tandem mass spectrometry using an ion-trap to analyse HAs. The collision-induced dissociation parameters for tandem ion-trap spectrometric analysis of these mutagenic compounds were optimised, and the full scan MS–MS spectra were used for unequivocal identification of the analytes. For aminoimidazoazaarenes, the most abundant ions were derived from the loss of a methyl group and the breaking of the aminoimidazole moiety, while for carbolines the major product ions arose from the loss of ammonia and HCN. Moreover, the performance of the LC–atmospheric pressure chemical ionisation MS–MS method was evaluated. The good precision (RSD lower than 11%) and the low detection limits achieved (10–60 pg injected) allow the determination of HAs at low part-per-billion level (0.4–5.0 ng g^{-1}) in a lyophilised meat extract.

Keywords: Food analysis; Amines, heterocyclic aromatic; Aminoimidazoazaarenes

1. Introduction

Diet is the main source of nutrients for humans; however, it can also contribute to the development of diseases [1]. As shown by several epidemiological studies, ~30–40% of cancers are related to diet [2,3]. Continuous exposure to mutagenic substances present in food, such as heterocyclic amines (HAs), can cause accumulated genetic alterations that can lead to the development of cancer [4]. Humans are regularly exposed to HAs through diet, since these compounds are produced during the cooking of meat and fish [5,6]. Depending on their chemical structure and their mechanism of formation, these xenobiotic genotoxic substances can be grouped into two main families. The first, named IQ type or amino-imidazoazaarenes (AIAs), includes mutagenic amines that have a 2-aminoimidazole group. These amines, also called thermic HAs, are generated from the reaction of free amino acids, creati(ni)ne and hexoses at ordinary cooking temperatures [7]. The other amines, called non-IQ type or pyrolytic HAs, are formed through the pyrolytic reaction of amino acids and proteins at temperatures above 300°C [8]. Some of these non-IQ type mutagens, the carbolines, contain a 2-aminopyridine moiety as a common structure.

To date, more than 25 HAs have been isolated from a number of food samples and model systems, and their structures elucidated. When tested both in

*Corresponding author. Tel.: +34-93-402-1100; fax: +34-93-402-1233.

E-mail address: galceran@apolo.qui.ub.es (M.T. Galceran).

0021-9673/02/$ – see front matter
PII: S0021-9673(01)01476-5

vivo and in vitro [9], most of these compounds are potent mutagens after metabolic activation. Harman and norharman are not mutagenic, but are considered comutagenic substances because they enhance the genotoxicity of mutagenic HAs. Moreover, the ten HAs so far tested in long-term animal experiments are carcinogenic in mice, rats and non-human primates [10,11]. These results support the hypothesis that HAs are involved in the aetiology of cancer. To establish the role of HAs in human health, an accurate determination of their dietary intake is required, which can be accomplished by combining information about types and quantities of food consumed and amounts of HAs in food products [12]. Nevertheless, the quantitative determination of HAs in food samples is mainly hindered by the low level of concentration of these microcomponents and the high complexity of the matrix. Therefore, the development of sensitive and selective analytical methodology is mandatory.

Until now, laborious clean-up procedures based on liquid–liquid extraction (LLE) [13], preparative liquid chromatography (LC) using different adsorbents [14], solid-phase extraction (SPE) with disposable columns [15] or tandem extraction procedures consisting of the coupling of LLE and SPE [16,17], have been developed. The sample treatment procedures employed in the analysis of mutagenic heterocyclic amines are reviewed in Ref. [18].

In addition, identification and quantification of HAs has been commonly carried out by means of chromatographic or related techniques [19]. Thus, gas chromatography (GC) with nitrogen-phosphorus selective detection (GC–NPD) [20] and gas chromatography–mass spectrometry (GC–MS) [21] have been used to analyse HAs. However, most of these compounds are polar and non-volatile, and consequently a derivatisation step is needed. This step can be avoided using liquid chromatography with different detection systems such as ultraviolet [22,23], electrochemical (ED) [24] and fluorescence [25] detection. Nevertheless, an essential aspect in the analysis of such complex matrices is the unequivocal identification of HAs. This can be efficiently achieved by coupling liquid chromatography with mass spectrometry (LC–MS) [26,27], a highly selective and sensitive detection system. To enhance the selectivity of the detection, LC–MS–MS using triple quadrupole [15,28–33] or ion-trap [34] instruments has been used. Recently, capillary electrophoresis, either with mass spectrometry (CE–MS) [35], ultraviolet (CE–UV) [36] or electrochemical (CE–ED) detection [37], has also been proposed although high detection limits have been obtained.

Here we describe a method based on LC–atmospheric pressure chemical ionisation (APCI) ion-trap (IT) MS–MS for the analysis of 16 HAs. The characteristic MS–MS spectrum of each analyte was used for unequivocal identification, which is important when real food samples are analysed. The LC–APCI-MS–MS method was used to determine HAs in a lyophilised meat extract [38]. To purify the sample, two tandem clean-up procedures were tested, both based on the well-known Gross method [16,17] which uses the coupling of LLE with diatomaceous earth as solid support and two SPE steps with propylsulfonic acid (PRS) and C_{18}.

2. Experimental

2.1. Chemicals

The solvents and chemicals used were HPLC or analytical grade, and the water was purified in an Elix-Milli-Q system (Millipore, Bedford, MA, USA). All the solutions were passed through a 0.45-μm nylon filter (Whatman, Clifton, NJ, USA) before injection into the HPLC system.

The compounds studied (Fig. 1) were 2-amino-3-methylimidazo[4,5-*f*]quinoline (IQ), 2-amino-3-trideuteromethylimidazo[4,5-*f*]quinoline (D_3-IQ), 2-amino-3,4-dimethylimidazo[4,5-*f*]quinoline (MeIQ), 2-amino-3,8-dimethylimidazo[4,5-*f*]quinoxaline (MeIQx), 2-amino-8-methyl-3-trideuteromethylimidazo[4,5-*f*]quinoxaline (D_3-MeIQx), 2-amino-3,4,8-trimethylimidazo[4,5-*f*]quinoxaline (4,8-DiMeIQx), 2-amino-3,7,8-trimethylimidazo[4,5-*f*]quinoxaline (7,8-DiMeIQx), 2-amino-3,4,7,8-tetramethylimidazo-[4,5-*f*]quinoxaline (TriMeIQx), 2-amino-1-methyl-6-phenylimidazo[4,5-*b*]pyridine (PhIP), 2-amino-1-trideuteromethyl-6-phenylimidazo[4,5-*b*]pyridine (D_3-PhIP), 2-amino-1,6-dimethylimidazo[4,5-*b*]pyridine (DMIP), 2-amino-9*H*-pyrido[2,3-*b*]indole (AαC), 2-amino-3-methyl-9*H*-pyrido[2,3-*b*]indole (MeAαC), 3-amino-1,4-dimethyl-5*H*-pyrido[4,3-*b*]indole (Trp-

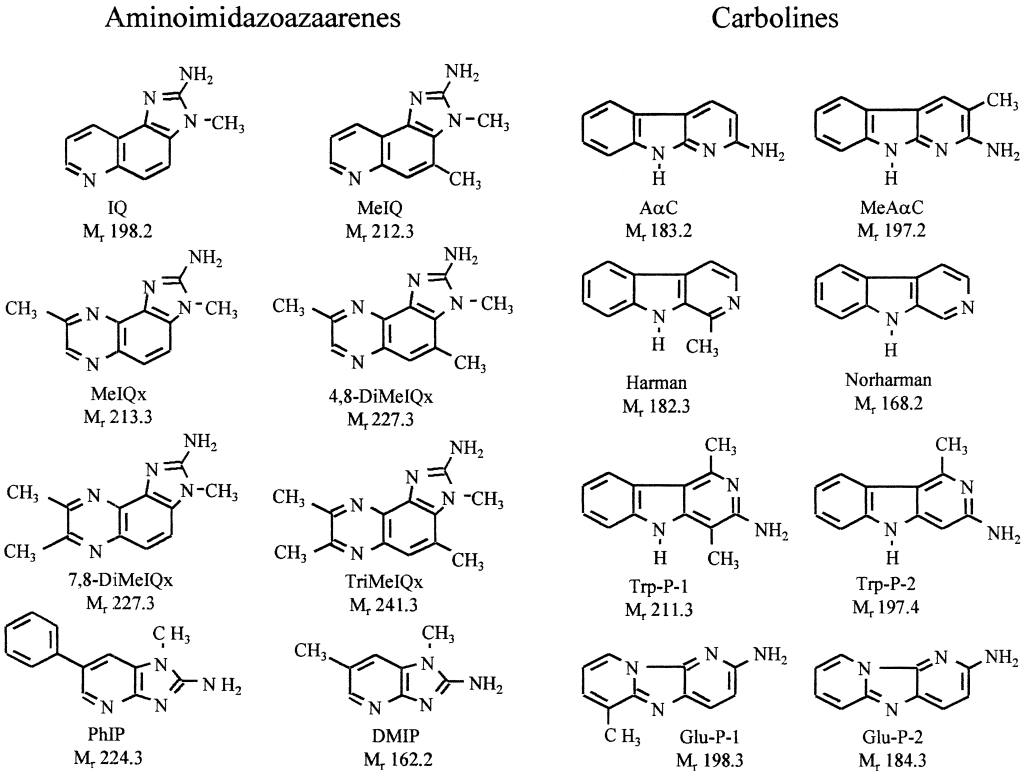

Fig. 1. Structure, abbreviated name and molecular mass of the compounds.

P-1), 3-amino-1-methyl-5*H*-pyrido[4,3-*b*]indole (Trp-P-2), 2-amino-6-methyldipyrido[1,2-*a*:3′,2′-*d*]imidazole (Glu-P-1) and 2-aminodipyrido[1,2-*a*:3′,2′-*d*]-imidazole (Glu-P-2), purchased from Toronto Research Chemicals (Toronto, Canada), and 1-methyl-9*H*-pyrido[3,4-*b*]indole (harman) and 9*H*-pyrido[3,4-*b*]indole (norharman), which were from Sigma (Steinheim, Germany). Stock standard solutions of 130 μg g^{-1} in methanol were prepared and used for further dilution. TriMeIQx was used as internal standard (1.2 μg g^{-1} methanolic solution).

Empty Extrelut-20 extraction cartridges were provided by Merck (Darmstadt, Germany), and Isolute diatomaceous earth refill material was obtained from IST (Hengoed, UK). Bond Elut PRS (500 mg) and endcapped Bond Elut C_{18} (100 and 500 mg) cartridges were from Varian (Harbor City, USA), and Isolute PRS (200 mg) and endcapped tridimensional Isolute C_{18} (100 mg) cartridges were from IST. Coupling pieces and stopcocks were purchased from Varian. A lyophilised meat extract was prepared from a commercial meat extract (Bovril) as described in Ref. [38].

2.2. Sample analysis

Two previously described purification methods [27,39] with some minor modifications were used to extract analytes from a lyophilised meat extract. Sample preparation method A was as follows. A 1-g sample of beef extract was homogenised in 12 ml 1 *M* NaOH with sonication, and the suspension was then shaken for 3 h using a rotating shaker Rotary Mixer 34526 (Breda Scientific, Breda, The Netherlands). The alkaline solution was mixed with Extrelut refill material (14 g) and was used to fill an empty Extrelut column. After being preconditioned with 7 ml dichloromethane (DCM), an Isolute PRS column was coupled on-line to the Extrelut column. To extract the analytes from diatomaceous earth, 75 ml of dichloromethane were passed through the tandem. The PRS cartridge was then dried and successively

rinsed with 15 ml methanol–water (4:6, v/v) and 2 ml water. The cationic exchanger column was then coupled to an Isolute C_{18} column, previously conditioned with 5 ml MeOH and 5 ml water, and HAs were then eluted with 20 ml of 0.5 *M* ammonium acetate at pH 8.5. Finally, the C_{18} cartridge was rinsed with 5 ml water and the sorbed HAs were eluted using 0.8 ml of methanol–ammonia (9:1, v/v). The solvent was gently evaporated under a stream of nitrogen and the analytes were redissolved in 50 μl of the internal standard in methanol.

For method B, the cation-exchange column was a Bond Elut PRS column. The washing solutions arising from this cartridge, which consisted of 6 ml 0.01 *M* HCl, 15 ml MeOH–0.1 *M* HCl (6:4, v/v) and 2 ml of water, were collected for the analysis of the less polar compounds (PhIP; α-carbolines: AαC and MeAαC; β-carbolines: harman and norharman; γ-carbolines: Trp-P-1 and Trp-P-2). After lowering their organic solvent content by adding 25 ml of water, the acidic washing solutions were neutralised with 500 μl ammonia. Less polar HAs were preconcentrated in a 500-mg Bond Elut C_{18} column, which had previously been conditioned with 5 ml of MeOH and 5 ml of water. Finally, the reversed-phase minicolumn was washed with 5 ml water and the analytes were eluted with 1.4 ml MeOH–ammonia (9:1, v/v). On the other hand, a 100-mg Bond Elut C_{18} cartridge was conditioned with 5 ml MeOH and 5 ml water, and was then coupled on-line with the PRS cartridge. After that, the most polar amines (DMIP; δ-carbolines: Glu-P-1 and Glu-P-2; aminoimidazoquinolines: IQ and MeIQ; aminoimidazoquinoxalines: MeIQx, 4,8-DiMeIQx and 7,8-DiMeIQx) were eluted from the cationic exchanger with 20 ml of 0.5 *M* ammonium acetate at pH 8.5. Finally, the C_{18} cartridge containing the most polar analytes was rinsed with 5 ml water and the sorbed HAs were eluted using 0.8 ml of methanol–ammonia (9:1, v/v). The extracts containing either the most or least polar analytes were gently evaporated to dryness under a stream of nitrogen and were then redissolved in 50 μl of the internal standard in methanol.

A Supelco Visiprep and a Visidry SPE vacuum manifold (Supelco, Gland, Switzerland) were used to manipulate the solid-phase extraction cartridges and solvent evaporation, respectively. The final extracts from both clean-up procedures were analysed using the LC–MS–MS method described in the next section.

Quantification and recovery calculation of the amines in the beef extract was carried out by standard addition. Before sample treatment, the meat extract was spiked at three different levels (50, 100 and 200 ng) by adding a methanolic solution of the analytes (4 μg g^{-1}). The solvent was allowed to evaporate for 30 min before applying the sample extraction procedure. Furthermore, D_3-IQ, D_3-MeIQx and D_3-PhIP were added to the meat extract at ~50 ng g^{-1}. Duplicate analyses of all the samples, including the fortified samples, were carried out.

2.3. Chromatographic conditions

LC was performed using a Waters 2690 Separations Module (Milford, MA, USA), equipped with a quaternary solvent delivery system and an autosampler. Amines were separated by reversed-phase LC using a TSK-Gel ODS 80T column (5 μm, 25.0×4.6 mm I.D.) (TosoHaas, Stuttgart, Germany) equipped with a Supelguard LC-8-DB precolumn (Supelco, Bellefonte, PA, USA).

Optimal separation was achieved with a ternary mobile phase at a flow-rate of 1 ml min^{-1}. Solvent A: 30 m*M* formic acid in water adjusted to pH 3.25 with a solution of ammonia; solvent B: 30 m*M* formic acid in water adjusted to pH 3.7 with a solution of ammonia; solvent C: acetonitrile. The gradient elution program was: 5–23% C in A, 0–18 min; 23% C in A, 18–21 min; 23% C in B, 21–25 min; 23–60% C in B, 25–33 min; 60% C in B, 33–40 min; return to the initial conditions, 40–50 min; 5 min equilibration. In all cases the amount injected was 15 μl.

2.4. Mass spectrometric conditions

MS analysis was carried out with an LCQ mass spectrometer (Finnigan MAT, San Jose, CA, USA) which operated using Excalibur 1.0 SR1 software. The mass spectrometer was provided with an atmospheric pressure chemical ionisation source and an ion trap as mass analyser. To prevent mass spectrometer contamination when running LC–MS, a divert valve

was used for a few minutes at the beginning of the chromatogram.

Optimal source working conditions for monitoring positive ions were as follows: spray current and discharge voltage were 5 μA and 5 kV, respectively; heated capillary temperature was 150°C, and that of the vaporiser 450°C; nitrogen was used as sheath gas at 72 l h^{-1} and as auxiliary gas at 360 l h^{-1}. The chromatographic separation was divided into three segments, corresponding to different eluting conditions (first segment: 0–18.5 min, second segment: 18.5–26 min, third segment: 26–40 min). Efficiency of ion transference from source to the ion trap was automatically optimised for each segment by infusing methanolic solutions of IQ, 4,8-DiMeIQx and Trp-P-1, respectively. Collision-induced dissociation (CID) conditions were optimised for each analyte as follows. Individual methanolic solutions (10 μg g^{-1}) were infused using a syringe pump (3 μl min^{-1}) and were mixed with the mobile phase corresponding to the eluting conditions of each HA by means a tee piece. Working activation Q (AQ) was 0.45, normalised collision energy (NCE) ranged from 36.3 to 43.6% and activation time (AT) was 30 ms. For data acquisition in full scan mode, the mass spectrometer operated over a range of m/z 150–250, and in full scan MS–MS the masses scanned varied from m/z 110 to m/z 250 (Table 1). In all cases, the acquisition of positive ions was performed in centroid mode, with a maximum injection time of 100 ms, three microscans, the automatic gain control activated and the inject waveform disconnected.

3. Results and discussion

3.1. Tandem mass spectrometry

In the positive mode, APCI provided only the peak corresponding to the protonated molecule ion $[M+H]^+$ in agreement with literature data [40,41]. Therefore, this ion was used as a precursor in MS–MS experiments. First of all, the effect of the value of isolation width (IW) on precursor ion intensity was studied. Maximum trapping efficiency, without interferences from isotopic species, was achieved using an IW of 1.5.

Fragmentation of precursor ions in an ion trap occurs by CID when a resonance excitation voltage is applied to the endcap electrodes. While the stability range of both precursor and product ions is defined by the magnitude of the trapping radio-frequency voltage (AQ) applied to the ring electrode, the energy applied is controlled by the amplitude (NCE) and the duration (AT) of the voltage applied to the endcap electrodes.

To determine the stability range of ions and to choose the optimum value for AQ, individual methanolic solutions (~10 μg g^{-1}) of HAs were infused at different AQ values ranging from 0 to 0.9. For precursor ions, NCE was zero, while for product ions an NCE value high enough to provide the major product ion as the base peak was used. AT was fixed at 30 ms for both precursor and product ions. As an example, Fig. 2 shows the AQ curves obtained for some of the compounds studied. Similar behavior was observed for all the HAs: while the precursor ions had a wide stability range, the product ions were stable in a narrower interval. An optimum AQ value of 0.45, which was inside the stability range of the precursor ions, was chosen to maximise the intensity of product ions.

The CID energy needed to fragment the precursor ion was optimised by studying the effect of NCE and AT on product ion intensity. For each compound, AQ was set at 0.45, AT was kept at 30 ms and NCE was varied from 0 to 70%. The precursor ions started to fragment at ~30% (Fig. 3). Beyond this value, an increase in NCE produced an enhancement of product ions intensity compared with the unfragmented precursor ion. At higher values, the abundance of product ions was generally constant and, in some cases, a decrease in the signal was produced because of further fragmentation. The optimum NCE value was selected to provide a maximum intensity of the product ion keeping a significant signal for the precursor ion. Finally, AQ and NCE were fixed to their selected values, and AT was studied between 20 and 40 ms, verifying that the optimum AT value was 30 ms. The final MS–MS working conditions are summarised in Table 1, together with a list of the main product ions for each compound and their tentative assignation.

In general, the most intense product ion in the MS–MS spectra of AIAs (aminoimidazoquinolines: IQ and MeIQ; aminoimidazoquinoxalines: MeIQx,

Table 1
Selected MS–MS conditions and product ions used for quantification of HAs

Analyte	MS spectra		MS–MS CID[a]	Product ions used for quantification		Full scan MS–MS range
	m/z (Rel.Ab.%)	Tentative Assign.	NCE (%)	*m/z* (Rel.Ab.%)	Tentative Assign.	
DMIP	163.2 (100)	$[M+H]^+$	40.7	148.2 (100)	$[M+H\text{-}CH_3]^{+\cdot}$	[140.0–170.0]
Glu-P-2	185.3 (100)	$[M+H]^+$	42.8	158.1 (100)	$[M+H–HCN]^+$	[150.0–190.0]
IQ	199.2 (100)	$[M+H]^+$	41.0	184.2 (100)	$[M+H–CH_3]^{+\cdot}$	[150.0–205.0]
MeIQ	213.3 (100)	$[M+H]^+$	40.3	198.2 (100)	$[M+H–CH_3]^{+\cdot}$	[165.0–220.0]
Glu-P-1	199.3 (100)	$[M+H]^+$	43.7	184.2 (89)	$[M+H–CH_3]^{+\cdot}$	[165.0–210.0]
				172.2 (100)	$[M+H–HCN]^+$	
MeIQx	214.3 (100)	$[M+H]^+$	41.3	199.2 (100)	$[M+H–CH_3]^{+\cdot}$	[165.0–220.0]
				173.2 (87)	$[M+H–C_2NH_3]^+$	
7,8-DiMeIQx	228.3 (100)	$[M+H]^+$	42.2	213.2 (89)	$[M+H–CH_3]^{+\cdot}$	[180.0–235.0]
				187.2 (100)	$[M+H–C_2NH_3]^+$	
4,8-DiMeIQx	228.3 (100)	$[M+H]^+$	41.1	213.3 (100)	$[M+H–CH_3]^{+\cdot}$	[180.0–235.0]
				187.2 (90)	$[M+H–C_2NH_3]^+$	
Norharman	169.2 (100)	$[M+H]^+$	44.6	167.2 (82)	$[M+H–2H]^+$	[110.0–175.0]
				142.1 (92)	$[M+H–HCN]^+$	
				115.1 (100)	$[M+H–2HCN]^+$	
TriMeIQx	242.3 (100)	$[M+H]^+$	41.3	227.2 (100)	$[M+H–CH_3]^{+\cdot}$	[195.0–250.0]
				201.2 (97)	$[M+H–C_2NH_3]^+$	
Harman	183.3 (100)	$[M+H]^+$	43.7	181.2 (40)	$[M+H–2H]^+$	[110.0–190.0]
				168.2 (100)	$[M+H–CH_3]^{+\cdot}$	
				115.1 (48)	$[M+H–CH_3CN–HCN]^+$	
Trp-P-2	198.4 (100)	$[M+H]^+$	40.3	222.1 (11)	$[M+H–NH_3+ACN]^+$	[175.0–225.0]
				199.2 (29)	$[M+H–NH_3+H_2O]^+$	
				181.1 (100)	$[M+H–NH_3]^+$	
PhIP	225.3 (100)	$[M+H]^+$	43.2	210.2 (100)	$[M+H–CH_3]^{+\cdot}$	[200.0–230.0]
Trp-P-1	212.3 (100)	$[M+H]^+$	40.1	236.0 (15)	$[M+H–NH_3+ACN]^+$	[190.0–240.0]
				213.2 (35)	$[M+H–NH_3+H_2O]^+$	
				195.2 (100)	$[M+H–NH_3]^+$	
AαC	184.2 (100)	$[M+H]^+$	38.5	208.1 (34)	$[M+H–NH_3+ACN]^+$	[165.0–215.0]
				185.2 (100)	$[M+H–NH_3+H_2O]^+$	
				167.1 (13)	$[M+H–NH_3]^+$	
MeAαC	198.2 (100)	$[M+H]^+$	37.2	222.0 (29)	$[M+H–NH_3+ACN]^+$	[175.0–225.0]
				199.2 (100)	$[M+H–NH_3+H_2O]^+$	
				183.2 (52)	$[M+H–CH_3]^{+\cdot}$	
				181.2 (20)	$[M+H–NH_3]^+$	

[a] In all cases, AQ value was 0.45 and AT was 30 ms.

7,8-DiMeIQx, 4,8-DiMeIQx and TriMeIQx; aminoimidazopyridines: DMIP, PhIP) arose from the loss of the 2-methyl group $[M+H–CH_3]^{+\cdot}$, as confirmed by the study of D_3-IQ, D_3-MeIQx and D_3-PhIP. The relative abundance of this fragment ion ranged from 89 to 100%. Moreover, aminoimidazoquinoxalines showed the cleavage of the aminoimidazole moiety $[M+H–C_2NH_3]^+$, with relative abundances from 87 to 100%. These fragmentation patterns are consistent with those obtained by other authors using triple quadrupole instruments [28,32,33].

In the case of carbolines (α-carbolines: AαC and MeAαC; β-carbolines: harman and norharman; γ-carbolines: Trp-P-1 and Trp-P-2; δ-carbolines: Glu-P-1 and Glu-P-2), the most abundant fragment ions were derived from the loss of a methyl $[M+H–CH_3]^{+\cdot}$ for the methylated carbolines (MeAαC, harman and Glu-P-1, relative abundances ranging

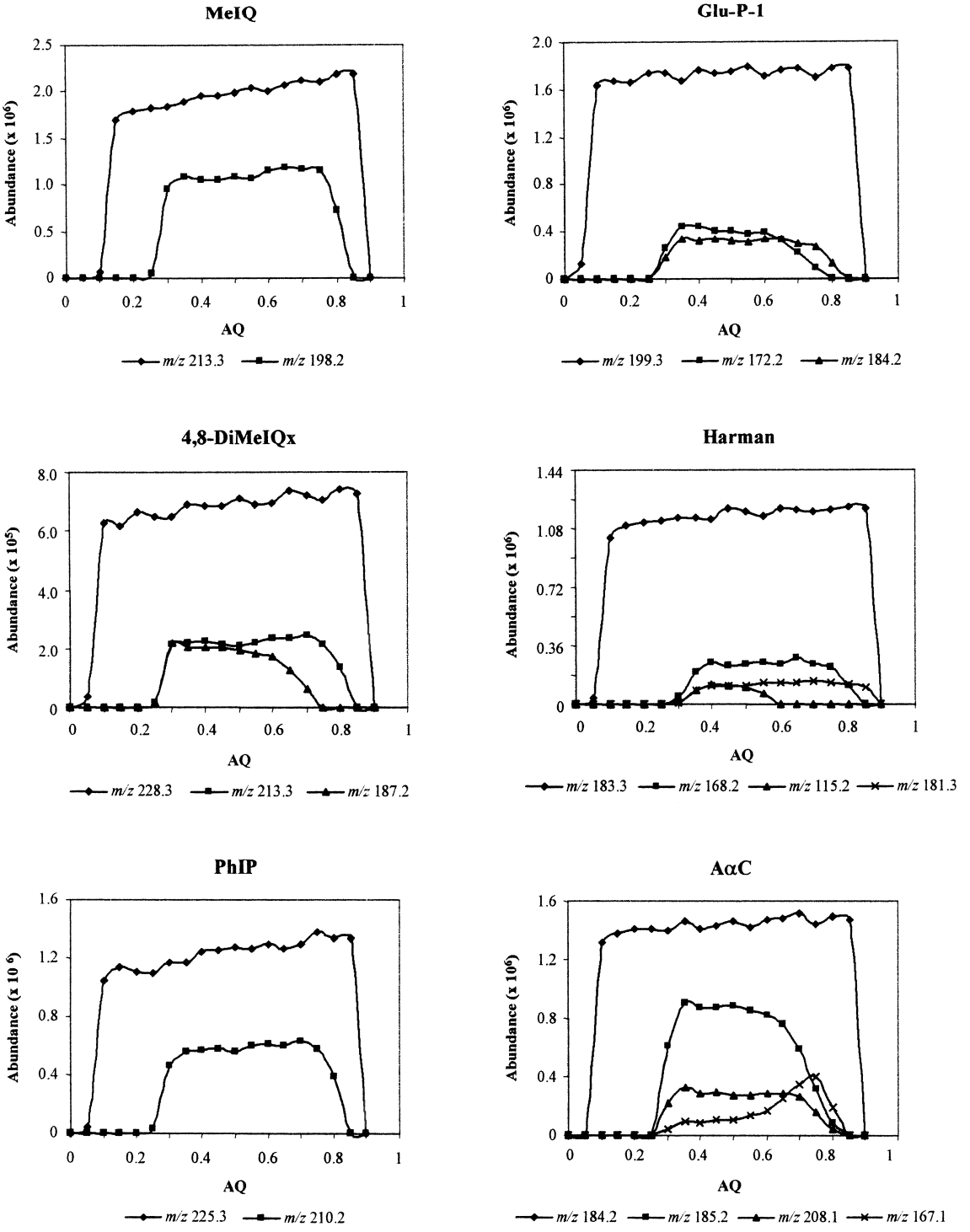

Fig. 2. Variation of precursor and product ion abundance as a function of the trapping radiofrequency voltage (AQ).

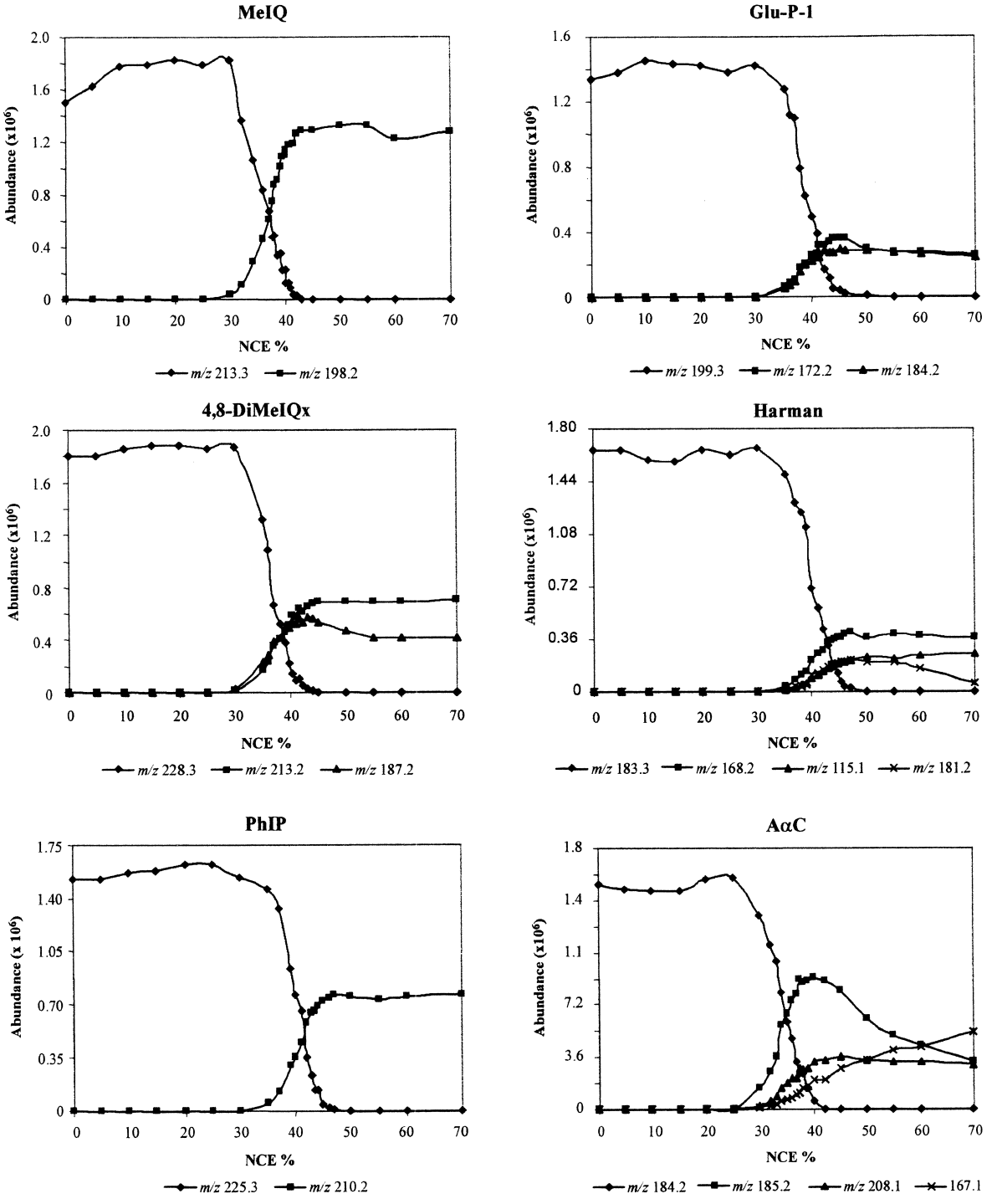

Fig. 3. Variation of precursor and product ion abundance as a function of the normalised collision energy (NCE).

from 52 to 100%), from the loss of ammonia $[M-NH_3]^+$ in the case of primary amines (100% of relative abundance for γ-carbolines, and in the range 13–20% for α-carbolines), and from the loss of HCN (100% for δ-carbolines and 92% for norharman). Moreover, other important fragment ions in the MS–MS spectra of harman and norharman corresponded to the loss of hydrogen atoms $[M-2H]^+$. In some cases, recombination of $[M+H-NH_3]^+$ with neutral molecules present in the ion trap, such as water or acetonitrile, was observed. These adducts are so abundant that, for instance, for α-carbolines they corresponded to the base peak, and for γ-carbolines they reached a relative abundance of 35%. The identity of these adducts was confirmed by changing the organic solvent of the mobile phase and also by carrying out higher-order multiple MS (MS^n) experiments. These adducts have not been observed by other authors working with triple quadrupole instruments [15,28].

Product ions with a relative abundance greater than 50% were chosen for the LC–MS–MS quantitative analysis. In the case of α-carbolines and γ-carbolines, the ion $[M-NH_3]^+$ and the adducts with water and acetonitrile were used to enhance the robustness of the quantitative analysis.

3.2. Performance of the LC–APCI-MS–MS method

Fig. 4 shows the chromatogram obtained after the injection of a standard solution (4 μg g^{-1}) at the selected conditions. A good resolution was obtained and the individual trace chromatograms were almost free of background noise.

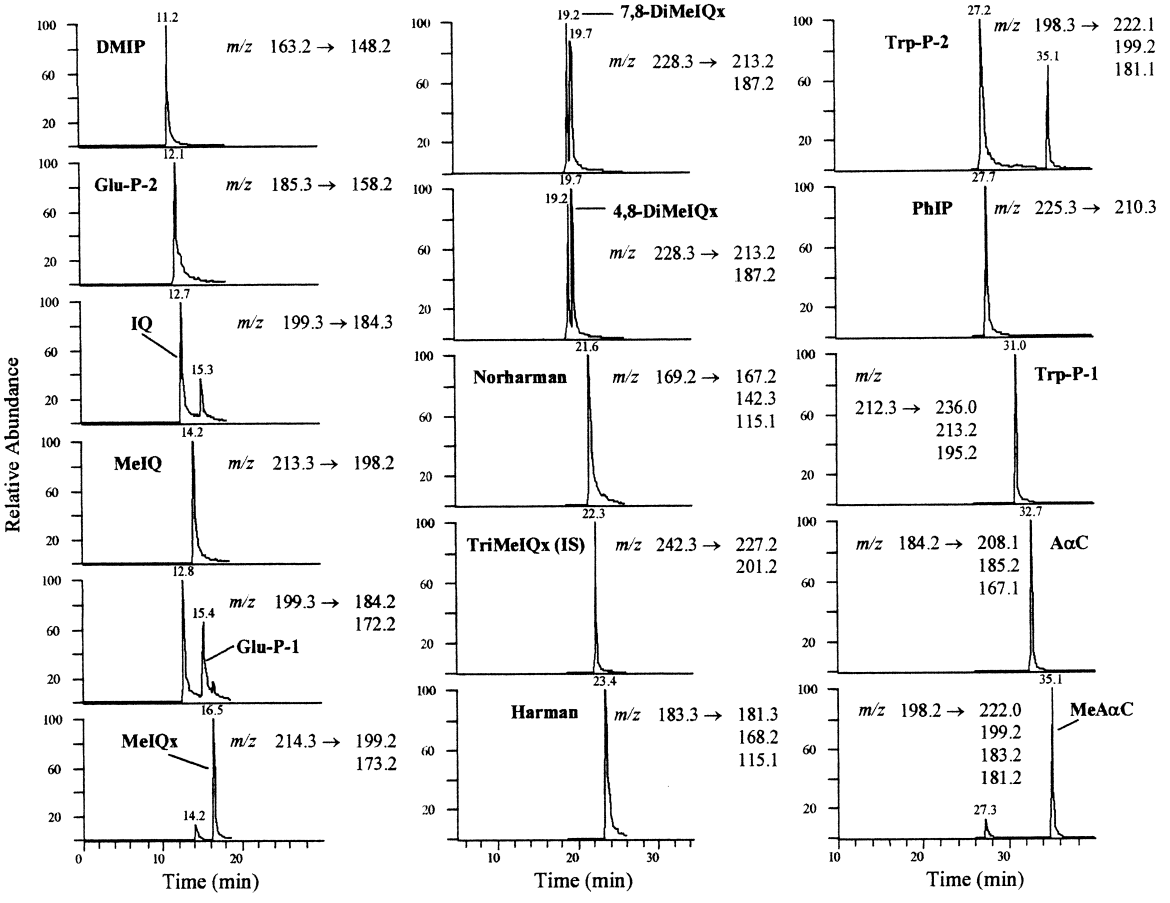

Fig. 4. LC–APCI-MS–MS chromatogram obtained for a standard solution (4 μg g^{-1}).

Calibration curves for the chromatographic method were performed at six concentration levels from 0.1 to 7.1 μg g^{-1} for each analyte. These curves were calculated daily from the representation of the ratio of the peak area of the analytes to the peak area of the internal standard (TriMeIQx) versus the ratio of the concentration of each compound to the concentration of the internal standard. Curves were fitted to a linear function, obtaining regression coefficients higher than 0.995 in all cases. To evaluate the analytical performance of the LC–MS–MS method, several quality parameters (repeatability or run-to-run precision, medium term or day-to-day precision and limit of detection) were determined. To calculate repeatability and medium term precision, five daily replicate analysis of a methanolic solution of all the analytes at ~1 μg g^{-1} were carried out on 3 successive days. A study of the variance of one factor for concentration and retention time was then performed. The RSD for concentration varied from 3.2 to 9.3% for run-to-run precision, and from 4.2 to 11.0% for day-to-day precision. For retention times, run-to-run precision, expressed as RSD, was between 0.1 and 0.5%, and day-to-day precision between 0.1 and 1.2% (Table 2).

Detection limits (LODs), based on a signal-to-noise ratio of 3:1, were determined in standard solutions and meat extracts. Full scan MS–MS LODs using standard solutions were from 2- to 8-fold lower than those obtained using full scan MS (Table 3). In the case of the meat extract, LODs were determined by fortifying blank samples at very low levels. For harman and norharman, which were present in the blank samples, LODs were obtained by extrapolating from a non-spiked sample. A comparison of LODs expressed as injected amount for standard solutions and meat extract (Table 3) shows that the LOD values were higher in the sample because of the effect of matrix on ionisation. Moreover, the improvement of LODs in MS–MS was greater in the sample than in the standard solutions, and this effect was more pronounced for the polar HAs using method A. This observation can be explained by the high selectivity of MS–MS, which allows reduction of background, thereby improving the signal-to-noise ratio.

In general and for both sample treatment procedures, limits of detection in the sample using full scan MS–MS were ~1 ng g^{-1}, which is a low value for such a complex sample. Except for DMIP,

Table 2
Run-to-run precision and day-to-day precision of the method for a standard solution

Analyte	Target conc. (μg g^{-1})	Mean value		Precision RSD % (n=15, α= 0.05)			
		Conc. (μg g^{-1})	t_r (min)	Conc.		t_r	
				Run-to-run	Day-to-day	Run-to-run	Day-to-day
DMIP	1.0502	1.078	11.2	5.7	7.7	0.1	1.0
Glu-P-2	1.0504	1.053	12.1	4.7	6.7	0.1	1.0
IQ	1.0445	1.058	12.8	4.9	5.5	0.5	1.0
MeIQ	1.0567	1.076	14.3	4.9	6.3	0.1	0.9
Glu-P-1	1.0447	1.049	15.4	5.0	10.1	0.1	0.9
MeIQx	1.0590	1.069	16.6	5.4	9.5	0.1	0.9
7,8-DiMeIQx	1.0690	1.096	19.2	6.4	10.6	0.1	0.8
4,8-DiMeIQx	1.0659	1.108	19.7	4.9	7.9	0.1	0.7
Norharman	1.0450	1.079	21.8	4.3	7.7	0.1	0.8
Harman	1.0278	1.093	23.6	4.6	4.2	0.1	0.8
Trp-P-2	1.0422	1.057	27.4	3.2	6.1	0.1	1.2
PhIP	1.0345	1.057	27.7	4.4	7.1	0.2	1.1
Trp-P-1	1.0378	1.139	31.0	6.3	10.5	0.1	0.6
AαC	1.0322	1.017	32.7	9.3	9.8	0.1	0.3
MeAαC	1.0401	1.026	35.1	7.7	11.0	0.1	0.1

Table 3
Limits of detection (LODs) in full scan MS and full scan MS–MS for a standard solution and a meat extract

Analyte	Standard solution				Meat extract							
	ng g^{-1}		Injected pg		Injected ng				ng g^{-1}			
	Full scan MS	Full scan MS–MS	Full scan MS	Full scan MS–MS	Full scan MS		Full scan MS–MS		Full scan MS		Full scan MS–MS	
					Clean-up A	Clean-up B	Clean-up A	Clean-up B	Clean-up A	Clean-up B	Clean-up A	Clean-up B
DMIP	18.8	2.3	358	44	6.7	3.3	0.7	0.5	101.0	32.2	10.3	4.9
Glu-P-2	14.8	2.4	283	45	5.0	2.9	0.5	0.7	11.9	11.5	1.2	2.7
IQ	12.3	2.0	235	38	4.8	3.2	0.5	0.5	10.6	14.7	1.0	2.3
MeIQ	10.6	2.0	202	39	4.7	3.3	0.5	0.5	10.4	16.6	1.1	2.4
Glu-P-1	13.6	2.1	259	41	5.4	3.3	0.7	1.0	13.5	14.7	1.7	4.6
MeIQx	10.2	1.2	196	24	3.9	2.2	0.5	0.4	10.0	9.2	1.2	1.6
7,8-DiMeIQx	4.1	1.7	79	33	2.6	2.0	0.4	0.4	6.7	9.1	0.9	1.5
4,8-DiMeIQx	3.4	1.8	66	34	2.7	1.9	0.4	0.3	6.4	9.4	1.0	1.7
Norharman	11.2	3.4	215	64	2.9[a]	3.0[a]	0.5[a]	0.5[a]	9.7[a]	10.1[a]	1.8[a]	1.6[a]
Harman	8.3	2.4	158	46	3.2[a]	3.5[a]	0.9[a]	0.8[a]	10.6[a]	11.5[a]	3.0[a]	2.5[a]
Trp-P-2	3.3	1.0	62	18	2.4	2.3	0.3	0.3	5.5	12.3	0.8	1.7
PhIP	2.1	0.8	41	16	2.8	2.7	0.3	0.3	6.5	13.5	0.7	1.6
Trp-P-1	2.8	0.6	53	12	2.0	2.0	0.4	0.7	4.3	9.2	0.8	3.1
AαC	2.1	0.5	40	10	0.6	0.7	0.1	0.1	2.0	4.8	0.4	1.0
MeAαC	2.4	0.6	46	11	0.6	0.5	0.1	0.2	1.8	2.9	0.4	0.8

[a] Extrapolated from the non-spiked meat extract.

slightly lower detection limits were achieved with clean-up method A, probably because of its higher extraction efficiency.

3.3. Determination of HAs in a meat extract

After optimisation of the chromatographic and spectrometric conditions, the LC–MS–MS method was used to analyse HAs in a lyophilised meat extract and the chromatogram is given in Fig. 5. The tandem mass spectrometry technique provided a high degree of selectivity, leading to chromatograms that were almost free of interfering peaks. Moreover, false peak identification was avoided by comparing the product ion full scan mass spectra of the sample with those of standards. Thus, we confirmed the presence of nine HAs in the sample. As an example, Fig. 6 shows the MS–MS spectra of Trp-P-1, AαC and MeAαC, which were present in the meat extract at very low concentrations, between the detection and quantification limits. IQ, MeIQx, 4,8-DiMeIQx, norharman, harman and PhIP were quantified by the standard addition method. Method A showed extraction efficiencies that ranged from 75 to 98% for all the HAs except DMIP, whose recovery was only 14%. In the case of method B, the recovery of DMIP was 35%, and for the rest of the analytes recovery values fell between 50 and 83% (Table 4). These values are comparable to those obtained in previous studies [42,43]. Although the extraction efficiencies varied slightly for the two sample treatments, the amounts of HAs detected are consistent (Table 4). Nevertheless, clean-up A is less time consuming and requires fewer materials.

Furthermore, recovery values using D_3-IQ, D_3-MeIQx and D_3-PhIP were calculated and used to quantify the respective non-labelled HAs in the meat extract. This quantification method gave more precise data because a correction of extraction efficiency and changes in instrument performance was achieved using labelled compounds. For these three compounds, the percentage recovered after sample treatment was comparable with that obtained with the standard addition method (Table 5). The other HAs present in the meat extract at levels higher than their limit of detection, namely 4,8-DiMeIQx, norharman

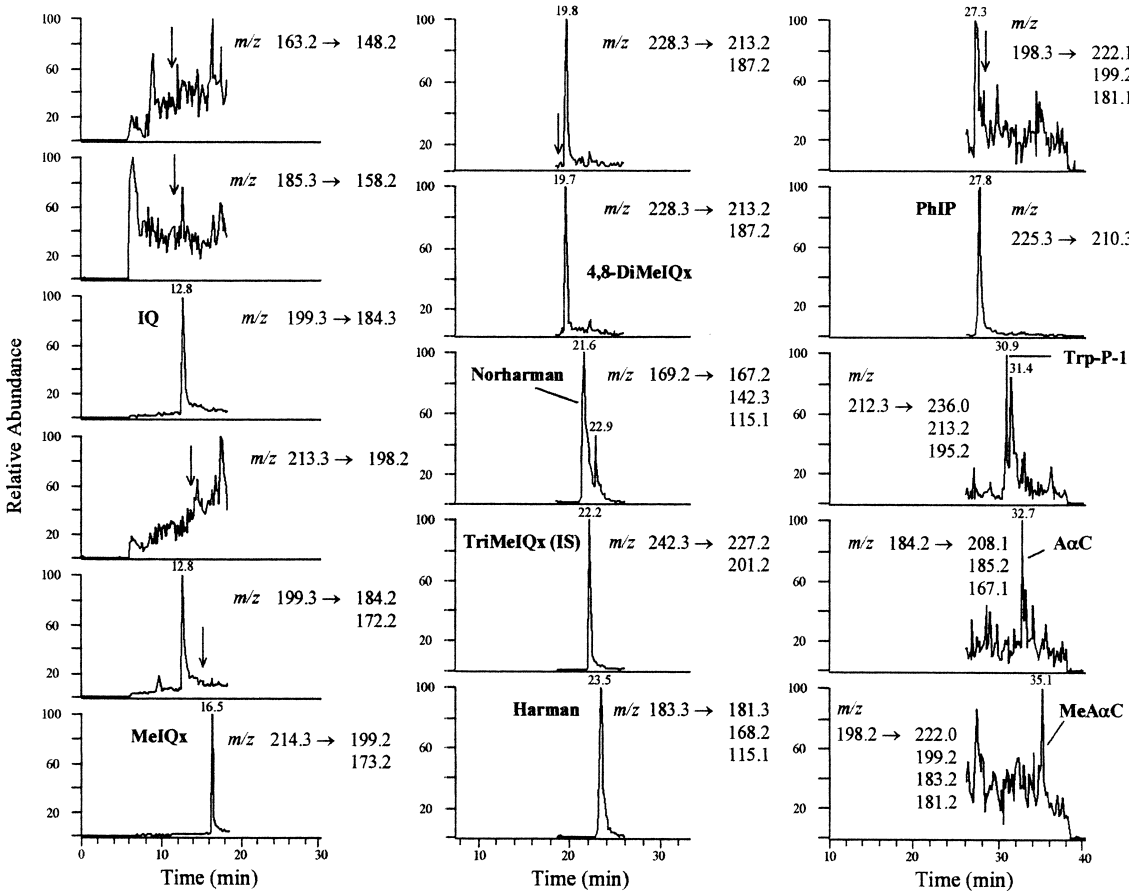

Fig. 5. LC–APCI-MS–MS chromatogram obtained for a meat extract purified with clean-up method A. Compounds identified: IQ, MeIQx, 4,8-DiMeIQx, norharman, harman, PhIP, Trp-P-1, AαC and MeAαC. The arrows indicate where the non-detected analytes would be expected.

and harman, were also quantified using the recovery values of the trideuterated HAs. In this case, higher standard deviations were obtained, because of differences in the extraction efficiency of the analytes. However, for clean-up A acceptable results were achieved because recovery values were very similar for most of the HAs.

4. Conclusions

The fragmentation of HAs in an ion trap was optimised to provide stable product ions for the analysis of these mutagenic amines by LC–APCI-MS–MS. For AIAs, the product ion derived from the loss of a methyl group was the base peak, while for carbolines the loss of ammonia and the corresponding adducts (water and acetonitrile) were the most relevant. The method was applied to the analysis of a lyophilised meat extract, and low LODs for such a complex matrix were found. The analytes present in this sample were determined, and reproducible and reliable data were obtained. False peak identification was prevented by matching the full scan MS–MS spectra of the sample with those of standards.

Moreover, although similar quantitative results

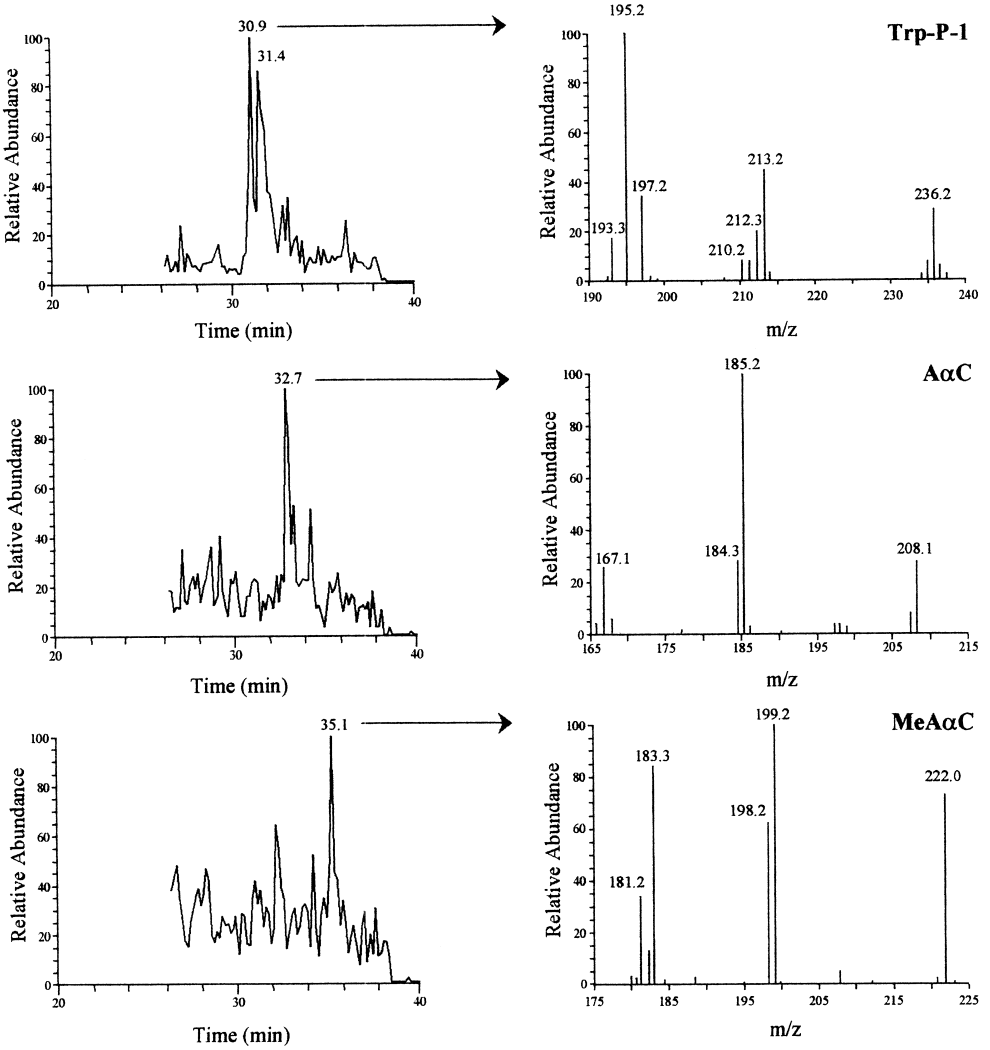

Fig. 6. Product ion scan confirmation of Trp-P-1, AαC and MeAαC in the meat extract.

were obtained using the two sample treatments, the clean-up that preconcentrates all the analytes in a single extract (method A) is less time consuming, requires the use of fewer materials and gives slightly higher recovery values. In addition, the use of deuterated analytes led to acquisition of more precise quantitative data for IQ, MeIQx and PhIP. Furthermore, for method A the use of labelled analytes also provided acceptable results for the other compounds analysed. Therefore this method could be used to estimate the content of HAs in food samples, reducing the number of spiked replicates in comparison with the classical standard addition method.

Acknowledgements

This work was carried out with financial support from the Commission of the European Community, specific RTD programme ''Quality of Life and Management of Living Resources'', project QLK1-

Table 4
Amount of HAs found in the lyophilised meat extract and recovery values for the two clean-up procedures[a]

Analyte	Clean-up A				Clean-up B			
	Recovery %	RSD %	Amount found (ng g^{-1})	SD	Recovery %	RSD %	Amount found (ng g^{-1})	SD
DMIP	14	4	n.d.		35	8	n.d.	
Glu-P-2	87	3	n.d.		83	5	n.d.	
IQ	87	3	31.3	3.3	72	6	36.5	3.4
MeIQ	93	3	n.d.		65	4	n.d.	
Glu-P-1	82	5	n.d.		74	7	n.d.	
MeIQx	81	4	40.5	6.4	80	5	40.2	7.6
7,8-DiMeIQx	78	5	n.d.		75	5	n.d.	
4,8-DiMeIQx	87	4	16.4	1.2	69	6	14.1	2.1
Norharman	89	7	180.2	20.5	58	8	169.7	14.8
Harman	87	10	240.7	35.5	50	16	304.5	53.1
Trp-P-2	90	3	n.d.		63	4	n.d.	
PhIP	87	3	25.0	3.0	67	6	24.1	3.2
Trp-P-1	98	3	n.q.		72	9	n.q.	
AαC	63	2	n.q.		46	5	n.q.	
MeAαC	75	5	n.q.		61	5	n.q.	

[a] n.d., not detected; n.q., below the limit of quantification (signal-to-noise ratio 10:1).

Table 5
Comparison of the quantitative data obtained for IQ, MeIQx and PhIP using standard addition and isotopic surrogates

Analyte		Standard addition				Isotopic surrogates			
		Recovery %	RSD %	Amount found (ng g^{-1})	SD	Recovery %	RSD %	Amount found (ng g^{-1})	SD
Clean-up A	IQ	87	3	31.3	3.3	81	6	36.3	3.1
	MeIQx	81	4	40.5	6.4	86	7	37.4	1.7
	PhIP	87	3	25.0	3.0	78	7	27.8	0.9
Clean-up B	IQ	72	6	36.5	3.4	67	4	37.2	2.5
	MeIQx	80	5	40.2	7.6	84	3	39.5	0.5
	PhIP	67	6	24.1	3.2	63	6	28.0	1.5

CT99-01197 ‘‘Heterocyclic Amines in Cooked Foods—Role in Human Health’’. Financial support has been also provided by the Ministerio de Ciencia y Tecnología, project AGL2000-0948. In addition, the authors thank International Sorbent Technology, Ltd. for kindly providing some sample extraction cartridges.

References

[1] T. Sugimura, Carcinogenesis 21 (2000) 387.
[2] J.H. Weisburger, Nutrition 16 (2000) 767.
[3] L.R. Ferguson, Mutat. Res. 443 (1999) 1.
[4] N.J. Gooderham, S. Murray, A.M. Lynch, M. Yadollahi-Farsani, K. Zhao, K. Rich, A.R. Boobis, D.S. Davies, Mutat. Res. 376 (1997) 53.
[5] K.I. Skog, M.A.E. Johansson, M.I. Jägerstad, Food Chem. Toxicol. 36 (1998) 879.
[6] R. Sinha, M.G. Knize, C.P. Salmon, E.D. Brown, D. Rhodes, J.S. Felton, O.A. Levander, N. Rothman, Food Chem. Toxicol. 36 (1998) 289.
[7] P. Arvidsson, M.A.J.S. Van Boekel, K. Skog, M. Jägerstad, J. Food Sci. 62 (1997) 911.
[8] K. Skog, A. Solyakov, M. Jägerstad, Food Chem. 68 (2000) 299.
[9] H. Okonogi, T. Ushijima, X.B. Zhang, J.A. Heddle, T. Suzuki, T. Sofuni, J.S. Felton, J.D. Tucker, T. Sugimura, M. Nagao, Carcinogenesis 18 (1997) 745.
[10] K. Wakabayashi, T. Sugimura, J. Nutr. Biochem. 9 (1998) 604.

[11] B.C. Pence, C.L. Shen, D.M. Dunn, M. Landers, M. Purewal, S. San Francisco, Z. Lebensm.-Unters.-Forsch. A 207 (1998) 455.
[12] G.A. Keating, D.W. Layton, J.S. Felton, Mutat. Res. 443 (1999) 149.
[13] L.M. Tikkanen, K.J. Latva-Kala, R.L. Heiniö, Food Chem. Toxicol. 34 (1996) 725.
[14] R.J. Turesky, H. Bur, T. Huynh-Ba, H.U. Aeschbacher, H. Milon, Food Chem. Toxicol. 26 (1988) 501.
[15] E. Richling, C. Decker, D. Häring, M. Herderich, P. Schreier, J. Chromatogr. A 791 (1997) 71.
[16] G. Gross, Carcinogenesis 11 (1990) 1597.
[17] G. Gross, A. Grüter, J. Chromatogr. 592 (1992) 271.
[18] F. Toribio, L. Puignou, M.T. Galceran, J. Chromatogr. B 747 (2000) 171.
[19] P. Pais, M.G. Knize, J. Chromatogr. B 747 (2000) 139.
[20] H. Kataoka, K. Kijima, J. Chromatogr. A 767 (1997) 187.
[21] S. Murray, A.M. Lynch, M.G. Knize, N.J. Gooderham, J. Chromatogr. 616 (1993) 211.
[22] G.A. Perfetti, J. AOAC Int. 79 (1996) 813.
[23] R. Sinha, N. Rothman, C.P. Salmon, M.G. Knize, E.D. Brown, C.A. Swanson, D. Rhodes, S. Rossi, J.S. Felton, O.A. Levander, Food Chem. Toxicol. 36 (1998) 279.
[24] C. Krach, G. Sontag, Anal. Chim. Acta 417 (2000) 77.
[25] P. Pais, C.P. Salmon, M.G. Knize, J.S. Felton, J. Agric. Food Chem. 47 (1999) 1098.
[26] P. Pais, E. Moyano, L. Puignou, M.T. Galceran, J. Chromatogr. A 775 (1997) 125.
[27] F. Toribio, E. Moyano, L. Puignou, M.T. Galceran, J. Chromatogr. A 869 (2000) 307.
[28] E. Richling, M. Herderich, P. Schreier, Chromatographia 42 (1996) 7.
[29] W.G. Stillwell, L.C.R. Kidd, J.S. Wishnok, S.R. Tannenbaum, R. Sinha, Cancer Res. 57 (1997) 3457.
[30] E. Richling, D. Häring, M. Herderich, P. Schreier, Chromatographia 48 (1998) 258.
[31] L.C.R. Kidd, W.G. Stillwell, M.C. Yu, J.S. Wishnok, P.L. Skipper, R.K. Ross, B.E. Henderson, S.R. Tannenbaum, Cancer Epidemiol. Biomarkers Prev. 8 (1999) 439.
[32] P.A. Guy, E. Gremaud, J. Richoz, R.J. Turesky, J. Chromatogr. A 883 (2000) 89.
[33] C.L. Holder, S.W. Preece, S.C. Conway, Y.M. Pu, D.R. Doerge, Rapid Commun. Mass Spectrom. 11 (1997) 1667.
[34] P. Pais, M.J. Tanga, C.P. Salmon, M.G. Knize, J. Agric. Food Chem. 48 (2000) 1721.
[35] Y.I. Zhao, M. Schelfaut, P. Sandra, F. Banks, Electrophoresis 19 (1998) 2213.
[36] S.D. Mendonsa, R.J. Hurtubise, J. Liq. Chromatogr. Rel. Technol. 22 (1999) 1027.
[37] J.C. Olsson, A. Dyremark, B. Karlberg, J. Chromatogr. A 765 (1997) 329.
[38] C. de Meester, M.T. Galceran, M. Rabache, Report EUR 17652 EN, BCR Information Series, Office for Official Publications of the European Communities, Luxembourg, 1997.
[39] M.T. Galceran, P. Pais, L. Puignou, J. Chromatogr. A 719 (1996) 203.
[40] P. Pais, E. Moyano, L. Puignou, M.T. Galceran, J. Chromatogr. A 778 (1997) 207.
[41] B. Stavric, B.P.Y. Lau, T.I. Matula, R. Klassen, D. Lewis, R.H. Downie, Food Chem. Toxicol. 35 (1997) 185.
[42] F. Toribio, L. Puignou, M.T. Galceran, J. Chromatogr. A 836 (1999) 223.
[43] F. Toribio, E. Moyano, L. Puignou, M.T. Galceran, J. Chromatogr. A 880 (2000) 101.

ANALYSIS OF HETEROCYCLIC AMINES BY LIQUID CHROMATOGRAPHY-TANDEM MASS SPECTROMETRY: TRIPLE QUADRUPOLE vs. ION TRAP

Running title: Analysis of Heterocyclic Amines by LC-MS/MS

F. Toribio, E. Moyano, L. Puignou and M.T. Galceran*.
Analytical Chemistry Department, University of Barcelona.

* Author to whom correspondence should be addressed:
Prof. M.T. Galceran
Martí i Franquès 1-11. E-08028 Barcelona. Spain.
Fax: +34 93 402 12 33
Phone: +34 93 402 12 75
e-mail: galceran@apolo.qui.ub.es

Abstract

MS/MS and in-source CID-MS/MS spectra of heterocyclic amines (HAs) were obtained with a triple quadrupole instrument. The results were compared with earlier results using an ion trap instrument. The main differences between the two instruments in the mass spectra provided were the greater fragmentation in the triple quadrupole and the formation of adducts due to ion-molecule reactions in the ion trap. For additional structural information in the triple quadrupole, ions of higher-order generation were obtained by combining in-source CID with tandem mass spectrometry.

In addition, an LC-APCI-MS/MS method using a triple quadrupole for determining HAs in food samples was developed. The method was checked and found to have good precision (RSD > 12%) and linearity ($r^2 < 0.997$). The lowest LODs (0.02-0.1 ng g^{-1}) were achieved working in the MRM mode.

Keywords: heterocyclic amines, liquid chromatography, mass spectrometry, triple quadrupole, ion trap.

1. Introduction

The presence of heterocyclic amines (HAs), a family including the highest mutagenic compounds formed during the thermal processing of muscle meats,[1,2] has been correlated with the generation of certain cancers, colorectal ones in particular.[3,4] The International Agency for Research on Cancer (IARC) considers some of the HAs tested as possible human carcinogens (Group 2 B: MeIQ, MeIQx, PhIP, AαC, MeAαC, Trp-P-1) and one as a probable human carcinogen (Group 2A: IQ).[5] Depending on their chemical structure, HAs can be classified into two groups. The amino-imidazoazaarenes (AIAs) have a 2-aminoimidazole group, whereas carbolines contain a 2-aminopyridine as a common structure.

The analysis of HAs in food is hindered by their low level of concentration in samples and the high complexity of the matrix. To purify samples, laborious clean-up procedures have been developed.[6] Analysis is usually performed with either GC or LC.[7] However, as GC has the drawback that HAs require a derivatising step before their injection, LC is a more suitable separation technique for the determination of these microcontaminants. One of the most important aspects in the analysis of HAs in such complex matrices is their on-line identification, which can be efficiently achieved by coupling LC with MS.

The high selectivity and sensitivity provided by mass spectrometry, together with the improvements introduced in the last decade in LC-MS coupling, have enabled this hyphenated technique to be widely used in the analytical chemistry field. The first studies of the analysis of HAs by LC-MS used a thermospray (TSP) interface and quadrupole instruments.[8,9] Later, TSP was replaced by the more robust atmospheric pressure ionisation (API) sources, namely electrospray (ES)[10-14] and atmospheric-pressure chemical ionisation (APCI).[15-18] Since API sources, the same as TSP, provide spectra with little fragmentation, the base peak corresponds to the protonated molecular ion $[M+H]^+$. To increase the selectivity provided by mass spectrometry, MS/MS experiments are usually performed.[13,17,19,20]

Most of the papers published describe the application of LC-MS to the confirmation and/or quantification of the analytes. This technique is also used in some cases to study the fragmentation of HAs. For example, the mass spectra obtained using single quadrupole instruments with in-source collision[10,15] and triple quadrupole instruments operating in MS/MS mode[21] were used to provide a tentative assignment of the fragments. In other studies, higher-order fragmentation was obtained by use of a triple quadrupole with in-source collision[19] or an ion trap.[22]

Despite the large amount of information available, the comparison of the results published is hindered by differences in experimental conditions, such as mobile phase, analytical column or even the sample analysed. In this study, we evaluate the use of an ion trap and a triple quadrupole instrument for the analysis of HAs. First, we studied the MS/MS and in-source CID-MS/MS spectra obtained in the triple quadrupole instrument using APCI. Then, the complementary information provided by labelled compounds was used to propose the fragmentation pathways of HAs. The results were compared with previous results using ion trap multistep mass spectrometry.[22] In addition, the triple quadrupole instrument was used to develop a method for the analysis of HAs. The LC-MS and LC-MS/MS methods were evaluated and contrasted with ion trap performance. Finally, the content of HAs in a lyophilised meat extract was determined with the triple quadrupole, and results were compared with those in the ion trap.

2. Experimental

2.1. Chemicals

The organic solvents (methanol, acetonitrile and dichloromethane, Merck, Darmstadt, Germany) were HPLC grade, and the water was purified in an Elix-Milli Q system (Millipore Corporation, Bedford, MA, USA). The chemicals used for sample treatment (sodium hydroxide, hydrochloric acid and ammonium acetate, Merck, Darmstadt, Germany) and for mobile phase preparation (ammonium formate, formic acid, Merck, Darmstadt, Germany) were analytical grade. Very pure He and N_2 (Air Liquide, Alcobendas, Spain) were used. All the solutions were passed

through a 0.45 μm nylon filter (Whatman Inc., Clifton, NJ, USA) before injection into the HPLC system.

The compounds studied (Figure 1) were 2-amino-3-methylimidazo[4,5-*f*]quinoline (IQ), 2-amino-3-trideuteromethylimidazo[4,5-*f*]quinoline (D_3-IQ), 2-amino-3,4-dimethylimidazo[4,5-*f*]quinoline (MeIQ), 2-amino-3,8-dimethylimidazo[4,5-*f*]quinoxaline (MeIQx), 2-amino-8-methyl-3-trideuteromethylimidazo[4,5-*f*]quinoxaline (D_3-MeIQx), 2-amino-3,4,8-trimethylimidazo[4,5-*f*]quinoxaline (4,8-DiMeIQx), 2-amino-3,7,8-trimethylimidazo[4,5-*f*]quinoxaline (7,8-DiMeIQx), 2-amino-3,4,7,8-tetramethylimidazo[4,5-*f*]quinoxaline (TriMeIQx), 2-amino-1-methyl-6-phenylimidazo[4,5-*b*]pyridine (PhIP), 2-amino-1-trideuteromethyl-6-phenylimidazo[4,5-*b*]pyridine (D_3-PhIP), 2-amino-1,6-dimethylimidazo[4,5-*b*]pyridine (DMIP), 2-amino-9*H*-pyrido[2,3-*b*]indole (AαC), 2-amino-3-methyl-9*H*-pyrido[2,3-*b*]indole (MeAαC), 3-amino-1,4-dimethyl-5*H*-pyrido[4,3-*b*]indole (Trp-P-1), 3-amino-1-methyl-5*H*-pyrido[4,3-*b*]indole (Trp-P-2), 2-amino-6-methyldipyrido[1,2-*a*:3',2'-*d*]imidazole (Glu-P-1) and 2-aminodipyrido[1,2-*a*:3',2'-*d*]imidazole (Glu-P-2), purchased from Toronto Research Chemicals Inc. (Toronto, Canada), and 1-methyl-9*H*-pyrido[3,4-*b*]indole (harman) and 9*H*-pyrido[3,4-*b*]indole (norharman), which were from the Sigma Chemical Company (Steinheim, Germany). Individual stock standard solutions of 100 μg mL^{-1} in methanol were prepared and used for further dilution, TriMeIQx was chosen as internal standard, and trideuterated IQ, MeIQx and PhIP were used for isotopic dilution analysis.

Isolute reservoirs and Isolute HM-N diatomaceous earth refill material were obtained from IST (Hengoed, Mid-Glamorgan, UK). Isolute PRS (200 mg) and endcapped tridimensional Isolute C_{18} (100 mg) cartridges also came from IST (Hengoed, Mid-Glamorgan, UK). Coupling pieces and stopcocks were purchased from Varian Associates (Harbor City, USA).

2.2. Liquid chromatography

As described previously,[18] amines were separated by reversed-phase LC using a TSK-Gel ODS 80TM column (5 μm, 25.0 X 4.6 mm I.D.) (TosoHaas, Stuttgart, Germany) equipped with a Supelguard LC-8-DB precolumn (Supelco, Bellefonte, PA, USA). Optimal conditions were achieved with a ternary mobile phase at a flow rate of 1 ml min^{-1}. Solvent A: 30 mM formic acid/ammonium formate buffer at pH 3.25; solvent B: 30 mM formic acid/ammonium formate buffer at pH 3.7; solvent C: acetonitrile. The gradient elution program was: 5-23% C in A, 0-18 min; 23% C in A, 18-21 min; 23% C in B, 21-25 min; 23-60% C in B, 25-33 min; 60% C in B, 33-40 min; return to the initial conditions, 40-50 min; 5 min equilibration.

Two different LC systems were used. The ion trap instrument was coupled to a Waters 2690 Separations Module (Waters, Milford, MA, USA), equipped with a quaternary solvent delivery system and an autosampler. In the case of the triple quadrupole, an Agilent 1100 Series (Agilent Technologies, Palo Alto, CA, USA) quaternary pumping system with autosampler and on-line vacuum degasser was used.

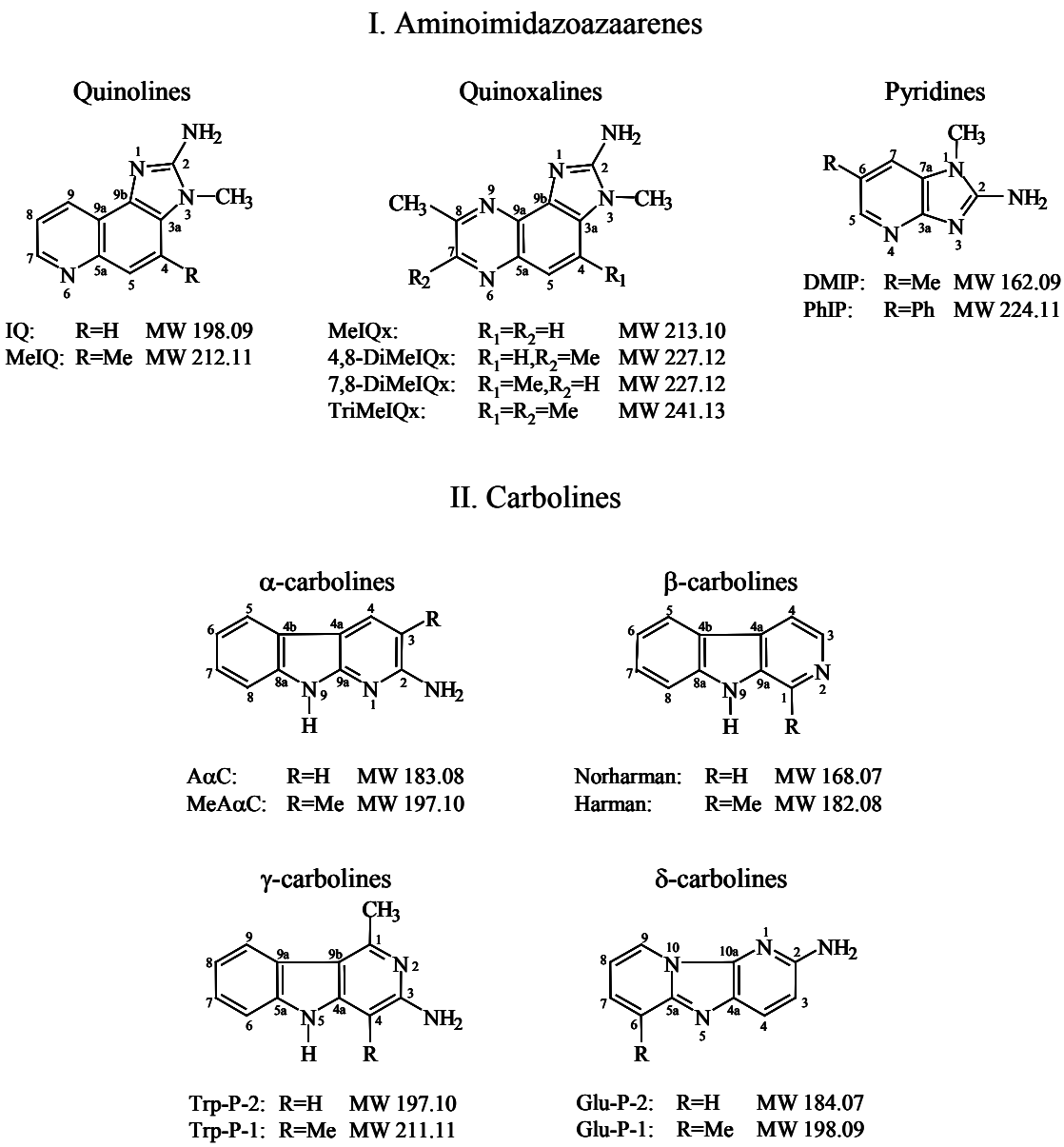

Figure 1.- Structure and molecular weight of the heterocyclic amines studied.

2.3. Mass spectrometry

- Triple quadrupole mass spectrometer

APCI experiments using a triple quadrupole mass spectrometer were carried out in a PE Sciex 3000 instrument (PerkinElmer Analytical Instruments, Shelton, CT, USA), which operated using a heated-nebuliser ionisation source and the Analyst software version 1.1.

Optimum source-dependent parameters to monitor positive ions were as follows: nitrogen was used as nebuliser gas at a flow rate of 11 arbitrary units (a.u.) and as curtain gas at 14 a.u.; vaporizer temperature was set at 460ºC; and the nebuliser current was 3.5 μA. Declustering potential, a compound-depending parameter, was set at 30 V.

MS/MS parameters were as follows: nitrogen was used as collision-induced dissociation (CID) gas at a pressure value of 6 a.u., and collision cell offset voltage ranged from 35 to 49 V depending on the analyte.

For full-scan acquisition mode, the mass analyser operated over a mass range of *m/z* 50-300 at a cycle time of 1 s and an interscan time of 5 ms. For the selected ion monitoring (SIM) mode, the chromatogram was segmented in three periods (first period: 0-17.5 min, second period: 17.5-25 min, third period: 25-40 min). The protonated molecular ions of the HAs were monitored in the first quadrupole, with a dwell time of 0.5 s and 5 ms interscan time. For MS/MS experiments, the chromatogram was also segmented in three periods. For the product ion mass spectra, the protonated molecular ion was selected as precursor ion at the first quadrupole, and the third quadrupole was scanned from 50 to 300 *m/z* using a 0.5 s dwell time and 5 ms interscan time. In the multiple reaction monitoring (MRM) mode, the transition between the precursor ion and the most abundant product ion for each analyte was monitored. A dwell time of 0.5 s and an interscan time of 5 ms were used.

-Ion trap mass spectrometer

The experiments using the ion trap mass analyser were carried out as we described in a previous paper.[20] The instrument was an LCQ mass spectrometer (Finnigan MAT, San Jose, CA, USA) which operated using Excalibur 1.0 SR1 software and was provided with an atmospheric pressure chemical ionisation (APCI) source. To prevent mass spectrometer contamination when running LC-MS, a divert valve was used for a few minutes at the beginning of the chromatogram.

Optimal source working conditions for monitoring positive ions were as follows: spray current at 5 μA, heated capillary temperature at 150ºC, and vaporiser temperature held at 450ºC. Nitrogen was used as sheath gas at 72 l h^{-1} (80 a.u.) and as auxiliary gas at 360 l h^{-1} (20 a.u.). The chromatogram was divided into three segments: first segment 0-18.5 min, second segment 18.5-26 min and third segment 26-40 min. The ion transference through the optics was automatically optimised in full scan mode for each segment by infusing individual methanolic solutions (8 μg mL^{-1}) of IQ, 4,8-DiMeIQx and Trp-P-1, respectively. A syringe pump (3 μL min^{-1}) and a tee piece were used to mix the solutions with the mobile phase. CID conditions were optimised for each compound, as described previously.[20] Maximum trapping efficiency was achieved using an isolation width of 1.5 *m/z* and an optimum activation Q value of 0.45 was chosen to maximise the intensity of product ions. The optimal normalised collision energy values ranged from 36% to 44%, and 30 ms were selected as activation time.

For data acquisition in full scan mode, the mass spectrometer operated over a range of *m/z* 150-250, and quantification was performed using the signal of the protonated molecular ion. In product ion full scan, the masses scanned varied from *m/z* 110 to *m/z* 250 depending on the analyte, and quantification used the most intense product ions for each compound. In all cases, ions were acquired in centroid mode, with a maximum injection time of 100 ms, 3 microscans, the automatic gain control activated and the inject waveform disconnected.

2.4. Sample analysis

A lyophilised meat extract, prepared from a commercial meat extract (Bovril™)[23] and contaminated with IQ, MeIQ, MeIQx, PhIP and AαC, was analysed. The target concentration for these analytes was 40-60 ng g^{-1}. Sample preparation method, developed in a previous study,[24] was

as follows: 1 g of material was homogenised in 12 ml 1 M NaOH with sonication, and the suspension was then shaken for 2 h in a Rotary Mixer 34526 rotating shaker (Breda Scientific, Breda, The Netherlands). The alkaline solution was mixed with Isolute HM-N refill material (14 g) and used to fill a 70 mL fritted reservoir. After preconditioning with 7 mL DCM, an Isolute PRS column was coupled on-line to the diatomaceous earth column. To extract the analytes from the Isolute HM-N material, 75 ml of dichloromethane were passed through the tandem. The PRS cartridge was then dried and successively rinsed with 15 ml methanol-H_2O (4:6, v/v) and 2 ml water. The cationic exchanger column was then coupled to an Isolute C_{18} column, previously conditioned with 5 mL MeOH and 5 mL water, and HAs were then eluted with 20 ml of 0.5 M ammonium acetate at pH 8.5. Finally, the C_{18} cartridge was rinsed with 5 ml water and the sorbed HAs were eluted using 0.8 ml of methanol-ammonia (9:1, v/v). The solvent was gently evaporated under a stream of nitrogen and the analytes were redissolved in either 80 (for LC-MS(IT) analysis) or 240 µl (for LC-MS(TQ) analysis) of the internal standard (TriMeIQx) in methanol.

The solid-phase extraction cartridges were handled with a Supelco Visiprep SPE vacuum manifold (Supelco, Gland, Switzerland), and solvent was evaporated with a Visidry device. The final extracts were analysed using the LC-MS methods described earlier.

The amines in the lyophilised meat extract were quantified, and their recovery calculated, by standard addition using four different levels (50-200%). For the determination of LODs in meat samples, a non-contaminated meat extract and a fried beef steak were analysed. For both samples, the treatment was as described previosly, although 3 g of the fried beef sample were purified. The meat extract contained only the comutagenic amines harman and norharman, and the fried beef was cooked under mild conditions to minimise the formation of HAs.

3. Results and Discussion

3.1. Tandem mass spectrometry of HAs

To establish a LC-APCI-MS method using the triple quadrupole instrument, several aspects of ionisation, ion transmission, fragmentation and acquisition were studied. The source-dependent parameters, namely nebuliser gas and curtain gas flow-rates, source temperature and nebuliser current, were optimised by flow injection of 2 µL of a methanolic solution containing TriMeIQx (4 µg mL^{-1}). Neither nebuliser gas nor curtain gas flow rate had much effect on the abundance of the protonated molecular ion, and optimal values were 11 and 14 a.u., respectively. In contrast, a pronounced decrease in the signal was observed for source temperature and nebuliser current at values higher than 470ºC and 4 µA, respectively. Thus, a source temperature value of 460ºC was selected as optimum, whereas nebuliser current value was set at 3.5 µA.

Declustering potential, a compound-depending parameter, was optimised by infusing (3 µL min^{-1}) individual methanol solutions for each HA (4 µg mL^{-1}) in the mobile phase. Three different eluting conditions corresponding to the three chromatographic segments were used, and declustering potential was ramped from 0 to 140 V. This potential allows a reduction of cluster formation, but also produces in-source CID fragmentation at high values, leading to the generation of characteristic product ions for each compound. For instance, aminoimidazoazaarenes (AIAs) showed the cleavage of the aminoimidazole moiety with losses of $^{\bullet}CH_3$, C_2NH_3 and CN_2H_2. For carbolines the loss of NH_3 for the primary amines, the loss of a methyl for the methylated

compounds and the loss of HCN for α-, β- and δ-carbolines were observed, in accord with literature data [10,15,19]. The maximum response for all the compounds was obtained with values from 20 to 40 V, as shown in Figure 2 for some HAs. Thus, for quantitative purposes an optimum DP value of 30 V was chosen as a compromise between declustering and fragmentation of the protonated molecular ion. Under optimum conditions, the mass spectra were dominated by the protonated molecular ion and only fragment ions with relative abundances lower than 5% were observed, as shown in Figure 2 for harman. At higher DP values the molecule fragmented, leading to product ions that confirm those previously observed in the MS/MS spectra.[22]

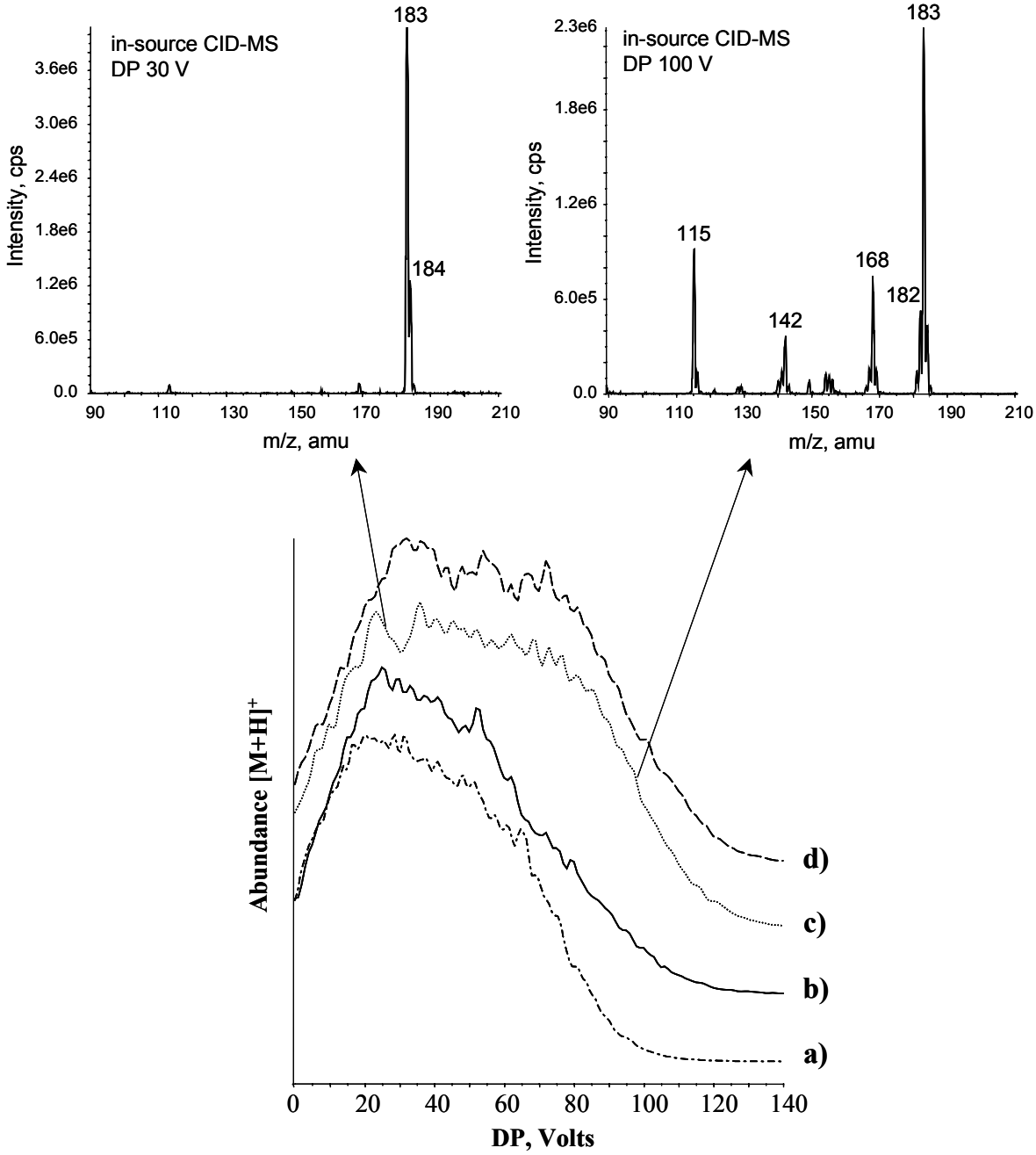

Figure 2.- Declustering potential curves for a) Glu-P-2, b) MeIQx, c) harman and d) PhIP.

After the selection of source working conditions, MS/MS parameters were studied. To optimise precursor ion transmission and fragmentation, CID gas pressure was varied from 0 to 12 a.u. An optimum value of 6 a.u. was found. The other important MS/MS parameter, the collision cell offset voltage, was optimised by infusing individual solutions of each compound and ramping the voltage value from 5 to 80 V. As an example, Figure 3 shows the voltage curves for Glu-P-2 and 4,8-DiMeIQx. The maximum of these curves provides information about the generation of product ions by multiple collisions inside the chamber when energy increases. For example, for 4,8-DiMeIQx the ions at *m/z* 212 and at *m/z* 160, which appear at voltages higher than 40 V, could arise from the fragmentation of the ions at *m/z* 213 and/or at *m/z* 187. The MS^n experiments performed using an ion trap analyser confirmed that the *m/z* 212 ion was produced by the fragmentation of the *m/z* 213 ion and that the *m/z* 160 ion was the base peak of the MS^3 spectra using the *m/z* 187 ion as precursor.

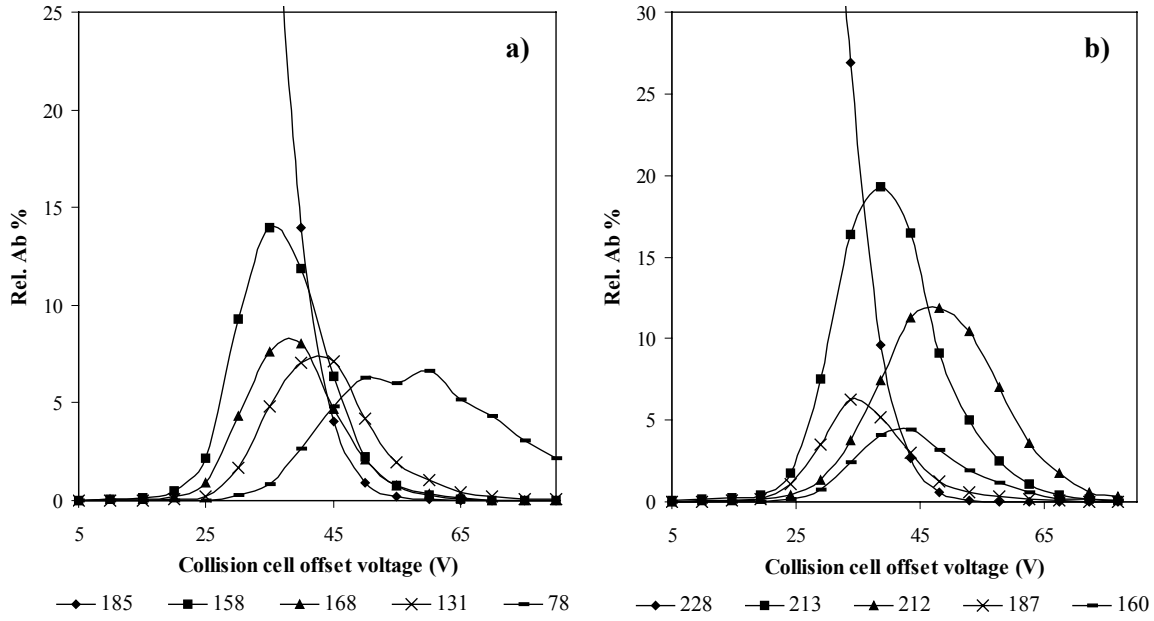

Figure 3.- Collision cell offset voltage curves for a) Glu-P-2 and b) 4,8-DiMeIQx.

To obtain the MS/MS spectra for all the HAs, collision cell offset voltage values providing maximum intensity of the main product ion and keeping at least 10% relative abundance for the precursor ion were selected. These optimum values are listed in Table 1 for aminoimidazoazaarenes and Table 2 for carbolines, together with the main ions observed and their relative abundances. The MS/MS spectra obtained using the triple quadrupole were generally consistent with those previously obtained using the ion trap.[22] For instance, AIAs showed the loss of a methyl group and the breaking of the aminoimidazole moiety. In the case of carbolines, the loss of ammonia, HCN and the breaking of the heterocyclic rings were observed.

Nevertheless, there were some significant differences between the two instruments in the mass spectra obtained. For example, the ions originated by the loss of C_2NH_3, NH_3 and HCN from the AIAs protonated molecular ion were less abundant in the triple quadrupole than in the ion trap. In contrast, ions such as *m/z* 157 for IQ or *m/z* 172 for MeIQx, assigned previously[22] as $[M+H-CN_2H_2]^+$, had higher intensities in the triple quadrupole. This increase could be due to the contribution of simultaneous fragmentation processes, namely the consecutive loss of $^{\bullet}CH_3$ and

HCN from the ion $[M+H]^+$ and the loss of CN_2H_2 from the same ion. This hypothesis was confirmed by the fragmentation of trideuterated IQ and MeIQx in the triple quadrupole and the comparison of the spectra with the MS^3 data in the ion trap. Moreover, new fragments appeared in some cases when the triple quadrupole was used. For example, the loss of CH_4 from the ion $[M+H]^+$ was observed for MeIQ, 4,8-DiMeIQx, TriMeIQx and DMIP. As previously, these ions could be explained by consecutive losses of $^{\bullet}CH_3$ and $^{\bullet}H$. In general, the higher fragmentation observed with the triple quadrupole analyser than with the ion trap was explained by the possibility of multiple collisions along the chamber in the triple quadrupole and the stabilisation of the fragment ions in the ion trap just after their generation.

The main differences in the case of carbolines were due to the absence in the triple quadrupole of the ions whose *m/z* was higher than the precursor ion's m/z previously observed in the ion trap. These absent ions were those derived from ion-molecule reactions.[22] As an example, Figure 4 shows the MS/MS spectra of Trp-P-1 obtained with both instruments. As is also found with the triple quadrupole, the ions at both *m/z* 213 and at *m/z* 236, corresponding to the adduct of the ion $[M+H-NH_3]^+$ with a molecule of water and a molecule of acetonitrile, respectively, disappeared. Ions arising from multiple collisions were also observed. For example, the ion of *m/z* 168, originated by consecutive losses of NH_3 and HCN from the protonated molecule, was present in the triple quadrupole MS/MS spectra of Trp-P-1. The same occurred with the ion of *m/z* 154 for Trp-P-2 (Table 2), and the *m/z* 140 and 154 ions for AαC and MeAαC, respectively. Other fragment ions arising from consecutive losses were those at *m/z* 115 for both harman and norharman, which led to the base peak of the MS/MS spectra of these analytes. All these consecutive fragmentation processes were consistent with the collision cell offset voltage curves in the triple quadrupole and were confirmed by the MS^2 and MS^3 experiments in the ion trap.

All the MS/MS spectra obtained using the triple quadrupole instrument are consistent with those obtained by other authors using the same analyser.[17,19,21] However, there is a lack of information about higher-order experiments with these instruments on all the HAs. Thus, the next step consisted of finding in-source CID-MS/MS spectra in the triple quadrupole for each analyte. To this end, a value of DP high enough to maximise the relative abundance of some major fragment ions in the ion source was established. Then, these ions were fragmented in the collision chamber to obtain their MS/MS spectra, which could provide information comparable to the MS^3 spectra or even the MS^4 spectra in the ion trap. As as example, Figure 5 shows the in-source CID-MS and in-source CID-MS/MS spectra of IQ in the triple quadrupole and the MS^3 and MS^4 in the ion trap. The in source-MS/MS experimental conditions and the relative abundance of each product ion are listed in Table 1 for AIAs and Table 2 for carbolines. Fragmentation was generally consistent with the multistep mass spectra using the ion trap.[22] The main differences were, as in the case of MS/MS, variation in the relative abundance of some product ions and the absence of adducts with neutral molecules in the spectra of carbolines obtained with the triple quadrupole.

Table 1.- Optimised triple quadrupole conditions and main product ions obtained for AIAs (aminoquinolines, aminoquinoxalines and aminopyridines).

Compound	**MS/MS**					**in source-MS/MS**				
	CE$^{\#}$ (V)	Precursor ion		Product ions		DP (V)	CE$^{\#}$ (V)	Precursor ion	Product ions	
		m/z (rel. Ab%)	Assign.	*m/z* (rel. Ab%)	Assign.			*m/z* (rel. Ab%)	*m/z* (rel. Ab%)	Assign.
IQ	37	199 (27)	$[M+H]^+$	184 (100)*	$[M+H-CH_3]^{+\cdot}$	100	35	184 (100)	157 (71)	$[M+H-CH_3-HCN]^{+\cdot}$
									156 (20)	$[M+H-CH_3-HCN-H]^+$
				158 (6)	$[M+H-C_2NH_3]^+$					
				157 (15)	$[M+H-CN_2H_2]^+$	115	28	157 (100)	156 (44)	$[M+H-CN_2H_2-H]^{+\cdot}$, $[M+H-CH_3-HCN-H]^+$
					$[M+H-CH_3-HCN]^{+\cdot}$				130 (40)	$[M+H-CN_2H_2-HCN]^+$, $[M+H-CH_3-HCN-HCN]^{+\cdot}$
				131 (6)	$[M+H-C_3N_2H_4]^+$	130	32	131 (100)	104 (48)	$[M+H-C_3N_2H_4-HCN]^+$
									78 (26)	$[M+H-C_3N_2H_4-C_3NH_3]^+$
MeIQ	37	213 (44)	$[M+H]^+$	198 (100)*	$[M+H-CH_3]^{+\cdot}$	105	34	198 (100)	197 (97)	$[M+H-CH_3-H]^+$
				197 (11)	$[M+H-CH_3-H]^+$	120	36	197 (100)	180 (31)	$[M+H-CH_3-H-NH_3]^+$
									170 (57)	$[M+H-CH_3-H-HCN]^+$
				172 (5)	$[M+H-C_2NH_3]^+$	100	32	172 (29)	145 (100)	$[M+H-C_2NH_3-HCN]^+$
				145 (5)	$[M+H-C_3N_2H_4]^+$					
MeIQx	37	214 (76)	$[M+H]^+$	199 (100)*	$[M+H-CH_3]^{+\cdot}$	95	34	199 (100)	198 (20)	$[M+H-CH_3-H]^+$
									172 (62)	$[M+H-CH_3-HCN]^{+\cdot}$
									171 (33)	$[M+H-CH_3-HCN-H]^+$
									131 (51)	$[M+H-CH_3-C_3N_2H_4]^{+\cdot}$
				197 (9)	$[M+H-NH_3]^+$					
				187 (11)	$[M+H-HCN]^+$					
				173 (29)	$[M+H-C_2NH_3]^+$	95	32	173 (86)	172 (27)	$[M+H-C_2NH_3-H]^{+\cdot}$
									158 (21)	$[M+H-C_2NH_3-CH_3]^{+\cdot}$
									156 (44)	$[M+H-C_2NH_3-NH_3]^+$
									146 (100)	$[M+H-C_2NH_3-HCN]^+$
				172 (21)	$[M+H-CN_2H_2]^+$	105	30	172 (100)	171 (78)	$[M+H-CN_2H_2-H]^{+\cdot}$, $[M+H-CH_3-HCN-H]^+$
					$[M+H-CH_3-HCN]^{+\cdot}$				145 (26)	$[M+H-CN_2H_2-HCN]^+$, $[M+H-CH_3-HCN-HCN]^{+\cdot}$
				160 (5)	$[M+H-C_2N_2H_2]^+$					
				156 (5)	$[M+H-C_2NH_3-NH_3]^+$					
				146 (21)	$[M+H-C_2NH_3-HCN]^+$					
				77 (7)	$[M+H-C_5N_5H_7]^+$	100	24	77 (100)	51 (90)	$[M+H-C_5N_5H_7-C_2H_2]^+$
4,8-DiMeIQx	39	228 (49)	$[M+H]^+$	213 (100)*	$[M+H-CH_3]^{+\cdot}$	100	35	213 (45)	212 (100)	$[M+H-CH_3-H]^{+\cdot}$
									145 (31)	$[M+H-CH_3-C_3N_2H_4]^{+\cdot}$
				212 (31)	$[M+H-CH_3-H]^+$	115	39	212 (100)	185 (85)	$[M+H-CH_3-H-HCN]^+$
				211 (7)	$[M+H-NH_3]^+$					
				187 (25)	$[M+H-C_2NH_3]^+$	95	30	187 (87)	170 (31)	$[M+H-C_2NH_3-NH_3]^+$
									160 (100)	$[M+H-C_2NH_3-HCN]^+$
				186 (12)	$[M+H-CN_2H_2]^+$					
				170 (5)	$[M+H-C_2NH_3-NH_3]^+$					
				160 (27)	$[M+H-C_2NH_3-HCN]^+$	105	30	160 (100)	133 (36)	$[M+H-C_2NH_3-HCN-HCN]^+$

				145 (5)	$[M+H-CH_3-C_3N_2H_4]^{+\cdot}$						
7,8-DiMeIQx	39	228 (88)	$[M+H]^+$	213 (100)*	$[M+H-CH_3]^{+\cdot}$	105	31	213 (100)	212 (21)	$[M+H-CH_3-H]^+$
									172 (33)	$[M+H-CH_3-C_2NH_3]^{+\cdot}$
									131 (51)	$[M+H-CH_3-C_4N_2H_6]^{+\cdot}$
				211 (7)	$[M+H-NH_3]^+$					
				187 (46)	$[M+H-C_2NH_3]^+$	100	29	187 (100)	172 (26)	$[M+H-C_2NH_3-CH_3]^{+\cdot}$
									160 (39)	$[M+H-C_2NH_3-HCN]^+$
									146 (21)	$[M+H-C_2NH_3-C_2NH_3]^+$
				186 (14)	$[M+H-CN_2H_2]^+$					
				172 (19)	$[M+H-CH_3-C_2NH_3]^+$					
				170 (7)	$[M+H-C_2N_2H_6]^+$					
				160 (20)	$[M+H-C_2NH_3-HCN]^+$					
				146 (15)	$[M+H-C_2NH_3-C_2NH_3]^+$					
				131 (14)	$[M+H-CH_3-C_4N_2H_6]^{+\cdot}$	125	24	131 (100)	130 (27)	$[M+H-CH_3-C_4N_2H_6-H]^+$
									104 (67)	$[M+H-CH_3-C_4N_2H_6-HCN]^{+\cdot}$
									77 (34)	$[M+H-CH_3-C_4N_2H_6-CN_3]^+$
TriMeIQx	39	242 (69)	$[M+H]^+$	227 (100)*	$[M+H-CH_3]^{+\cdot}$	105	38	227 (40)	226 (86)	$[M+H-CH_3-H]^+$
									186 (27)	$[M+H-CH_3-C_2NH_3]^{+\cdot}$
									185 (23)	$[M+H-CH_3-C_2NH_3-H]^+$
									145 (100)	$[M+H-CH_3-C_4N_2H_6]^{+\cdot}$
				226 (19)	$[M+H-CH_3-H]^+$					
				225 (6)	$[M+H-NH_3]^+$					
				201 (31)	$[M+H-C_2NH_3]^+$	95	34	201 (61)	174 (100)	$[M+H-C_2NH_3-HCN]^+$
				200 (6)	$[M+H-CN_2H_2]^+$					
				186 (8)	$[M+H-CH_3-C_2NH_3]^+$					
				174 (20)	$[M+H-C_2NH_3-HCN]^+$					
				160 (7)	$[M+H-C_4N_2H_6]^+$					
				145 (7)	$[M+H-CH_3-C_4N_2H_6]^{+\cdot}$					
DMIP	35	163 (84)	$[M+H]^+$	148 (100)*	$[M+H-CH_3]^{+\cdot}$	90	29	148 (59)	147 (100)	$[M+H-CH_3-H]^+$
				147 (27)	$[M+H-CH_3-H]^+$	105	30	147 (100)	120 (25)	$[M+H-CH_3-H-HCN]^+$
									105 (30)	$[M+H-CH_3-H-CN_2H_2]^+$
				146 (9)	$[M+H-NH_3]^+$					
				121 (7)	$[M+H-CN_2H_2]^+$					
				105 (6)	$[M+H-CH_3-H-CN_2H_2]^+$					
PhIP	42	225 (51)	$[M+H]^+$	210 (100)*	$[M+H-CH_3]^{+\cdot}$	110	36	210 (100)	183 (32)	$[M+H-CH_3-HCN]^{+\cdot}$
									168 (24)	$[M+H-CH_3-CN_2H_2]^{+\cdot}$
				183 (10)	$[M+H-CH_3-HCN]^{+\cdot}$					
				168 (6)	$[M+H-CH_3-CN_2H_2]^{+\cdot}$					

CE[#] Collision cell offset voltage.

* Product ion used in the MRM mode.

Table 2.- Optimised triple quadrupole MS^n conditions and main product ions obtained for α-, β-, γ- and δ-carbolines.

Compound	MS/MS					in source-MS/MS				
	CE# (V)	Precursor ion		Product ions		DP (V)	CE# (V)	Precursor ion	Product ions	
		m/z (rel. Ab%)	Assign.	*m/z* (rel. Ab%)	Assign.			*m/z* (rel. Ab%)	*m/z* (rel. Ab%)	Assign.
AαC	33	184 (53)	$[M+H]^+$	167 (100)*	$[M+H-NH_3]^+$	90	32	167 (16)	140 (100)	$[M+H-NH_3-HCN]^+$
				140 (21)	$[M+H-NH_3-HCN]^+$	115	36	140 (85)	113 (100)	$[M+H-NH_3-HCN-HCN]^+$
MeAαC		198 (65)	$[M+H]^+$	183 (32)	$[M+H-CH_3]^{+\cdot}$	85	35	183 (100)	156 (96)	$[M+H-CH_3-HCN]^{+\cdot}$
									129 (22)	$[M+H-CH_3-C_2N_2H_2]^{+\cdot}$
				181 (100)*	$[M+H-NH_3]^+$	90	31	181 (100)	154 (60)	$[M+H-NH_3-HCN]^+$
									129 (35)	$[M+H-NH_3-C_3NH_2]^{+\cdot}$
				154 (21)	$[M+H-NH_3-HCN]^+$	110	36	154 (55)	127 (100)	$[M+H-NH_3-HCN-HCN]^+$
				129 (16)	$[M+H-NH_3-C_3NH_2]^{+\cdot}$					
Harman	49	183 (22)	$[M+H]^+$	182 (12)	$[M+H-H]^{+\cdot}$	100	36	182 (73)	181 (100)	$[M+H-H-H]^+$
									155 (21)	$[M+H-H-HCN]^{+\cdot}$
									154 (62)	$[M+H-H-H-HCN]^+$
				181 (6)	$[M+H-H-H]^+$					
				168 (20)	$[M+H-CH_3]^{+\cdot}$	105	44	168 (25)	167 (30)	$[M+H-CH_3-H]^+$
									141 (29)	$[M+H-CH_3-HCN]^{+\cdot}$
									140 (100)	$[M+H-CH_3-HCN-H]^+$
									114 (45)	$[M+H-CH_3-C_2N_2H_2]^{+\cdot}$
				142 (6)	$[M+H-C_2NH_3]^+$	100	29	142 (23)	115 (100)	$[M+H-C_2NH_3-HCN]^+$
				141 (6)	$[M+H-CH_3-HCN]^{+\cdot}$	110	31	141 (100)	140 (87)	$[M+H-CH_3-HCN-H]^+$
									114 (87)	$[M+H-CH_3-HCN-HCN]^{+\cdot}$
				140 (6)	$[M+H-CH_3-HCN-H]^+$					
				115 (100)*	$[M+H-C_2NH_3-HCN]^+$	115	34	115 (100)	89 (52)	$[M+H-C_2NH_3-HCN-C_2H_2]^+$
Norharman	49	169 (34)	$[M+H]^+$	168 (30)	$[M+H-H]^{+\cdot}$	105	36	168 (100)	167 (34)	$[M+H-H-H]^+$
									141 (32)	$[M+H-H-HCN]^{+\cdot}$
									140 (28)	$[M+H-H-HCN-H]^+$
				142 (9)	$[M+H-HCN]^+$	100	28	142 (40)	115 (100)	$[M+H-HCN-HCN]^+$
				141 (9)	$[M+H-HCN-H]^{+\cdot}$	120	31	141 (100)	140 (88)	$[M+H-HCN-H-H]^+$
									114 (76)	$[M+H-HCN-H-HCN]^{+\cdot}$
				140 (7)	$[M+H-HCN-2H]^+$					
				115 (100)*	$[M+H-HCN-HCN]^+$	115	36	115 (100)	89 (68)	$[M+H-HCN-HCN-C_2H_2]^+$
Trp-P-1	35	212 (81)	$[M+H]^+$	197 (5)	$[M+H-CH_3]^{+\cdot}$					
				195 (100)*	$[M+H-NH_3]^+$	95	30	195 (83)	168 (100)	$[M+H-NH_3-HCN]^+$
									167 (44)	$[M+H-NH_3-HCN-H]^{+\cdot}$

				168 (37)	$[M+H-NH_3-HCN]^+$	105	35	168 (65)	167 (100)	$[M+H-NH_3-HCN-H]^{+\cdot}$
									141 (24)	$[M+H-NH_3-HCN-HCN]^+$
				167 (11)	$[M+H-NH_3-HCN-H]^{+\cdot}$	125	40	167 (72)	166 (100)	$[M+H-NH_3-HCN-H-H]^+$
Trp-P-2	33	198 (100)	$[M+H]^+$	181 (70)*	$[M+H-NH_3]^+$	90	29	181 (58)	154 (100)	$[M+H-NH_3-HCN]^+$
				157 (7)	$[M+H-C_2NH_3]^+$					
				154 (32)	$[M+H-NH_3-HCN]^+$	110	35	154 (60)	128 (75)	$[M+H-NH_3-HCN-C_2H_2]^+$
									127 (100)	$[M+H-NH_3-HCN-HCN]^+$
Glu-P-1	37	199 (100)	$[M+H]^+$	184 (22)	$[M+H-CH_3]^{+\cdot}$	80	34	184 (100)	157 (28)	$[M+H-CH_3-HCN]^{+\cdot}$
									144 (39)	$[M+H-CH_3-C_2NH_2]^+$
				182 (23)	$[M+H-NH_3]^+$	100	34	182 (100)	181 (55)	$[M+H-NH_3-H]^{+\cdot}$
									167 (33)	$[M+H-NH_3-CH_3]^{+\cdot}$
									155 (23)	$[M+H-NH_3-HCN]^+$
									128 (15)	$[M+H-NH_3-C_2N_2H_2]^+$
				172 (28)*	$[M+H-HCN]^+$	100	35	172 (38)	145 (100)	$[M+H-HCN-HCN]^+$
									92 (92)	$[M+H-HCN-C_4N_2H_4]^+$
				145 (16)	$[M+H-HCN-HCN]^+$	100	20	145 (100)	92 (20)	$[M+H-HCN-HCN-C_3NH_3]^+$
				92 (7)	$[M+H-HCN-C_4N_2H_4]^+$	115	22	92 (53)	65 (100)	$[M+H-HCN-C_4N_2H_4-HCN]^+$
Glu-P-2	37	185 (100)	$[M+H]^+$	168 (31)	$[M+H-NH_3]^+$	100	30	168 (100)	141 (36)	$[M+H-NH_3-HCN]^+$
				158 (53)*	$[M+H-HCN]^+$	90	30	158 (35)	131 (100)	$[M+H-HCN-HCN]^+$
				131 (30)	$[M+H-HCN-HCN]^+$	100	24	131 (100)	105 (22)	$[M+H-HCN-HCN-C_2H_2]^+$
									78 (60)	$[M+H-HCN-HCN-C_3NH_3]^+$
				78 (5)	$[M+H-HCN-HCN-C_3NH_3]^+$					

CE# Collision cell offset voltage.
* Product ion used in the MRM mode.

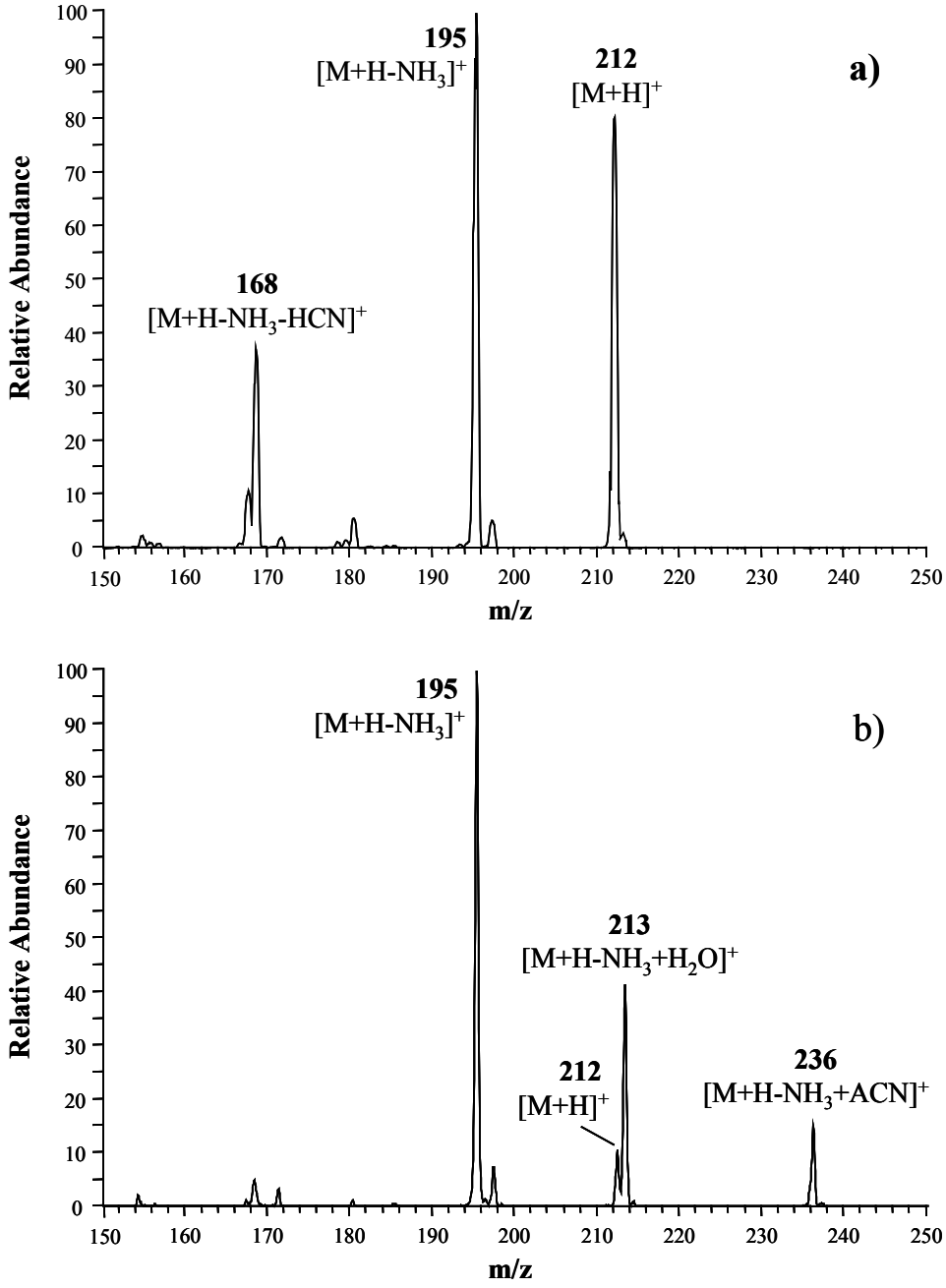

Figure 4.- MS/MS spectra of Trp-P-1 in a) a triple quadrupole mass analyser and b) an ion trap mass analyser.

The in-source CID-MS/MS spectra using the triple quadrupole together with information extracted from collision cell offset voltage curves were used to propose fragmentation patterns which were consistent with those previously established for AIAs with the ion trap.[22] In the case of carbolines, the proposal of fragmentation pathways using the ion trap was hindered by the existence of adducts of the product ion derived from the loss of ammonia with neutral molecules, which led to very low abundances of the other product ions. Therefore, the information provided by the triple quadrupole was used to analyse in depth the fragmentation of these compounds. It was observed that for α-, γ- and δ-carbolines the main fragmentation pathway started with the loss of the primary amino group (70-100% relative abundance for α- and γ-carbolines). After this initial

loss, the pyridine ring broke, which led to the loss of HCN (60-100% relative abundance for α- and γ-carbolines, and 23-36% for δ-carbolines). For some of these compounds, further fragmentation of the pirrole ring was observed, causing the loss of HCN (α- and γ-carbolines). Other important product ions in the MS/MS spectra of carbolines were those derived from the breaking of the pyridine ring, with losses of CH_3 (MeAαC, harman, Trp-P-1 and Glu-P-1), HCN (norharman and δ-carbolines) and C_2NH_3 (harman and Trp-P-2). In these cases, further fragmentation was produced in the heterocyclic rings, leading mainly to the loss of HCN. Although the information on carbolines extracted from the triple quadrupole is valuable, the lack of labelled compounds prevented the establishment of reliable fragmentation pathways.

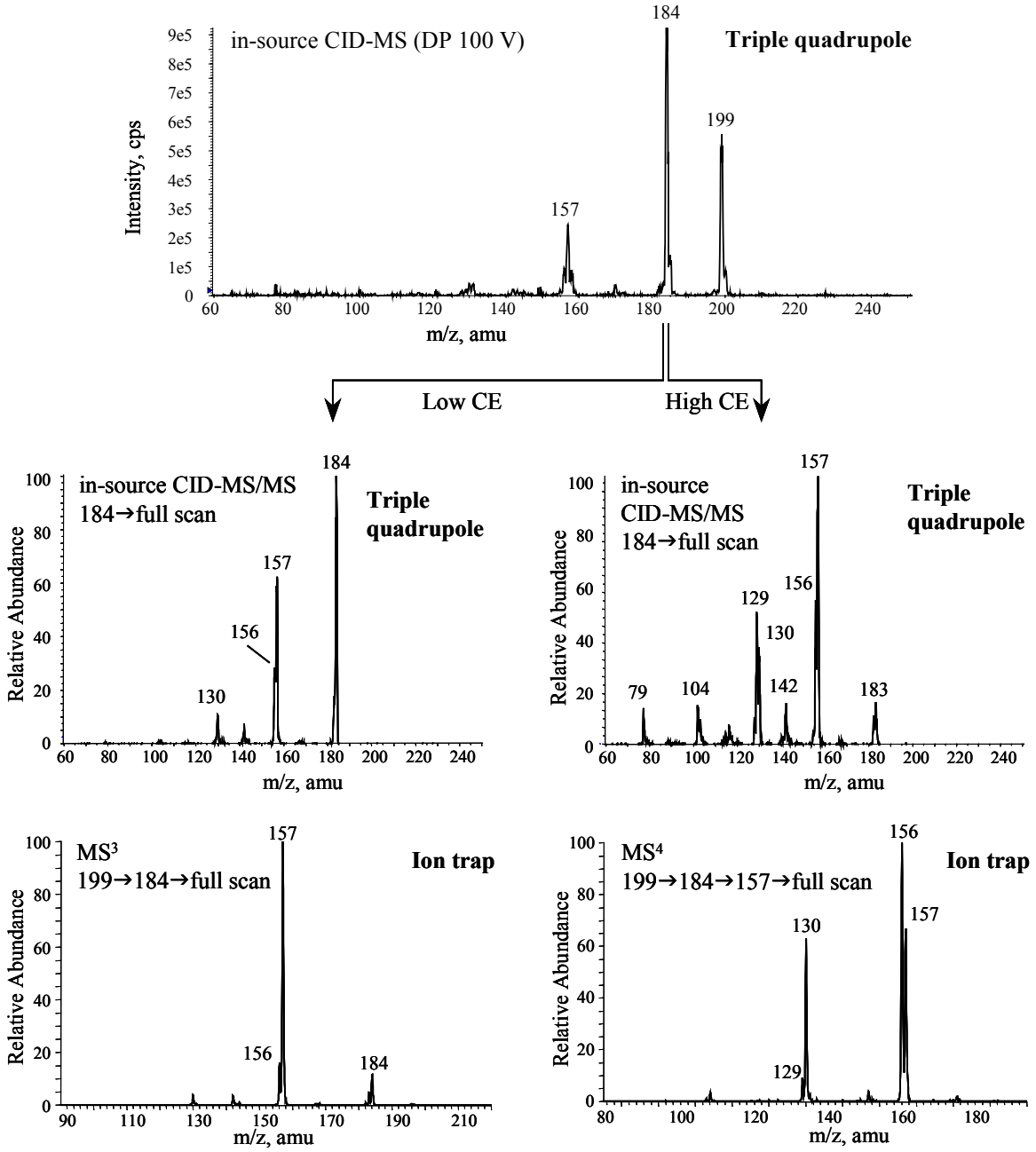

Figure 5.- In-source CID-MS and in-source CID-MS/MS of IQ in a triple quadrupole mass analyser and MS^3 and MS^4 in an ion trap mass analyser.

3.2. LC-MS method performance

Quantitative determinations were carried out in either SIM or MRM mode. Since in the MS spectra of HAs the ion $[M+H]^+$ was the most abundant, this ion was monitored in the SIM acquisition mode and was used as precursor ion in MS/MS experiments. Precursor-product ion transitions chosen for MRM mode corresponded to the most abundant fragment for each analyte, as shown in Table 1 for AIAs and Table 2 for carbolines. Once the quantitative methodology was established, several quality parameters were studied.

Limits of detection (LODs), based on a signal-to-noise ratio of 3, were calculated by injecting 15 µL of diluted HA standard solutions (Table 3). LODs ran in the range 15-239 pg injected for SIM and 3-12 pg injected for MRM, showing a major improvement in the signal when using the latter. Generally lower LODs were achieved for HAs eluting later, due to the higher content of acetonitrile in the mobile phase, which helps ionization and leads to narrower chromatographic peaks. LODs in the triple quadrupole are consistent with those published in the literature, in which values ranging from 0.5 to 670 pg injected for SIM mode[10,15] and 0.1-250 pg injected for MRM mode[21] can be found. The LODs obtained were also very similar to those found using the ion trap instrument.[18,20]

Linearity of the triple quadrupole was studied by injecting standard solutions with concentrations ranging from the limit of quantification (LOQ, from 0.6 pg mL^{-1} to 40 pg mL^{-1} depending on the analyte and the MS mode) to 3.2 µg mL^{-1}. As the signal was linear below 1.5 µg mL^{-1} ($r^2 > 0.997$), the system was calibrated for quantification purposes with six standard solutions at concentrations ranging from LOQ to 1.5 µg mL^{-1}. Run-to-run precision and day-to-day precision based on concentration were established by daily injection of the calibration standards followed by five consecutive injections of a standard solution (0.4 µg mL^{-1} for SIM and 0.09 µg mL^{-1} for MRM) for three days. Analysis of the variance of one factor was carried out to evaluate the precision, whose values in terms of RSD % are listed in Table 4. As can be seen, run-to-run and day-to-day precision for SIM mode are in the 3-11% and 2-12% ranges, respectively, whereas for MRM mode run-to-run precision ranged from 3 to 6% and day-to-day precision from 3 to 9%. These values are very similar to those obtained with the ion trap in MS mode[18] or MS/MS mode[20], which ranged in all cases from 2 to 11%. Table 4 also shows the relative errors obtained in the quantification of the analytes. As can be seen, relative differences when using the SIM mode were below 13%, whereas for the MRM mode values were under 4%.

Table 3.- Limits of detection in both instruments.

Analyte	Standard solution		Lyophilised meat extract								Fried Beef							
	Triple quadrupole		Ion Trap				Triple quadrupole				Ion Trap				Triple quadrupole			
	SIM	MRM	MS		MS/MS		SIM		MRM		MS		MS/MS		SIM		MRM	
	pg inj.	pg inj.	ng inj.	ng g^{-1}	ng inj.	ng g^{-1}	ng inj.	ng g^{-1}	ng inj.	ng g^{-1}	ng inj.	ng g^{-1}	ng inj.	ng g^{-1}	ng inj.	ng g^{-1}	ng inj.	ng g^{-1}
DMIP	239	10	2.7	157	0.3	17	1.3	53	0.1	5	0.7	13	0.2	3	0.8	11	0.03	0.4
Glu-P-2	180	12	1.3	12	0.4	3	1.3	12	0.1	0.9	0.4	1.3	0.3	0.7	0.7	1.9	0.03	0.09
IQ	66	10	0.9	6	0.2	1.4	0.6	5	0.03	0.2	0.4	0.8	0.2	0.5	0.5	1.4	0.02	0.05
MeIQ	57	10	0.5	3	0.2	0.9	0.5	3	0.04	0.2	0.5	0.9	0.2	0.3	0.7	1.6	0.02	0.04
Glu-P-1	48	10	0.9	8	0.4	3	0.6	5	0.1	0.9	0.3	0.9	0.2	0.5	0.5	1.2	0.04	0.1
MeIQx	-	9	1.3	10	0.2	1.1	-	-	0.04	0.3	0.2	0.5	0.2	0.4	-	-	0.04	0.09
7,8-DiMeIQx	65	9	0.7	5	0.1	0.7	0.7	5	0.04	0.3	0.3	0.6	0.2	0.3	0.5	1.0	0.02	0.04
4,8-DiMeIQx	68	8	0.7	5	0.1	0.7	0.7	5	0.03	0.2	0.3	0.6	0.2	0.3	0.4	1.0	0.02	0.03
Norharman	40	10	0.4[a]	3[a]	0.09[a]	0.7[a]	0.7[a]	5[a]	0.03[a]	0.2[a]	0.2	0.7	0.2	0.8	0.4	1.0	0.03	0.07
Harman	43	8	0.3[a]	3[a]	0.08[a]	0.6[a]	0.7[a]	5[a]	0.04[a]	0.2[a]	0.2	0.7	0.2	0.7	0.4	1.0	0.04	0.07
Trp-P-2	24	8	0.4	4	0.08	0.6	0.4	4	0.03	0.3	0.2	0.7	0.08	0.2	0.09	0.3	0.02	0.04
PhIP	29	4	0.7	4	0.07	0.4	0.7	4	0.02	0.1	0.2	0.5	0.03	0.05	0.3	0.7	0.01	0.03
Trp-P-1	31	6	0.4	8	0.08	1.3	0.5	8	0.05	0.8	0.3	1.7	0.04	0.2	0.1	0.7	0.02	0.09
AαC	-	4	0.6	5	0.04	0.3	0.3	2.0	0.01	0.1	0.06	0.2	0.03	0.06	0.2	0.5	0.01	0.02
MeAαC	15	3	0.3	2.0	0.04	0.3	0.2	1.0	0.02	0.1	0.06	0.1	0.03	0.06	0.05	0.1	0.01	0.02

[a] Value estimated from the non-spiked sample.

Table 4.- Quality parameters of the triple quadrupole methodology.

Analyte	tr (min)		Calculated concentration (ng mL^{-1})		Relative error[a] (%, n=15)		Concentration precision (RDS%, n= 15, α=0.05)			
							run-to-run		*day-to-day*	
	SIM	MRM	SIM	MRM	SIM	MRM	SIM	MRM	SIM	MRM
DMIP	11.0	11.0	431	85.6	7	4	4	3	4	4
Glu-P-2	12.1	12.2	451	87.9	2	1	3	4	4	7
IQ	12.7	12.8	440	91.8	4	4	5	3	7	5
MeIQ	14.5	14.7	405	90.3	13	1	6	3	10	3
Glu-P-1	15.3	15.3	458	87.9	0.2	0.5	8	3	12	7
MeIQx	16.3	16.4	405	87.1	13	3	11	4	8	8
7,8-DiMeIQx	19.1	19.2	417	94.2	11	4	5	3	6	4
4,8-DiMeIQx	19.6	19.7	419	86.4	10	2	7	6	9	9
Norharman	21.6	21.8	457	84.8	0.4	4	6	4	10	6
Harman	23.2	23.3	433	84.8	4	2	6	3	9	6
Trp-P-2	26.2	26.3	444	87.1	3	1	7	3	9	5
PhIP	26.8	26.8	426	87.1	6	0.4	3	3	2	6
Trp-P-1	30.5	30.6	465	87.1	2	0.7	9	5	11	6
AαC	32.9	33.0	448	86.4	1	1	5	4	9	4
MeAαC	35.4	35.4	455	88.7	0.4	0.8	5	5	7	5

[a] Calculated relative to the target value.

3.3. Analysis of meat samples

To evaluate the performance of the LC-MS method in meat sample analysis, LOD values were calculated. Two samples, a meat extract that contained only the comutagens harman and norharman and a fried beef sample free of HAs, were spiked at very low levels. LOD values obtained using the ion trap and the triple quadrupole instruments are listed in Table 3, expressed as ng injected and ng g^{-1} of sample. For the triple quadrupole, the improvement when using MRM instead of SIM was on average about 20-fold, due to the higher selectivity of the tandem mode. Moreover, for both acquisition modes, LOD values were always higher for the meat extract than for the fried beef, due to the greater matrix complexity of the former. The same behaviour was observed for the ion trap when working in MS/MS mode (Table 3).

However, comparison of LODs when using the ion trap in MS mode and using the triple quadrupole in SIM mode shows that very similar values are obtained for both the meat extract and the fried beef. However, when applying tandem mass spectrometry, about 3 to 6-fold lower LODs were found for the triple quadrupole instrument. Nevertheless, the ion trap in MS/MS mode provides the product ion scan for each chromatographic peak, avoiding false positives.

The level of HAs in the lyophilised meat extract was determined by standard addition using the four LC-MS methods developed. The concentration of IQ, MeIQ, MeIQx, PhIP and AαC was in the 29-62 ng g^{-1} range, whereas the comutagens harman and norharman were at a concentration level of about 200-275 ng g^{-1}. The results of the quantification are given in Table 5, together with the corresponding confidence intervals. As can be seen, results obtained with the different methods are generally consistent with each other, and RSD are in most cases lower than 15%.

Table 5.- Quantification results in the analysis of a lyophilised meat extract.

Analyte	Ion trap		Triple quadrupole	
	MS	*MS/MS*	*SIM*	*MRM*
	conc.* ($ng\ g^{-1}$)	conc.* ($ng\ g^{-1}$)	conc.* ($ng\ g^{-1}$)	conc.* ($ng\ g^{-1}$)
IQ	33 ± 7	29 ± 6	46 ± 17	43 ± 17
MeIQ	39 ± 16	31 ± 10	45 ± 6	40 ± 12
MeIQx	43 ± 13	41 ± 16	-	52 ± 20
PhIP	38 ± 11	36 ± 16	42 ± 11	40 ± 10
AαC	40 ± 16	43 ± 19	47 ± 11	62 ± 12

* Confidence interval determined for n= 6, α= 0.05.

4. Conclusions

This paper has compared the MS, MS/MS and in-source CID-MS/MS spectra, as well as the collision cell offset voltage curves, provided by a triple quadrupole analyser with those obtained with an ion trap. Although similarities have been observed, in general higher fragmentation occurred in the triple quadrupole due to multiple collisions in the collision chamber. In-source CID-MS/MS and high collision energies can be used in a triple quadrupole to obtain higher-generation ions that can be used as a complementary confirmation tool. Moreover, the absence of ion-molecule reactions for carbolines in the triple quadrupole allowed a higher fragmentation of parent ions, providing structural information additional to that obtained with an ion trap analyser.

For the determination of HAs in food samples, both instruments provided similar precision. Tandem mass spectrometry, due to its high selectivity and sensitivity, is recommended. Although the lowest LODs were obtained with the triple quadrupole instrument working in MRM acquisition mode, the ability of the ion trap to provide a full scan of product ions enables the analytes in food analysis to be confirmed without loss of sensitivity. Nevertheless, false positives can also be avoided in the triple quadrupole by the monitoring of several transitions, although this causes a decrease in the signal.

Acknowledgements

This research was supported by the European Commission's specific RTD programme "Quality of Life and Management of Living Resources", project QLK1-CT99-01197 "Heterocyclic Amines in Cooked Foods -- Role in Human Health". Financial support was also provided by the Ministerio de Ciencia y Tecnología, project AGL2000-0948. The authors also want to thank Dr. Olga Jáuregui of the Serveis Científico-Tècnics of the University of Barcelona for her valuable technical and scientific help.

References

1. Zimmerli B, Rhyn P, Zoller O, Schlatter J. *Food Addit.Contam.* 2001; **18**: 533-551.
2. Sugimura T, Nagao M, Wakabayashi K. *Mutat.Res.* 2000; **447**: 15-25.
3. Norat T, Riboli E. *Nutr.Rev.* 2001; **59**: 37-47.
4. Sinha R, Chow WH, Kulldorff M, Denobile J, Butler J, Garcia-Closas M, Weil R, Hoover RN, Rothman N. *Cancer Res.* 1999; **59**: 4320-4324.
5. International Agency for Research on Cancer. IARC monographs on the evaluation of carcinogenic risks to humans. Lyon, 1993; **56:** 163-242.
6. Toribio F, Puignou L, Galceran MT. *J.Chromatogr.B* 2000; **747**: 171-202.
7. Pais P, Knize MG. *J.Chromatogr.B* 2000; **747**: 139-169.
8. Edmons CG, Sethi SK, Yamaizumi Z, Kasai H, Nishimura S, McCloskey JA. *Environ.Health Perspect.* 1986; **67**: 35-40.
9. Gross GA, Turesky RJ, Fay LB, Stillwell WG, Skipper PL, Tannenbaum SR. *Carcinogenesis* 1993; **14**: 2313-2318.
10. Pais P, Moyano E, Puignou L, Galceran MT. *J.Chromatogr.A* 1997; **775**: 125-136.
11. Stillwell WG, Kidd LCR, Wishnok JS, Tannenbaum SR, Sinha R. *Cancer Res.* 1997; **57**: 3457-3464.
12. Paehler A, Richoz J, Soglia J, Vouros P, Turesky RJ. *Chem.Res.Toxicol.* 2002; **15**: 551-561.
13. Knize MG, Kulp KS, Malfatti MA, Salmon CP, Felton JS. *J.Chromatogr.A* 2001; **914**: 95-103.
14. Gangl ET, Turesky RJ, Vouros P. *Anal.Chem.* 2001; **73**: 2397-2404.
15. Pais P, Moyano E, Puignou L, Galceran MT. *J.Chromatogr.A* 1997; **778**: 207-218.
16. Stavric B, Lau BPY, Matula TI, Klassen R, Lewis D, Downie RH. *Food Chem.Toxicol.* 1997; **35**: 185-197.
17. Holder CL, Preece SW, Conway SC, Pu YM, Doerge DR. *Rapid.Commun.Mass Spectrom.* 1997; **11**: 1667-1672.
18. Toribio F, Moyano E, Puignou L, Galceran MT. *J.Chromatogr.A* 2000; **869**: 307-317.
19. Guy PA, Gremaud E., Richoz J, Turesky RJ. *J.Chromatogr.A* 2000; **883**: 89-102.
20. Toribio F, Moyano E, Puignou L, Galceran MT. *J.Chromatogr.A* 2002; **948**: 267-281.
21. Richling E, Herderich M, Schreier P. *Chromatographia* 1996; **42**: 7-11.
22. Toribio F, Moyano E, Puignou L, Galceran MT. *J.Mass Spectrom.* 2002; **37**: 812-828.
23. Bermudo E, Puignou L, Galceran MT. *J.Chromatog.B* 2003; submitted**.**
24. Toribio F, Puignou L, Galceran MT. *J.Chromatogr.A* 1999; **836**: 223-233.